

Matrix Inference in Growing Rank Regimes

Farzad Pourkamali^{†,*}, Jean Barbier[‡], Nicolas Macris[†]

[†] *School of Computer and Communication Science, Ecole Polytechnique Fédérale de Lausanne*

[‡] *The Abdus Salam International Center for Theoretical Physics, Trieste*

Abstract

The inference of a large symmetric signal-matrix $\mathbf{S} \in \mathbb{R}^{N \times N}$ corrupted by additive Gaussian noise, is considered for two regimes of growth of the rank M as a function of N . For *sub-linear* ranks $M = \Theta(N^\alpha)$ with $\alpha \in (0, 1)$ the mutual information and minimum mean-square error (MMSE) are derived for two classes of signal-matrices: (a) $\mathbf{S} = \mathbf{X}\mathbf{X}^\top$ with entries of $\mathbf{X} \in \mathbb{R}^{N \times M}$ independent identically distributed; (b) \mathbf{S} sampled from a rotationally invariant distribution. Surprisingly, the formulas match the rank-one case. Two efficient algorithms are explored and conjectured to saturate the MMSE when no statistical-to-computational gap is present: (1) Decimation Approximate Message Passing; (2) a spectral algorithm based on a Rotation Invariant Estimator. For *linear* ranks $M = \Theta(N)$ the mutual information is rigorously derived for signal-matrices from a rotationally invariant distribution. Close connections with scalar inference in free probability are uncovered, which allow to deduce a simple formula for the MMSE as an integral involving the limiting spectral measure of the data matrix only. An interesting issue is whether the known information theoretic phase transitions for rank-one, and hence also sub-linear-rank, still persist in linear-rank. Our analysis suggests that only a smoothed-out trace of the transitions persists. Furthermore, the change of behavior between low and truly high-rank regimes only happens at the linear scale $\alpha = 1$.

1 Introduction

We consider the estimation of a large matrix from noisy observations. A real symmetric signal matrix $\mathbf{S} \in \mathbb{R}^{N \times N}$ is observed through an additive white Gaussian noise channel with output

$$\mathbf{Y} = \sqrt{\gamma}\mathbf{S} + \mathbf{Z} \quad (1)$$

with \mathbf{Z} a symmetric Gaussian matrix and $\gamma > 0$ proportional to the signal-to-noise ratio (SNR). We adopt the point of view of Bayesian inference where the prior law of \mathbf{S} and the channel are known, and the task is to infer the signal \mathbf{S} from observations \mathbf{Y} . This problem is known as matrix denoising and is part of many modern data analysis tasks, for example cleaning covariance matrices in statistics or finance [1], signal and image analysis [2], matrix recovery or completion [3, 4]. Matrix denoising is intimately connected to the more involved problem of matrix factorization, where one must estimate two matrices $\mathbf{X} \in \mathbb{R}^{N \times K}$ and $\mathbf{T} \in \mathbb{R}^{M \times K}$ (up to certain symmetries) from noisy observation of $\mathbf{X}\mathbf{T}^\top$. Many problems in signal processing and learning can be formulated as matrix factorization, for example sparse coding [5, 6], blind source separation [7], robust principal component analysis [8], interpretations of patterns in images [9] or also in genomics data [10]. Given this ubiquity both matrix denoising and factorization have gained much attention. But, their theoretical underpinnings still present great challenges.

Much progress has been made in the last decade when the matrix-signal \mathbf{S} is low-rank, meaning the rank is fixed as the matrix dimension grows. Fundamental information theoretical and algorithmic limits, as well as phase transitions and computational-to-statistical gaps, are determined in various statistical settings, see [11–21]. However, when the matrix rank grows with the dimension, the problem remains very challenging and solid results are scarce. Here we consider regimes where the rank grows *sub-linearly* and *linearly* with matrix dimension. We first describe our main findings and then discuss how they compare with the literature. A global view of existing and new results is summarized in Table 1.

1.1 Sub-linear rank regime

This corresponds to $M = \Theta(N^\alpha)$ with $N \rightarrow +\infty$ and $\alpha \in (0, 1)$ fixed. We study two types of priors for the signal matrix: (a) $\mathbf{S} = \mathbf{X}\mathbf{X}^\top$ with entries of $\mathbf{X} \in \mathbb{R}^{N \times M}$ independent identically distributed; (b) \mathbf{S} sampled from

Authors contributed equally to this work.

* Corresponding author: farzad.pourkamali@epfl.ch

a rotationally invariant distribution. Surprisingly we find that for *any* $\alpha \in (0, 1)$ the statistical behavior matches the rank-one case (in particular this implies that there can be phase transitions). For model (a) a new version of the (non-rigorous) replica method [22] is used to derive the asymptotic mutual information between signal and observation matrices in the form of a low dimensional variational formula. The result coincides with the asymptotic mutual information of the rank-one case; see Statement 4. For model (b) we adapt methods of [1, 23] using so-called Rotation Invariant Estimators (RIE). These turn out to be Bayesian optimal estimators which can be used to compute the MMSE and hence the mutual information under Gaussian noise. Two efficient algorithms are also discussed and conjectured to saturate the MMSE when no statistical-to-computational gap is present. For model (a) we introduce Decimation Approximate Message Passing inspired from [24], while for model (b) a RIE estimator [1, 23] adapted to the sub-linear regime provides a natural spectral algorithm.

1.2 Linear rank regime

This corresponds to $M = \Theta(N)$ with $N \rightarrow +\infty$. In this regime, we restrict ourselves to rotationally invariant prior distributions for \mathcal{S} . The mutual information (between signal and observation matrices) and MMSE are rigorously computed under natural assumptions. In this linear regime, the behavior of these quantities is qualitatively different from the low-rank case. We answer a previously open question about the continuity of MMSE as a function of SNR in the affirmative, which rules out the existence of first-order phase transitions in general. However, it remains unclear if higher-order phase transitions might exist in specific examples. Based on a mix of numerical and analytical evidence on specific examples, we observe that only smoothed-out traces of phase transitions seem to persist. We also check that for $\mathcal{S} = \frac{1}{N} \mathbf{X} \mathbf{X}^\top$ with $\mathbf{X} \in \mathbb{R}^{N \times M}$ a Gaussian matrix and $M/N = \epsilon \rightarrow 0$ (taken after the infinite size limit) the MMSE curve tends to the rank-one MMSE of a Gaussian spiked model, thus recovering a second-order phase transition (MMSE continuous and first derivative discontinuous). This limiting behavior is “compatible” with the findings of the sub-linear rank regime.

We first prove Theorem 1 relating the asymptotic mutual information to the limit of a log-spherical-integral, known as an Harish Chandra-Itzykson-Zuber (HCIZ) integral in the mathematical physics literature. Computing the asymptotic behavior of HCIZ integrals is a notoriously difficult problem that we address indirectly here. Indeed we approach the problem from a completely independent perspective making use of the class of RIEs introduced in [23]. The best estimator in this class is in fact optimal and equal to the minimum-mean-square estimator. Thus using the mean-square error of RIE, we are able to directly compute the MMSE; see Theorem 2. Then, integrating an I-MMSE relation [25], we derive an explicit expression for the asymptotic mutual information; see Theorem 3. As a bonus, comparing Theorems 1 and 3 we directly find the asymptotic expression of the *particular* log-spherical integral occurring in the present setting.

1.3 Comparison with literature and discussion

Table 1 summarizes existing results and our main new contributions. The relationship between mutual information and log-spherical integral appearing in Theorem 1 was already found in [22] and [26], but in these works the derivation is far from rigorous. References [27], [26] use Matytsin’s formalism to compute the asymptotic log-spherical integral. This requires dealing with an optimal transportation problem which is usually not exactly solvable; however, in the present setting with additive Gaussian noise, it turns out an exact solution can be computed. We stress that our derivation of the MMSE and mutual information in Theorems 2 and 3 (using the RIE) entirely avoids the use of Matytsin’s formalism and can therefore be viewed as a new calculation of the asymptotic log-spherical integral. It remains to be seen if such methods can be extended beyond the additive Gaussian noise in order to deal with more general spherical integrals (as Matytsin’s formalism does). The denoising problem of rectangular matrices was investigated in [22, 28, 29] for rotationally invariant priors, and an optimal denoiser is also proposed in [28, 29].

For non-rotational invariant priors and linear rank regimes, the matrix denoising problem is wide open. There have been several attempts to derive the mutual information and MMSE for general i.i.d. priors using the replica method from statistical mechanics [30], [22]. However, this method involves largely heuristic ansatzes that have been very difficult to justify for large rank, and it is suspected that the proposed solutions to date are doubtful.

Given the difficulties encountered by the replica method for linear rank, we believe it is of great interest that the sub-linear rank case with i.i.d. priors seems to be amenable to this method. We note that this regime is also particularly relevant practically, as it captures the “not-so-low rank” regime of matrix inference which was recently understood to capture numerous applications [31]. Although we cannot prove Statement 4 there are indications that it is correct. The rank-one formula derived here for separable priors can be shown to be an upper bound to the true mutual information [32]. Also, for \mathbf{X} i.i.d. Gaussian the signal matrix \mathcal{S} has a rotation invariant Wishart prior and we can check consistency with the MMSE obtained from the RIE and the formula for the mutual information recently proven in rotationally invariant sub-linear rank settings [33].

Table 1: Summary of known and new results on matrix inference, on the information-theoretic limits (IT) and optimal algorithms (Alg)

	Separable priors	Rotationally invariant priors
Finite rank $M = \Theta(1)$	(IT) Rigorous MI, MMSE formulas [11–13, 16–19] (Alg) Approximate message-passing (AMP) [34–37]	(IT) Rigorous MI, MMSE formulas [14, 15, 20, 21] (Alg) Spectral PCA [38, 39]
Sub-linear rank $1 \ll M \ll N$	(IT) <u>New</u> : Stat. 4: rank-one MI and MMSE formulas (Alg) <u>New</u> : Decimation-AMP, conjectured optimal	(IT) Rigorous rank-one MI formula [33] (Alg) <u>New</u> : Sub-linear RIE, conjectured optimal
Linear rank $M = \Theta(N)$	Open problem	(IT) <u>New</u> : Thm. 1: relation between MI and log-spherical integrals <u>New</u> : Thm. 2 and 3: explicit expressions of MMSE and MI via free probability In [26] expressions via Matytsin’s formalism and in [22] via perturbative expansions (Alg) Rotational Invariant Estimator (RIE) [23]

2 Inference of matrices with growing rank: settings

2.1 Sub-linear rank matrix factorization and denoising

We start with the setting for matrix *factorization*. Let $\mathbf{X} \in \mathbb{R}^{N \times M}$, with $M = \lfloor N^\alpha \rfloor$ and $\alpha \in (0, 1)$ independent of N , be drawn with i.i.d. entries according to a symmetric distribution $p_X(x) = p_X(-x)$ and variance $\mathbb{E}_X(x^2) = \rho$. The rank M of the matrix $\mathbf{S}(\mathbf{X}) = \mathbf{X}\mathbf{X}^\top/N$ (to be recovered) is sub-linear compared to N . The statistician has access to a symmetric data matrix $\mathbf{Y} = \sqrt{\gamma}\mathbf{S}(\mathbf{X}) + \mathbf{Z}$ where $\mathbf{Z} \sim \exp(-\frac{N}{4}\text{Tr}\mathbf{Z}^2)$ is a standard Wigner matrix and $\gamma \in \mathbb{R}_+$ controls SNR. The Bayesian task here is to infer \mathbf{S} by exploiting the knowledge that it admits a decomposition $\mathbf{X}\mathbf{X}^\top$, with a separable prior for \mathbf{X} .

We also consider symmetric signal matrices $\mathbf{S} \in \mathbb{R}^{N \times N}$ distributed according to a rotation invariant prior supported on matrices with sublinear rank $M = \lfloor N^\alpha \rfloor$. Such signal instances can be realized by taking $\mathbf{S} = \mathbf{V}\mathbf{\Lambda}\mathbf{V}^\top$ with $\mathbf{V} \in \mathbb{R}^{N \times M}$ a matrix uniformly sampled from the Stiefel manifold of full column-rank matrices such that $\mathbf{V}^\top\mathbf{V} = \mathbf{I}_M$ and $\mathbf{\Lambda} = \text{diag}(\lambda_1^S, \dots, \lambda_M^S)$ a set of random i.i.d. M real eigenvalues. Again, the statistician has access to the observation matrix $\mathbf{Y} = \sqrt{\gamma}\mathbf{S} + \mathbf{Z}$. This setting corresponds to a *denoising* problem, namely, the task of recovering a certain matrix \mathbf{S} which has no specific factorized structure, but with a prior on the law of \mathbf{S} itself. Note that if all of the eigenvalues are set to 1, this model and the factorized one with Gaussian i.i.d. elements for \mathbf{X} , are asymptotically equivalent [40].

For both models the main objects of interest are the mutual information $I_N(\mathbf{S}; \mathbf{Y})/(MN)$ between signal and data and the MMSE

$$\text{MMSE}_N(\gamma) = \frac{1}{M} \mathbb{E} \|\mathbf{S} - \mathbb{E}[\mathbf{S} | \mathbf{Y}]\|_F^2$$

when $N \rightarrow \infty$, both suitably scaled in order to have non-trivial limits.

2.2 Linear rank matrix denoising

We consider $\mathbf{S} = \mathbf{S}^\top \in \mathbb{R}^{N \times N}$ distributed according to a rotation invariant prior, i.e., $dP_{S,N}(\mathbf{O}\mathbf{S}\mathbf{O}^\top) = dP_{S,N}(\mathbf{S})$ for any $N \times N$ orthogonal matrix \mathbf{O} . The matrix \mathbf{S} is again corrupted by Gaussian Wigner noise $\mathbf{Y} = \sqrt{\gamma}\mathbf{S} + \mathbf{Z}$ and we are interested in the same information-theoretic quantities as in the sub-linear rank regime.

The empirical spectral distribution of \mathbf{S} is denoted as $\rho_S^{(N)}(x)dx = \frac{1}{N} \sum_{i \leq N} \delta(x - \lambda_i^S)dx$ where (λ_i^S) are the eigenvalues of \mathbf{S} . For the rigorous analysis throughout the linear rank case we shall assume the following:

Assumption 1. The empirical spectral distribution $\rho_S^{(N)}$ converges almost surely weakly to a well-defined probability measure ρ_S with support in $[-C, C]$ for some finite $C > 0$ independent of N . Moreover, the second moment of $\rho_S^{(N)}$ is almost surely bounded.

Signal instances satisfying this assumption can be constructed as $\mathbf{S} = \mathbf{O}\mathbf{\Lambda}\mathbf{O}^\top$ with \mathbf{O} uniformly sampled over the manifold of orthogonal matrices (or Haar distributed) and $\mathbf{\Lambda} = \text{diag}(\lambda_1^S, \dots, \lambda_N^S)$ i.i.d. eigenvalues distributed according to ρ_S with compact support. Note that for measures ρ_S containing a weight $\epsilon \in [0, 1]$ at 0 the random matrices \mathbf{S} have rank $M = (1 - \epsilon)N$. When $M = N$ there is another popular way to construct rotation invariant matrix ensembles, namely by setting $dP_{S,N}(\mathbf{S}) \propto \exp(-\frac{N}{2}\text{Tr}V(\mathbf{S}))d\mathbf{S}$ where $V(\mathbf{S})$ is a rotation invariant ‘‘matrix potential’’. For such priors almost sure weak convergence of the empirical spectral distribution is proved in [41] whenever $\liminf_{|x| \rightarrow \infty} V(x)/(\beta \ln|x|) > 1$ for some $\beta > 1$. Moreover, under some additional conditions, the largest eigenvalue of such a random matrix satisfies a large deviation principle, which implies the almost sure boundedness of the top eigenvalue [41]. Therefore, our assumption holds for a large class of ensembles described by rotation invariant potentials.

3 Main results

It is convenient to start the discussion with the linear case.

3.1 Linear rank matrix denoising

We slightly abuse notation and use $\mu(x) dx$ for $d\mu(x)$ even if the measure is not absolutely continuous. For a sequence of matrices $\mathbf{A}_N \in \mathbb{R}^{N \times N}$, we denote the limiting empirical spectral measure by ρ_A . The free additive convolution [42] of two probability distributions is $\rho_A \boxplus \rho_B$. For real symmetric matrices $\mathbf{A}, \mathbf{B} \in \mathbb{R}^{N \times N}$, the log-spherical integral is defined as $\mathcal{J}_N(\mathbf{A}, \mathbf{B}) := \frac{1}{N} \ln \langle \exp(\frac{N}{2} \text{Tr} \mathbf{A} \mathbf{U} \mathbf{B} \mathbf{U}^\top) \rangle_{\mathbf{U}}$, where the average is w.r.t. the Haar measure over $N \times N$ orthogonal matrices.

Let $\mathcal{J}[\rho_{\sqrt{\gamma}S}, \rho_{\sqrt{\gamma}S} \boxplus \rho_{\text{sc}}] = \lim_{N \rightarrow +\infty} \mathcal{J}_N(\sqrt{\gamma}S, \mathbf{Y})$ where $\rho_{\sqrt{\gamma}S}$ is the limiting spectral distribution of $\sqrt{\gamma}S$, and ρ_{sc} is the usual Wigner semi-circle distribution. Ref. [43] proves that under assumption 1 the limit exists. Our first result for matrix denoising in the linear rank regime is a rigorous formula for the mutual information.

Theorem 1 (Mutual Information for linear rank matrix denoising). *Under assumption 1,*

$$\frac{I_N(\mathbf{S}; \mathbf{Y})}{N^2} \xrightarrow{N \rightarrow \infty} \frac{\gamma}{2} \int x^2 \rho_S(x) dx - \mathcal{J}[\rho_{\sqrt{\gamma}S}, \rho_{\sqrt{\gamma}S} \boxplus \rho_{\text{sc}}]. \quad (2)$$

The complete proof is presented in the SI, Section 1. Although we know that the limiting log-spherical integral is given by a variational problem, see [43], its computation requires going through Matytsin's formalism [44] and is, in general, highly non-trivial. Here we will provide another formula (Theorem 3) for the mutual information, which is much simpler and explicit and which, in turn, also provides an expression for the log-spherical integral.

The route to this program goes first through the class of RIE. An estimator $\hat{\Xi}(\mathbf{Y})$ is called *rotation invariant* if for any orthogonal matrix \mathbf{O} , $\mathbf{O} \hat{\Xi}(\mathbf{Y}) \mathbf{O}^\top = \hat{\Xi}(\mathbf{O} \mathbf{Y} \mathbf{O}^\top)$. We may define the best possible reconstruction error *within the RIE class* as

$$\text{MMSE}_{\text{RIE}, N}(\gamma) = \min_{\hat{\Xi} \in \text{RIE}} \frac{1}{N} \mathbb{E} \|\mathbf{S} - \hat{\Xi}(\mathbf{Y})\|_{\text{F}}^2. \quad (3)$$

Obviously $\text{MMSE}_N(\gamma) \leq \text{MMSE}_{\text{RIE}, N}(\gamma)$. However, it is easy to check explicitly that the MMSE estimator $\mathbb{E}[\mathbf{S} | \mathbf{Y}]$ belongs to the RIE class. Thus we also have $\text{MMSE}_{\text{RIE}, N}(\gamma) \leq \text{MMSE}_N(\gamma)$ and hence $\text{MMSE}_N(\gamma) = \text{MMSE}_{\text{RIE}, N}(\gamma)$.

Because of rotation invariance, \mathbf{Y} and $\hat{\Xi} \in \text{RIE}$ can be diagonalized in the same basis (\mathbf{y}_i) . Thus any RIE is expressed as $\hat{\Xi}(\mathbf{Y}) = \sum \hat{\xi}_i \mathbf{y}_i \mathbf{y}_i^\top$ where $(\hat{\xi}_i)$ are the eigenvalues of the estimator. Therefore (3) requires minimizing over $(\hat{\xi}_i)$ only. In [23] the heuristic replica method is used to show that *in the large N limit*, the optimal $(\hat{\xi}_i)$ can be expressed only in terms of the limiting spectral measure ρ_Y of the data \mathbf{Y} and its eigenvalues (λ_i^Y) :

$$\hat{\Xi}^*(\mathbf{Y}) = \sum_{i \leq N} \xi_i^* \mathbf{y}_i \mathbf{y}_i^\top, \quad \xi_i^* = \frac{1}{\sqrt{\gamma}} (\lambda_i^Y - 2\pi \text{H}[\rho_Y](\lambda_i^Y)), \quad (4)$$

where $\text{H}[\rho_Y](z) := \text{P.V.} \frac{1}{\pi} \int \rho_Y(x)/(z-x) dx$ is the *Hilbert transform* of ρ_Y . Note that ρ_Y is given by the free convolution $\rho_Y = \rho_{\sqrt{\gamma}S} \boxplus \rho_{\text{sc}}$ which is a continuous density due to the smoothing effect of the semi-circle law [45]. Based on this result we make the following assumption here:

Assumption 2. The estimator (4) is asymptotically optimal in the RIE class, i.e.,

$$\text{MMSE}_{\text{RIE}, N}(\gamma) = \frac{1}{N} \mathbb{E} \|\mathbf{S} - \hat{\Xi}^*(\mathbf{Y})\|_{\text{F}}^2 + o_N(1). \quad (5)$$

Using (4) and (5) we prove in the SI Sec. 4 the following explicit formula for the MMSE in linear rank matrix denoising:

Theorem 2 (MMSE for linear rank matrix denoising). *Under assumptions 1, 2 we have*

$$\text{MMSE}_N(\gamma) \xrightarrow{N \rightarrow \infty} \frac{1}{\gamma} \left(1 - \frac{4\pi^2}{3} \int \rho_Y^3(x) dx \right) \quad (6)$$

where the data spectral density $\rho_Y = \rho_{\sqrt{\gamma}S} \boxplus \rho_{\text{sc}}$. Moreover $\text{MMSE}(\gamma) := \lim_{N \rightarrow \infty} \text{MMSE}_N(\gamma)$ is continuous in $\gamma > 0$.

This is an explicit formula that can be used to concretely compute the $\text{MMSE}(\gamma)$ curves for various models of rotation invariant signal ensembles, and in particular, allows to investigate the existence and nature of phase transitions¹. The continuity of $\text{MMSE}(\gamma)$ guarantees that there is no first order phase transition. In low-rank matrix denoising (as well as other inference problems) when there is no first order phase transition (but possibly higher order continuous transitions) the model does not display an algorithmically “hard phase” for low complexity algorithms (e.g., message passing algorithms are optimal). The present linear-rank rotation invariant case is no exception to this picture. Indeed equation (4) suggests an optimal spectral algorithm to estimate the signal: given an observation \mathbf{Y} one computes its eigenvalues and an estimate of the Hilbert transform replacing the integral by an empirical sum to use in (4). This algorithm is optimal since as remarked above $\text{MMSE}_N(\gamma) = \text{MMSE}_{\text{RIE},N}(\gamma)$. Note however that in the (sub-linear rank) *factorized* model it is not the spectral algorithms that are optimal (apart from the special case of Gaussian \mathbf{X} and $\mathbf{X}\mathbf{X}^\top$ Wishart), but rather the decimation-AMP we provide in this paper. Finally, we also mention that the optimality of RIE was also discussed in [26] in a different manner where the authors show heuristically that the posterior mean $\mathbb{E}[\mathbf{S} | \mathbf{Y}]$ equals $\hat{\Xi}^*(\mathbf{Y})$ as $N \rightarrow +\infty$, and also before in [1].

We now proceed to deduce a simpler formula for the mutual information (than in Thm. 1) using the I-MMSE relation [25]

$$\text{MMSE}_N(\gamma) = 4 \frac{d}{d\gamma} \frac{I_N(\mathbf{S}; \mathbf{Y})}{N^2} \quad (7)$$

and free probability. Using the concavity of the mutual information w.r.t. the SNR, (7) also holds as $N \rightarrow +\infty$. One can thus permute the limit $N \rightarrow +\infty$ with the derivative w.r.t. γ . Therefore, it suffices to compute the integral over the *asymptotic* MMSE to find the *asymptotic* mutual information; this is done using basic results from free probability in Sec. “Methodology”. The final result reads:

Theorem 3 (Explicit Mutual Information for linear rank matrix denoising). *Let $\rho_Y = \rho_{\sqrt{\gamma}S} \boxplus \rho_{sc}$. Under assumptions 1, 2 we have*

$$\frac{I_N(\mathbf{S}; \mathbf{Y})}{N^2} \xrightarrow{N \rightarrow \infty} \frac{1}{2} \iint \ln |s - t| \rho_Y(s) \rho_Y(t) ds dt + \frac{1}{8}. \quad (8)$$

In Sec. 4 of the SI we also provide a generalization of this result to a larger class of (non-Gaussian) rotation invariant noise ensembles.

3.2 Sub-linear rank matrix factorization and denoising

Our first result for the sub-linear rank case says that, from the information-theoretic perspective, for matrix factorization with separable priors, sub-linear rank is equivalent to having a rank-one signal.

Statement 4 (Replica prediction). *For the setting of sub-linear rank matrix factorization described above with an entry-wise prior for \mathbf{X} the mutual information matches the rank-one prediction, i.e.,*

$$\frac{I_N(\mathbf{S}; \mathbf{Y})}{MN} \xrightarrow{N \rightarrow \infty} \inf_{\sigma \geq 0} \left\{ \frac{\gamma}{4} (\sigma - \rho)^2 + I(X; \sqrt{\gamma\sigma}X + Z) \right\} \quad (9)$$

where $X \sim p_X$, $Z \sim \mathcal{N}(0, 1)$ and ρ is the variance of p_X . If the minimizer σ_* in (9) is unique, the MMSE reads

$$\text{MMSE}_N(\gamma) \xrightarrow{N \rightarrow \infty} \rho^2 - \sigma_*^2. \quad (10)$$

In the limit $M = \lfloor N^\alpha \rfloor$, $N \rightarrow +\infty$, this statement holds for any $\alpha \in [0, 1)$. The collapse of asymptotic mutual information for all sub-linear rank regimes (including finite rank) to a single rank-one formula might seem implausible. However, similar behavior is known in random matrix theory problems [33, 46] and the surprise here is that such a reduction is *also* valid in the framework of Bayesian inference.

A rigorous validation of this reduction in a special case comes from the recent work [33] which derived the asymptotic mutual information for sub-linear matrix denoising with rotationally invariant priors. For Wishart signals with \mathbf{X} Gaussian the two formulas should therefore coincide. This consistency check indeed works and is presented in the Sec 6.2.2 of the SI. We also provide in the Sec. 6 of SI an independent check using a sub-linear RIE to rederive (along lines similar to the linear case) the information theoretic quantities for a few specific priors, and among them the Wishart signals.

We now discuss novel *algorithmic* approaches for the sub-linear regime: a decimation-AMP for the factorized model with separable priors and a spectral sub-linear RIE algorithm for denoising with rotational invariant priors *and* noise.

¹Phase transitions are non-analyticity points in the asymptotic mutual information as a function of SNR. This is a concave and continuous function, and k -th order phase transitions correspond to discontinuities in the k -th derivative. In particular for a first order transition the MMSE is discontinuous because of the I-MMSE relation (7).

Decimation-AMP algorithm. We use the standard AMP algorithm for *rank-one* matrix inference [34–36] applied together with a *decimation* procedure. The idea is to iteratively subtract from the data at each “inference round” the estimated rank-one spike. This is inspired from [24] where the authors look at linear ranks and instead employ an exponentially costly inference algorithm at each step. The surprise is that in the sub-linear case, using AMP “one spike at a time” works and yields an algorithm of complexity $\Theta(MN^2)$. Its pseudo-code is as follows: set $t = 1$ and $\mathbf{Y}^{(1)} = \mathbf{Y}$, then

- (i) *Rank-one AMP*: Run standard AMP for rank-one matrices (with an optimal denoiser associated to p_X if known, or else any other denoiser) until convergence, whose output is a vector $\hat{\mathbf{x}}^{(t)} = \text{AMP}_{M=1}(\mathbf{Y}^{(t)}) \in \mathbb{R}^N$.
- (ii) *Decimation*: If $t < M$ set $\mathbf{Y}^{(t+1)} = \mathbf{Y}^{(t)} - \sqrt{\gamma}\hat{\mathbf{x}}^{(t)}(\hat{\mathbf{x}}^{(t)})^\top$, $t = t + 1$ and go to step (i); else go to step (iii).
- (iii) *Estimator*: Output $\sum_{t \leq M} \hat{\mathbf{x}}^{(t)}(\hat{\mathbf{x}}^{(t)})^\top$ as estimator of $\mathcal{S}(\mathbf{X})$.

Sub-linear RIE algorithm. We construct a RIE applicable to rotation invariant signals *and* noises. This estimator is derived based on the results on sub-linear perturbations of random matrices [46], details of which can be found in Sec. 6 of the SI. This yields a spectral algorithm in the spirit of PCA which requires the data \mathbf{Y} and knowledge of the noise distribution. Let G_{ρ_Z} the Cauchy transform of the limiting spectral measure ρ_Z and G'_{ρ_Z} its derivative. Define the following *thresholding function* (which is *not* the same as the one employed in the linear rank regime (4))

$$f_Z(x) = -\frac{1}{\sqrt{\gamma}}\mathbb{I}(x \notin [a, b])\frac{G_{\rho_Z}(x)}{G'_{\rho_Z}(x)},$$

where $[a, b]$ is the support of ρ_Z . For example with Wigner noise $f_Z(x) = \gamma^{-1/2}\mathbb{I}(|x| > 2)\text{sign}(x)\sqrt{x^2 - 4}$. Algorithmic steps are:

- (i) *Spectral step*: Compute eigen-data $(\lambda_i^Y, \mathbf{y}_i)_{i \leq N}$ from \mathbf{Y} .
- (ii) *Thresholded estimator*: Output $\hat{\mathbf{S}} = \sum_{i \leq N} f_Z(\lambda_i^Y)\mathbf{y}_i\mathbf{y}_i^\top$.

We conjecture that these two algorithms are Bayes-optimal in the sense that their mean square error matches the MMSE, for any regime $M = \lfloor N^\alpha \rfloor$ with $\alpha \in (0, 1)$ when N is large. This is supported by the theoretical checks for the Wishart priors and also, at least for some range of exponents, by the numerical results presented in Sec. 4. Our numerics do not yet allow to pinpoint whether the conjecture holds for any $\alpha < 1$ or only up to some maximal exponent.

4 Numerical examples and discussion

4.1 Performance of algorithms in sub-linear rank regimes

Fig. 1 illustrates the performance of the proposed algorithms for two examples in the sub-linear rank regime. The left plot corresponds to a Wishart matrix signal $\mathbf{X}\mathbf{X}^\top$ where $\mathbf{X} \in \mathbb{R}^{N \times M}$ has i.i.d. $\mathcal{N}(0, 1)$ entries. Thus $\mathcal{S}_N(\mathbf{X})$ has a rotationally invariant distribution, and we observe that, as expected, both sub-linear RIE and decimation-AMP with MMSE denoiser achieve the MMSE (predicted by the rank-one formula). The right plot corresponds to a Rademacher matrix: $\mathbf{X} \in \mathbb{R}^{N \times M}$ has i.i.d. ± 1 entries with equal probability. The regime of ranks we can attain without particular optimization and for all instances is smaller for Rademacher signals ($M = \lfloor N^{0.3} \rfloor$) than for Gaussian ($M = \lfloor N^{0.5} \rfloor$); this higher level of difficulty may be inherent to the Rademacher setting. Indeed, after relating matrix factorization to the Hopfield model [24] this is not surprising as it is known that continuous variables allow for greater recovery properties than binary variables [47]. Note also that since the Rademacher prior is not rotationally invariant, the sub-linear RIE algorithm is sub-optimal for that case and decimation-AMP is needed.

4.2 MMSE in linear rank regimes

As first example in the linear rank regime, we consider the case where $\rho_S = \frac{1}{2}\delta_{-1} + \frac{1}{2}\delta_{+1}$. Using the technique introduced in [45], we obtain an explicit analytical expression for $\rho_Y = \rho_{\sqrt{\gamma}S} \boxplus \rho_{SC}$. For $\gamma \geq 1$ the support of ρ_Y consists of two disjoint intervals, and for $\gamma < 1$ we get a single interval. Therefore, we expect that, if a phase transition in the mutual information and MMSE exists, it should happen at $\gamma_c = 1$. As noted before, because of Theorem 2 we know that $\text{MMSE}(\gamma)$ is continuous, so a phase transition can only be second or higher order. Furthermore, from the explicit formula for ρ_Y we get integral representations of the first few derivatives of $\text{MMSE}(\gamma)$. Fig. 3 displays the results of precise numerical integrations for the MMSE and its first two derivatives, while the third derivative

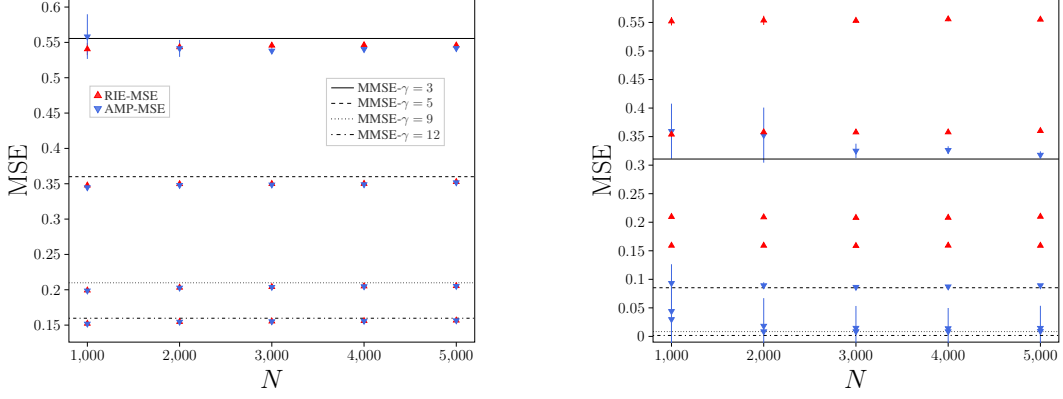


Figure 1: Comparison of the MSE reached by our proposed Sub-linear RIE (red) and Decimation AMP (blue) algorithms for sub-linear matrix inference as a function of the size N for various SNR γ , compared to the rank-one MMSE (Statement 4). Each point is the average over 10 experiments. (left) Signal with Gaussian spikes, $M = \lfloor N^{0.5} \rfloor$. (right) Signal with Rademacher spikes, $M = \lfloor N^{0.3} \rfloor$.

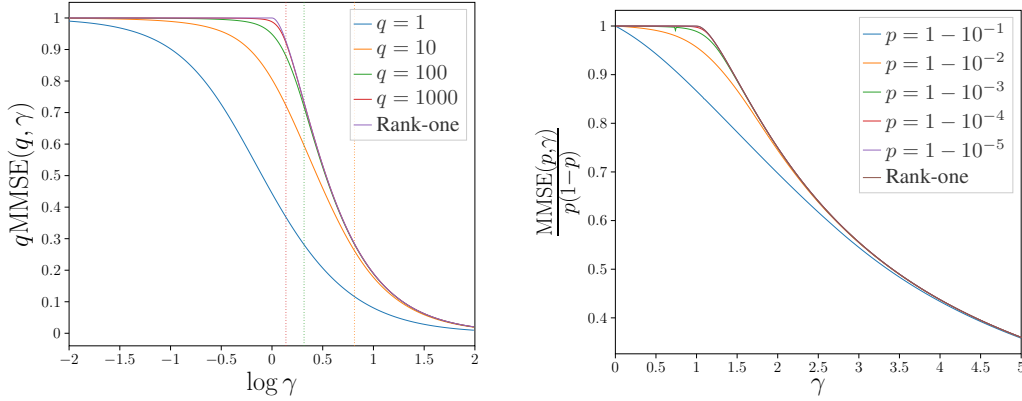


Figure 2: MMSE in the linear-rank regime with sparse spectral priors. The MMSE of the rank-one problem is also plotted for comparison. (left) Signal with Marchenko-Pastur spectral distribution for large q 's. The vertical dashed lines corresponds to the critical value where the support of ρ_Y splits. (right) Signal with rank $M = (1-p)N$ and Bernoulli spectral distribution, $\rho_S = p\delta_0 + (1-p)\delta_{+1}$, for p 's close to 1.

is computed by numerically differentiating the second derivative. These plots suggest that there is 4-th order phase transition for this example model at $\gamma_c = 1$. All details and additional figures can be found in the Sec. 7 of the SI.

In a second example we consider $\mathbf{S} = \mathbf{X}\mathbf{X}^\top/N$ where $\mathbf{X} \in \mathbb{R}^{N \times M}$ has i.i.d. standard Gaussian entries. The limiting spectral distribution of \mathbf{S} when the aspect ratio $N/M \rightarrow q$ (fixed) is the *Marchenko-Pastur* law. For this model it is not difficult to directly compute ρ_Y (see SI). Its support is a single interval for $q \leq 1$, and two disjoint intervals for $q > 1$ and $\gamma > q(q^{1/3} - 1)^{-3}$. However, when the intervals merge in this case there does not seem to exist a phase transition, at least on low order derivatives (investigated numerically). Fig. 2 (left) shows the MMSE as a function of $\log \gamma$.

4.3 Transition between the sub-linear and linear rank regimes

A surprising prediction of our analysis is the collapse of the formulas for the mutual information and MMSE of sub-linear matrix inference with separable priors, onto rank-one expressions; see Statement 4. Our replica analysis is however not able to assess for what precise regime of M this prediction fails. But, we can exploit our rigorous results on linear rank inference to pinpoint when this happens, namely, when does the transition between the low and truly extensive rank regime occurs. For the aforementioned case of a Wishart signal, we observe in the left part of Fig. 2 that as $q \rightarrow +\infty$ the MMSE tends to the one of the rank-one version of matrix denoising with Gaussian prior. In particular, we recover the second-order phase transition of the rank-one problem at $\gamma = 1$, which matches the famous Ben Arous-Baik-Péché transition [38]. This convergence towards the rank-one prediction can also be observed in a model with Bernoulli spectral distribution, see right part of Fig.2.

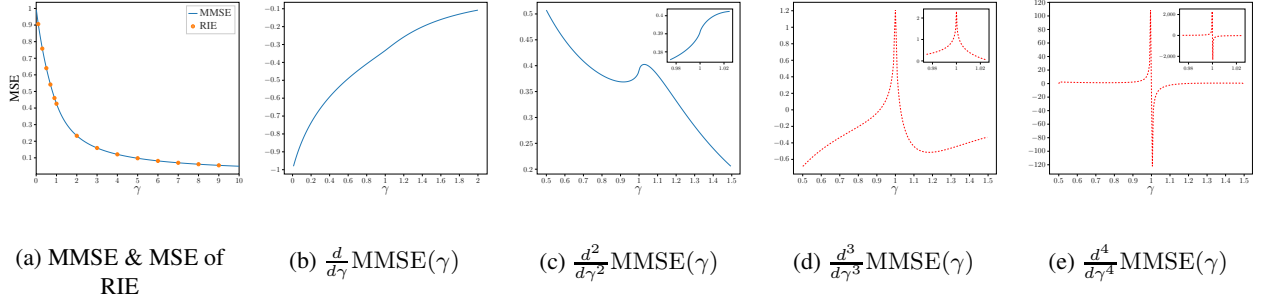


Figure 3: MMSE for the Rademacher spectral distribution. From left to right: Plot (a) $\text{MMSE}(\gamma)$ computed from (6) and $\text{MSE}_{N,\text{RIE}}(\gamma)$ points computed from (4) for $N = 1000$ averaged over 20 runs (error bars are invisible). Plots (b) and (c): first and second derivatives of $\text{MMSE}(\gamma)$ computed using their integral representation (integral computed numerically). Plots (d) and (e): first and second numerical differentiation of (c). These suggest that the $\text{MMSE}''(\gamma)$ has a vertical tangent at $\gamma_c = 1$, and a possible phase transition (if present) would be 4-th order. A numerical analysis in the SI, Sec 7 is compatible with a weak singularity at $\gamma_c = 1$ of the form $(\gamma - 1)^3 \ln |\gamma - 1|$.

5 Methodology

This work combines four main tools, namely *spherical integrals*, *free probability*, the *replica method*, and *RIE's*. The use of the later has been sketched in the previous sections so we restrict the discussion to the first three. The *spherical integrals* involved in this work are defined for two real symmetric matrices $\mathbf{A}, \mathbf{B} \in \mathbb{R}^{N \times N}$ as $\mathcal{I}_N(\mathbf{A}, \mathbf{B}) := \int DU \exp \frac{N}{2} \text{Tr} \mathbf{A} \mathbf{U} \mathbf{B} \mathbf{U}^T$, where DU is the Haar measure over the group of orthogonal matrices. The asymptotic behavior of HCIZ integrals in the symmetric case has been extensively studied in the literature, both in mathematics [43] and in physics communities [44]. In particular, it is possible to compute perturbative expansions, used in the matrix denoising problem in [22], or sometimes work out explicit solutions to Matytsin's theory [26]. Besides spherical integrals, we also use results from *free probability*. Free probability (see [48, 49]) was initially introduced to study operator algebras, but has gained considerable importance in other realms due to its connection with the asymptotic behavior of random matrices. While free probability has been exploited in linear estimation and wireless communication problems [50–53], the connection with matrix inference setting studied here is to the best of our knowledge new. The *replica method* [54] has been broadly used in inference and is known to lead to successful and provable –by other methods– results for low rank problems. As already said for the linear rank regime, it still needs to be understood how to correctly use the method, if this is at all possible. Here we propose a new replica calculation for the large but sub-linear rank regime. As already mentioned, our prediction is compatible with existing rigorous results [33].

Among our various results, the proof of Theorem 3 is particularly insightful due to the connections it establishes between matrix inference and free probability. To compute the integral over the MMSE (7), first we show that the MMSE can be expressed as the free Fisher information of a non-commutative random variable, and then carry out the integration using basic relations in free probability to obtain the expression for the mutual information. Let X be a self-adjoint *non-commutative* random variable X associated to a probability measure μ_X with compact support on the real line. According to [55, 56] the *free entropy* $\chi(X)$ and the *free Fisher information* $\Phi(X)$ are given as

$$\chi(X) = \iint \ln |s - t| \mu_X(s) \mu_X(t) ds dt + \frac{3}{4} + \frac{1}{2} \ln 2\pi, \quad (11)$$

$$\Phi(X) = \frac{4\pi^2}{3} \int \mu_X^3(s) ds. \quad (12)$$

Moreover, these two quantities are related through the relation:

$$\chi(X) = \frac{1}{2} \int_0^\infty \left(\frac{1}{1+t} - \Phi(X + \sqrt{t}Z) \right) dt + \frac{1}{2} \ln 2\pi + \frac{1}{2} \quad (13)$$

where Z is a semicircular non-commutative random variable, and X and Z are *free*. We apply these relations to $X = S$ and Z , two free non-commutative random variables (not to confused with the $N \times N$ matrices \mathbf{S} and \mathbf{Z}) associated to the probability measures ρ_S and ρ_{sc} . Since S and Z are free, the sum $\sqrt{\gamma}S + Z$ is a non-commutative random variable associated to the measure $\rho_{\sqrt{\gamma}S} \boxplus \rho_{\text{sc}} = \rho_Y$. Clearly then (6) can be written in the free probability language as

$$\text{MMSE}(\gamma) = \frac{1}{\gamma} \left(1 - \Phi(\sqrt{\gamma}S + Z) \right). \quad (14)$$

Integrating both sides of (14) over γ and using (13) and (7) (the latter for $N \rightarrow \infty$), we conclude that (see details in Sec. 4 of SI)

$$\frac{I_N(\mathbf{S}; \mathbf{Y})}{N^2} \xrightarrow{N \rightarrow \infty} \frac{1}{2} \chi(\sqrt{\gamma}S + Z) - \frac{1}{4} \ln 2\pi - \frac{1}{4}. \quad (15)$$

This implies an explicit expression for the asymptotic mutual information. It is shown in [57] that $\Phi(\sqrt{\gamma}S + Z)$ is a continuous function of γ . Thus, (14) implies that the $\text{MMSE}(\gamma)$ is a continuous function of γ .

Acknowledgments

We acknowledge important insights from Léo Miolane in early stages of this project. We are also thankful to Antoine Maillard for interesting discussions. The work of F. P has been supported by Swiss National Science Foundation grant no 200021-204119. J. B was funded by the European Union (ERC, CHORAL, project number 101039794). Views and opinions expressed are those of the author(s) only and do not reflect those of the European Union or the European Research Council. Neither the European Union nor the granting authority are responsible for them.

References

- [1] Joël Bun, Jean-Philippe Bouchaud, and Marc Potters. Cleaning large correlation matrices: tools from random matrix theory. *Physics Reports*, 666:1–109, 2017.
- [2] Thierry Bouwmans, Necdet Serhat Aybat, and El-hadi Zahzah. *Handbook of robust low-rank and sparse matrix decomposition: Applications in image and video processing*. CRC Press, 2016.
- [3] David L Donoho, Matan Gavish, and Andrea Montanari. The phase transition of matrix recovery from gaussian measurements matches the minimax mse of matrix denoising. *Proceedings of the National Academy of Sciences*, 110(21):8405–8410, 2013.
- [4] Weiran Wang, Miguel Carreira-Perpiñán, and Zhengdong Lu. A denoising view of matrix completion. *Advances in Neural Information Processing Systems*, 24, 2011.
- [5] Bruno A Olshausen and David J Field. Emergence of simple-cell receptive field properties by learning a sparse code for natural images. *Nature*, 381(6583):607–609, 1996.
- [6] Bruno A Olshausen and David J Field. Sparse coding with an overcomplete basis set: A strategy employed by v1? *Vision research*, 37(23):3311–3325, 1997.
- [7] Adel Belouchrani, Karim Abed-Meraim, J-F Cardoso, and Eric Moulines. A blind source separation technique using second-order statistics. *IEEE Transactions on signal processing*, 45(2):434–444, 1997.
- [8] Emmanuel J Candès, Xiaodong Li, Yi Ma, and John Wright. Robust principal component analysis? *Journal of the ACM (JACM)*, 58(3):1–37, 2011.
- [9] Daniel D Lee and H Sebastian Seung. Learning the parts of objects by non-negative matrix factorization. *Nature*, 401(6755):788–791, 1999.
- [10] Andrew V Kossenkov and Michael F Ochs. Matrix factorisation methods applied in microarray data analysis. *International journal of data mining and bioinformatics*, 4(1):72–90, 2010.
- [11] Satish Babu Korada and Nicolas Macris. Exact solution of the gauge symmetric p-spin glass model on a complete graph. *Journal of Statistical Physics*, 136(2):205–230, 2009.
- [12] Mohamad Dia, Nicolas Macris, Florent Krzakala, Thibault Lesieur, Lenka Zdeborová, et al. Mutual information for symmetric rank-one matrix estimation: A proof of the replica formula. *Advances in Neural Information Processing Systems*, 29, 2016.
- [13] Marc Lelarge and Léo Miolane. Fundamental limits of symmetric low-rank matrix estimation. *Probability Theory and Related Fields*, 173(3):859–929, 2019.
- [14] Farzad Pourkamali and Nicolas Macris. Mismatched estimation of rank-one symmetric matrices under gaussian noise. *arXiv preprint arXiv:2107.08927*, 2021.
- [15] Jean Barbier, TianQi Hou, Marco Mondelli, and Manuel Sáenz. The price of ignorance: how much does it cost to forget noise structure in low-rank matrix estimation? *arXiv preprint arXiv:2205.10009*, 2022.

- [16] Thibault Lesieur, Florent Krzakala, and Lenka Zdeborová. Mmse of probabilistic low-rank matrix estimation: Universality with respect to the output channel. In *2015 53rd Annual Allerton Conference on Communication, Control, and Computing (Allerton)*, pages 680–687. IEEE, 2015.
- [17] Jean Barbier and Nicolas Macris. The adaptive interpolation method: a simple scheme to prove replica formulas in bayesian inference. *Probability theory and related fields*, 174(3):1133–1185, 2019.
- [18] Jean Barbier and Nicolas Macris. The adaptive interpolation method for proving replica formulas. applications to the curie–weiss and wigner spike models. *Journal of Physics A: Mathematical and Theoretical*, 52(29):294002, 2019.
- [19] Léo Miolane. Fundamental limits of low-rank matrix estimation: the non-symmetric case. *arXiv preprint arXiv:1702.00473*, 2017.
- [20] Clément Luneau, Nicolas Macris, and Jean Barbier. High-dimensional rank-one nonsymmetric matrix decomposition: the spherical case. In *2020 IEEE International Symposium on Information Theory (ISIT)*, pages 2646–2651. IEEE, 2020.
- [21] Farzad Pourkamali and Nicolas Macris. Mismatched estimation of non-symmetric rank-one matrices under gaussian noise. In *2022 IEEE International Symposium on Information Theory (ISIT)*, pages 1288–1293. IEEE, 2022.
- [22] Jean Barbier and Nicolas Macris. Statistical limits of dictionary learning: random matrix theory and the spectral replica method. *arXiv preprint arXiv:2109.06610*, 2021.
- [23] Joël Bun, Romain Allez, Jean-Philippe Bouchaud, and Marc Potters. Rotational invariant estimator for general noisy matrices. *IEEE Transactions on Information Theory*, 62(12):7475–7490, 2016.
- [24] Francesco Camilli and Marc Mézard. Matrix factorization with neural networks. *arXiv preprint arXiv:2212.02105*, 2022.
- [25] Dongning Guo, Shlomo Shamai, and Sergio Verdú. Mutual information and minimum mean-square error in gaussian channels. *IEEE transactions on information theory*, 51(4):1261–1282, 2005.
- [26] Antoine Maillard, Florent Krzakala, Marc Mézard, and Lenka Zdeborová. Perturbative construction of mean-field equations in extensive-rank matrix factorization and denoising. *arXiv preprint arXiv:2110.08775*, 2021.
- [27] Hinnerk Christian Schmidt. *Statistical Physics of Sparse and Dense Models in Optimization and Inference*. PhD thesis, Université Paris Saclay (COmUE), 2018.
- [28] Emanuele Troiani, Vittorio Erba, Florent Krzakala, Antoine Maillard, and Lenka Zdeborová. Optimal denoising of rotationally invariant rectangular matrices. *arXiv preprint arXiv:2203.07752*, 2022.
- [29] Farzad Pourkamali and Nicolas Macris. Rectangular rotational invariant estimator for general additive noise matrices. *arXiv preprint arXiv:2304.12264*, 2023.
- [30] Yoshiyuki Kabashima, Florent Krzakala, Marc Mézard, Ayaka Sakata, and Lenka Zdeborová. Phase transitions and sample complexity in bayes-optimal matrix factorization. *IEEE Transactions on information theory*, 62(7):4228–4265, 2016.
- [31] Chanwoo Lee and Miaoyan Wang. Statistical and computational rates in high rank tensor estimation. *arXiv preprint arXiv:2304.04043*, 2023.
- [32] Jean Barbier, Justin Ko, and Anas Rahman. Private communication. 2023.
- [33] Jonathan Husson and Justin Ko. Spherical integrals of sublinear rank. *arXiv preprint arXiv:2208.03642*, 2022.
- [34] Yash Deshpande and Andrea Montanari. Information-theoretically optimal sparse pca. In *2014 IEEE International Symposium on Information Theory*, pages 2197–2201. IEEE, 2014.
- [35] Sundeep Rangan and Alyson K Fletcher. Iterative estimation of constrained rank-one matrices in noise. In *2012 IEEE International Symposium on Information Theory Proceedings*, pages 1246–1250. IEEE, 2012.
- [36] Thibault Lesieur, Florent Krzakala, and Lenka Zdeborová. Constrained low-rank matrix estimation: Phase transitions, approximate message passing and applications. *Journal of Statistical Mechanics: Theory and Experiment*, 2017(7):073403, 2017.

- [37] Jean Barbier, Francesco Camilli, Marco Mondelli, and Manuel Saenz. Bayes-optimal limits in structured pca, and how to reach them. *arXiv preprint arXiv:2210.01237*, 2022.
- [38] Jinho Baik, Gérard Ben Arous, and Sandrine Péché. Phase transition of the largest eigenvalue for nonnull complex sample covariance matrices. *The Annals of Probability*, 33(5):1643–1697, 2005.
- [39] Florent Benaych-Georges and Raj Rao Nadakuditi. The eigenvalues and eigenvectors of finite, low rank perturbations of large random matrices. *Advances in Mathematics*, 227(1):494–521, 2011.
- [40] Dag Jonsson. Some limit theorems for the eigenvalues of a sample covariance matrix. *Journal of Multivariate Analysis*, 12(1):1–38, 1982.
- [41] Greg W Anderson, Alice Guionnet, and Ofer Zeitouni. *An introduction to random matrices*. Cambridge university press, 2010.
- [42] Dan Voiculescu. Limit laws for random matrices and free products. *Inventiones mathematicae*, 104(1):201–220, 1991.
- [43] Alice Guionnet and Ofer Zeitouni. Large deviations asymptotics for spherical integrals. *Journal of functional analysis*, 188(2):461–515, 2002.
- [44] A Matytsin. On the large-N limit of the Itzykson-Zuber integral. *Nuclear Physics B*, 411(2-3):805–820, 1994.
- [45] Philippe Biane. On the free convolution with a semi-circular distribution. *Indiana University Mathematics Journal*, pages 705–718, 1997.
- [46] Jiaoyang Huang. Mesoscopic perturbations of large random matrices. *Random Matrices: Theory and Applications*, 7(02):1850004, 2018.
- [47] Carlo Lucibello and Marc Mézard. The exponential capacity of dense associative memories. *arXiv preprint arXiv:2304.14964*, 2023.
- [48] Alexandru Nica and Roland Speicher. *Lectures on the combinatorics of free probability*, volume 13. Cambridge University Press, 2006.
- [49] James A Mingo and Roland Speicher. *Free probability and random matrices*, volume 35. Springer, 2017.
- [50] Ralf R Müller. Random matrices, free probability and the replica method. In *2004 12th European Signal Processing Conference*, pages 189–196. IEEE, 2004.
- [51] Sergio Verdú. Mismatched estimation and relative entropy. *IEEE Transactions on Information Theory*, 56(8):3712–3720, 2010.
- [52] Alexandru Nica, Roland Speicher, Antonia Tulino, and Dan Voiculescu. Free probability extensions and applications. In *Proc. BIRS*, pages 3–10. Citeseer, 2008.
- [53] Galen Reeves, Henry D Pfister, and Alex Dytso. Mutual information as a function of matrix snr for linear gaussian channels. In *2018 IEEE International Symposium on Information Theory (ISIT)*, pages 1754–1758. IEEE, 2018.
- [54] Marc Mezard and Andrea Montanari. *Information, physics, and computation*. Oxford University Press, 2009.
- [55] Dan Voiculescu. The analogues of entropy and of fisher’s information measure in free probability theory, i. *Communications in mathematical physics*, 155(1):71–92, 1993.
- [56] Dan Voiculescu. The analogues of entropy and of fisher’s information measure in free probability theory, ii. *Inventiones mathematicae*, 118(1):411–440, 1994.
- [57] Dan Voiculescu. The derivative of order 1/2 of a free convolution by a semicircle distribution. *Indiana University Mathematics Journal*, pages 697–703, 1997.
- [58] Cédric Villani. *Topics in optimal transportation*, volume 58. American Mathematical Soc., 2021.
- [59] Godfrey Harold Hardy, John Edensor Littlewood, and George Pólya. *Inequalities*. Cambridge university press, 1952.
- [60] Dimitri Shlyakhtenko and Terence Tao Jekel. Fractional free convolution powers. *arXiv preprint arXiv:2009.01882*, 2020.

- [61] Marc Mézard, Giorgio Parisi, and Miguel Angel Virasoro. *Spin glass theory and beyond: An Introduction to the Replica Method and Its Applications*, volume 9. World Scientific Publishing Company, 1987.
- [62] Hidetoshi Nishimori. *Statistical physics of spin glasses and information processing: an introduction*. Number 111. Clarendon Press, 2001.
- [63] Alice Guionnet and Jiaoyang Huang. Large deviations asymptotics of rectangular spherical integral. *arXiv preprint arXiv:2106.07146*, 2021.
- [64] Kenneth R Davidson and Stanislaw J Szarek. Local operator theory, random matrices and banach spaces. *Handbook of the geometry of Banach spaces*, 1(317-366):131, 2001.
- [65] Timothy Sauer. *Numerical analysis*. Addison-Wesley Publishing Company, 2011.
- [66] Svante Janson. Resultant and discriminant of polynomials. *Notes*, September, 22, 2007.

A Proof of Theorem 1

We present the steps needed to prove theorem 1. It is convenient to decompose Assumption 1 in the main text in two parts.

Assumption 1.A The empirical spectral distribution of \mathbf{S} converges almost surely weakly to a well-defined probability measure ρ_S with support included in $[-C, C]$ for some finite positive constant $0 < C < +\infty$ independent of N .

Assumption 1.B The second moment of the empirical spectral distribution of \mathbf{S} is almost surely bounded.

Remark 1. These assumptions taken together imply that the second moment of the empirical measure $\rho_S^{(N)}$ converges almost surely to the second moment of ρ_S .

Remark 2. By Theorem 7.12 in ref. [58], these assumptions are equivalent to the convergence of the empirical distribution in the Wasserstein-2 metric to ρ_S .

We start from the posterior distribution of the model, which is proportional to

$$P_N(\mathbf{X}|\mathbf{Y}) \propto e^{-\frac{N}{4}\|\mathbf{Y}-\sqrt{\gamma}\mathbf{X}\|_F^2} P_{S,N}(\mathbf{X}) \propto e^{\frac{N}{2}\text{Tr}[\sqrt{\gamma}\mathbf{X}\mathbf{Y}-\frac{\gamma}{2}\mathbf{X}^2]} P_{S,N}(\mathbf{X}). \quad (16)$$

The partition function is defined as the normalizing factor of the posterior distribution (16)

$$Z(\mathbf{Y}) = \int d\mathbf{X} e^{\frac{N}{2}\text{Tr}[\sqrt{\gamma}\mathbf{X}\mathbf{Y}-\frac{\gamma}{2}\mathbf{X}^2]} P_{S,N}(\mathbf{X}) \quad (17)$$

and the free energy is defined as

$$F_N(\gamma) = -\frac{1}{N^2}\mathbb{E}_Y[\ln Z(\mathbf{Y})]. \quad (18)$$

One can easily see that the free energy is linked to the average mutual information via the identity

$$\frac{1}{N^2}I_N(\mathbf{S}; \mathbf{Y}) = F_N(\gamma) + \frac{\gamma}{4N}\mathbb{E}[\text{Tr}\mathbf{S}^2] \quad (19)$$

in which $\frac{1}{N}\mathbb{E}[\text{Tr}\mathbf{S}^2]$ converges to the second moment of ρ_S by assumption. Therefore, to prove theorem 1 it is enough to show

$$\lim_{N \rightarrow \infty} F_N(\gamma) = \frac{\gamma}{4} \int x^2 \rho_S(x) dx - \mathcal{J}[\rho_{\sqrt{\gamma}\mathbf{S}}, \rho_{\sqrt{\gamma}\mathbf{S}} \boxplus \rho_{\text{sc}}]. \quad (20)$$

The proof of (20) is done in two main steps. First we show that such a limit holds for the free energy of an *independent eigenvalue model*. Second, using the *pseudo-Lipschitz* continuity of the free energy w.r.t. to the prior distribution, we deduce that the same limit holds for the free energy of the original model.

We make the convention that in the eigen-decomposition of a $N \times N$ matrix $\mathbf{S} = \mathbf{U}\mathbf{\Lambda}\mathbf{U}^\top$ with $\mathbf{\Lambda} = \text{diag}(\boldsymbol{\lambda})$, the eigenvalues $\lambda_1, \dots, \lambda_N$ are in non-decreasing order.

A.1 An independent eigenvalue model

Suppose $\boldsymbol{\lambda}^0 \in \mathbb{R}^N$ is generated with i.i.d. elements from ρ_S and is ordered in non-decreasing way. Fix $\boldsymbol{\lambda}^0$ once for all. Let $\tilde{\mathbf{S}} \in \mathbb{R}^{N \times N}$ the matrix constructed as $\mathbf{U}\tilde{\mathbf{\Lambda}}\mathbf{U}^\top$ where \mathbf{U} is distributed according to the Haar measure, and $\tilde{\mathbf{\Lambda}} = \text{diag}(\tilde{\boldsymbol{\lambda}})$ is a diagonal matrix. The distribution of the matrix $\tilde{\mathbf{S}}$ is

$$dP_{\tilde{\mathbf{S}},N}(\tilde{\mathbf{S}}) = d\mu_N(\mathbf{U})dp_{\tilde{\mathbf{S}},N}(\tilde{\boldsymbol{\lambda}}) = d\mu_N(\mathbf{U}) \prod_{i=1}^N \delta(\tilde{\lambda}_i - \lambda_i^0) d\tilde{\boldsymbol{\lambda}}. \quad (21)$$

The independent eigenvalue model is defined as an inference model where the matrix $\tilde{\mathbf{S}}$ is observed through an AWGN channel $\tilde{\mathbf{Y}} = \sqrt{\gamma}\tilde{\mathbf{S}} + \tilde{\mathbf{Z}}$ with SNR proportional to γ and $\tilde{\mathbf{Z}}$ a symmetric Gaussian Wigner matrix. The associated partition function and the free energy are defined in the same way as in (17),(18)

$$\tilde{Z}(\tilde{\mathbf{Y}}) = \int d\mathbf{X} e^{\frac{N}{2}\text{Tr}[\sqrt{\gamma}\mathbf{X}\tilde{\mathbf{Y}}-\frac{\gamma}{2}\mathbf{X}^2]} P_{\tilde{\mathbf{S}},N}(\mathbf{X}). \quad (22)$$

$$\tilde{F}_N(\gamma) = -\frac{1}{N^2}\mathbb{E}_{\tilde{\mathbf{Y}}}[\ln \tilde{Z}(\tilde{\mathbf{Y}})]. \quad (23)$$

For this independent eigenvalue model, we have

Proposition 1. For ρ_S with compact support and any $\gamma > 0$, ρ_S -almost surely

$$\lim_{N \rightarrow \infty} \tilde{F}_N(\gamma) = \frac{\gamma}{4} \int x^2 \rho_S(x) dx - \mathcal{J}[\rho_{\sqrt{\gamma}S}, \rho_{\sqrt{\gamma}S} \boxplus \rho_{sc}]. \quad (24)$$

Proof. We start from the partition function (22),

$$\begin{aligned} \tilde{Z}(\tilde{Y}) &= \int d\mathbf{X} e^{\frac{\gamma}{2} \text{Tr}[\sqrt{\gamma} \mathbf{X} \tilde{Y} - \frac{\gamma}{2} \mathbf{X}^2]} P_{\tilde{S}, N}(\mathbf{X}) \\ &= \int d\boldsymbol{\lambda} d\mu_N(\mathbf{U}) \prod_{i=1}^N \delta(\lambda_i - \lambda_i^0) e^{\frac{\gamma}{2} \text{Tr}[\sqrt{\gamma} \mathbf{U} \boldsymbol{\Lambda} \mathbf{U}^\top \tilde{Y} - \frac{\gamma}{2} \boldsymbol{\lambda}^2]} \\ &= e^{-\frac{\gamma}{4} \text{Tr} \boldsymbol{\Lambda}^0} \int d\mu_N(\mathbf{U}) e^{\frac{\gamma}{2} \text{Tr}[\sqrt{\gamma} \mathbf{U} \boldsymbol{\Lambda}^0 \mathbf{U}^\top \tilde{Y}]} \\ &= e^{-\frac{\gamma}{4} \text{Tr} \boldsymbol{\Lambda}^0} \mathcal{I}_N(\sqrt{\gamma} \boldsymbol{\Lambda}^0, \tilde{Y}) \end{aligned} \quad (25)$$

Recall that $\tilde{Y} = \sqrt{\gamma} \mathbf{U} \boldsymbol{\Lambda}^0 \mathbf{U}^\top + \tilde{\mathbf{Z}}$, so the free energy can be written as

$$\begin{aligned} \tilde{F}_N(\gamma) &= \mathbb{E}_{\tilde{Y}} \left[\frac{\gamma}{4N} \text{Tr} \boldsymbol{\Lambda}^0{}^2 - \mathcal{J}_N(\sqrt{\gamma} \boldsymbol{\Lambda}^0, \tilde{Y}) \right] \\ &= \frac{\gamma}{4N} \text{Tr} \boldsymbol{\Lambda}^0{}^2 - \mathbb{E}_{\mathbf{U}} \mathbb{E}_{\tilde{\mathbf{Z}}} \left[\mathcal{J}_N(\sqrt{\gamma} \boldsymbol{\Lambda}^0, \tilde{Y}) \right] \\ &= \frac{\gamma}{4N} \text{Tr} \boldsymbol{\Lambda}^0{}^2 - \mathbb{E}_{\mathbf{U}} \mathbb{E}_{\tilde{\mathbf{Z}}} \left[\mathcal{J}_N(\sqrt{\gamma} \boldsymbol{\Lambda}^0, \sqrt{\gamma} \mathbf{U} \boldsymbol{\Lambda}^0 \mathbf{U}^\top + \mathbf{U} \tilde{\mathbf{Z}} \mathbf{U}^\top) \right] \quad (\text{By rotational invariance of } \tilde{\mathbf{Z}}) \\ &= \frac{\gamma}{4N} \text{Tr} \boldsymbol{\Lambda}^0{}^2 - \mathbb{E}_{\mathbf{U}} \mathbb{E}_{\tilde{\mathbf{Z}}} \left[\mathcal{J}_N(\sqrt{\gamma} \boldsymbol{\Lambda}^0, \sqrt{\gamma} \boldsymbol{\Lambda}^0 + \tilde{\mathbf{Z}}) \right] \quad (\mathcal{J}_N \text{ is invariant under rotation by } \mathbf{U}) \\ &= \frac{\gamma}{4N} \text{Tr} \boldsymbol{\Lambda}^0{}^2 - \mathbb{E}_{\tilde{\mathbf{Z}}} \left[\mathcal{J}_N(\sqrt{\gamma} \boldsymbol{\Lambda}^0, \sqrt{\gamma} \boldsymbol{\Lambda}^0 + \tilde{\mathbf{Z}}) \right]. \end{aligned} \quad (26)$$

By the strong law of large numbers the first term in (26) converges to $\frac{\gamma}{4} \int x^2 \rho_S(x) dx$ almost surely. Finally proposition 1 follows from the lemma

Lemma A.1. For any $\gamma \in \mathbb{R}_+$, the sequence $\mathbb{E}_{\tilde{\mathbf{Z}}} \left[\mathcal{J}_N(\sqrt{\gamma} \boldsymbol{\Lambda}^0, \sqrt{\gamma} \boldsymbol{\Lambda}^0 + \tilde{\mathbf{Z}}) \right]$ converges to $\mathcal{J}[\rho_{\sqrt{\gamma}S}, \rho_{\sqrt{\gamma}S} \boxplus \rho_{sc}]$ as $N \rightarrow \infty$, ρ_S -almost surely.

This lemma is based on an important result on the convergence of log-spherical integrals [43]. We refer to Appendix H.1 for the details. \square

A.2 Pseudo-Lipschitz continuity of the free energy

Consider any two rotationally invariant matrix ensembles $P_N^{(1)}, P_N^{(2)}$. Let $\mathbf{S} \sim P_N^{(1)}(\mathbf{S})$, $\tilde{\mathbf{S}} \sim P_N^{(2)}(\tilde{\mathbf{S}})$ with eigendecompositions $\mathbf{S} = \mathbf{U} \boldsymbol{\Lambda} \mathbf{U}^\top$, $\tilde{\mathbf{S}} = \tilde{\mathbf{U}} \tilde{\boldsymbol{\Lambda}} \tilde{\mathbf{U}}^\top$ and

$$dP_N^{(1)}(\mathbf{S}) = d\mu_N(\mathbf{U}) P_N^{(1)}(\boldsymbol{\lambda}) d\boldsymbol{\lambda}, \quad dP_N^{(2)}(\tilde{\mathbf{S}}) = d\mu_N(\tilde{\mathbf{U}}) P_N^{(2)}(\tilde{\boldsymbol{\lambda}}) d\tilde{\boldsymbol{\lambda}} \quad (27)$$

where $P_N^{(1)}(\boldsymbol{\lambda}), P_N^{(2)}(\tilde{\boldsymbol{\lambda}})$ are the joint probability density functions for the eigenvalues, induced by the priors. Now consider the two inference problems corresponding to reconstructing the signals from outputs of an AWGNC channel and define as before the corresponding free energies $F_N^{(1)}(\gamma), F_N^{(2)}(\gamma)$. Then we have

Proposition 2. For all $\gamma > 0$ and N

$$|F_N^{(1)}(\gamma) - F_N^{(2)}(\gamma)| \leq \frac{\gamma}{4N} \left(\sqrt{\mathbb{E}_{\boldsymbol{\lambda}} [\|\boldsymbol{\lambda}\|_2^2]} + \sqrt{\mathbb{E}_{\tilde{\boldsymbol{\lambda}}} [\|\tilde{\boldsymbol{\lambda}}\|_2^2]} \right) \sqrt{\mathbb{E}_{\boldsymbol{\lambda}, \tilde{\boldsymbol{\lambda}}} [\|\boldsymbol{\lambda} - \tilde{\boldsymbol{\lambda}}\|_2^2]}. \quad (28)$$

Proof. The proof is based on an interpolation between the two matrix ensembles. We refer to appendix H.2. \square

A.3 The distance between the original and independent eigenvalue models

Consider the original and independent eigenvalue models, in other words, the models with prior distributions

$$dP_{S,N}(\mathbf{S}) = d\mu_N(\mathbf{U}) P_{S,N}(\boldsymbol{\lambda}) d\boldsymbol{\lambda}^S, \quad dP_{\tilde{S},N}(\tilde{\mathbf{S}}) = d\mu_N(\mathbf{U}) \prod_{i=1}^N \delta(\tilde{\lambda}_i - \lambda_i^0) d\tilde{\boldsymbol{\lambda}} \quad (29)$$

where $P_{S,N}(\boldsymbol{\lambda})$ is the joint p.d.f. of eigenvalues of \mathbf{S} , and $\boldsymbol{\lambda}^0$ is generated with i.i.d. elements from ρ_S . Denote $\prod_{i=1}^N \delta(\tilde{\lambda}_i - \lambda_i^0)$ by $P_{\tilde{S},N}(\tilde{\boldsymbol{\lambda}})$.

Lemma A.2. *Under assumption 1 for $\boldsymbol{\lambda} \sim P_{S,N}(\boldsymbol{\lambda})$ and $\tilde{\boldsymbol{\lambda}} \sim P_{\tilde{S},N}(\tilde{\boldsymbol{\lambda}})$ we have*

$$\lim_{N \rightarrow \infty} \frac{1}{N} \mathbb{E}_{\boldsymbol{\lambda}, \tilde{\boldsymbol{\lambda}}} [\|\boldsymbol{\lambda} - \tilde{\boldsymbol{\lambda}}\|^2] = 0. \quad (30)$$

Proof. Since $P_{\tilde{S},N}(\tilde{\boldsymbol{\lambda}})$ is a delta distribution, we can write

$$\mathbb{E}_{\boldsymbol{\lambda}, \tilde{\boldsymbol{\lambda}}} [\|\boldsymbol{\lambda} - \tilde{\boldsymbol{\lambda}}\|^2] = \mathbb{E}_{\boldsymbol{\lambda}} [\|\boldsymbol{\lambda} - \boldsymbol{\lambda}^0\|^2]. \quad (31)$$

For a vector $\boldsymbol{\lambda}$, denote the empirical distribution of its components by $\hat{\mu}_{\boldsymbol{\lambda}}$. The Wasserstein-2 distance between two empirical distributions, $\hat{\mu}_{\boldsymbol{\lambda}}, \hat{\mu}_{\boldsymbol{\lambda}^0}$ is defined as

$$W_2(\hat{\mu}_{\boldsymbol{\lambda}}, \hat{\mu}_{\boldsymbol{\lambda}^0}) = \sqrt{\inf_{\gamma \in \Gamma(\hat{\mu}_{\boldsymbol{\lambda}}, \hat{\mu}_{\boldsymbol{\lambda}^0})} \mathbb{E}_{\gamma(x,y)} [(x-y)^2]}$$

with $\Gamma(\hat{\mu}_{\boldsymbol{\lambda}}, \hat{\mu}_{\boldsymbol{\lambda}^0})$ the set of couplings of $(\hat{\mu}_{\boldsymbol{\lambda}}, \hat{\mu}_{\boldsymbol{\lambda}^0})$. By lemma H.5 in Appendix H.3, we have

$$W_2(\hat{\mu}_{\boldsymbol{\lambda}}, \hat{\mu}_{\boldsymbol{\lambda}^0}) = \sqrt{\min_{\pi \in \mathcal{S}_N} \frac{1}{N} \|\boldsymbol{\lambda} - \boldsymbol{\lambda}_{\pi}^0\|^2}$$

where $\boldsymbol{\lambda}_{\pi}^0$ is the permuted version of $\boldsymbol{\lambda}^0$, and \mathcal{S}_N is the group of all permutations of N elements. So, for given $\boldsymbol{\lambda}$ and $\boldsymbol{\lambda}^0$ (which have a non-decreasing order), we have (considering the identity permutation)

$$\|\boldsymbol{\lambda} - \boldsymbol{\lambda}^0\|^2 \geq N W_2(\hat{\mu}_{\boldsymbol{\lambda}}, \hat{\mu}_{\boldsymbol{\lambda}^0})^2. \quad (32)$$

Now we recall the *rearrangement inequality*: for real numbers $x_1 \leq x_2 \leq \dots \leq x_n, y_1 \leq y_2 \leq \dots \leq y_n$, for every permutation $\pi \in \mathcal{S}_N$ we have [59]

$$x_n y_1 + \dots + x_1 y_n \leq x_{\pi(1)} y_1 + \dots + x_{\pi(n)} y_n \leq x_1 y_1 + \dots + x_n y_n.$$

For any permutation of $\boldsymbol{\lambda}^0$ (in particular the one which achieves the minimum in (32)), using the rearrangement inequality, we get (recall that $\boldsymbol{\lambda}^0$ is ordered in non-decreasing order)

$$\begin{aligned} \|\boldsymbol{\lambda} - \boldsymbol{\lambda}_{\pi}^0\|^2 &= \|\boldsymbol{\lambda}\|^2 + \|\boldsymbol{\lambda}_{\pi}^0\|^2 - 2\boldsymbol{\lambda}^{\top} \boldsymbol{\lambda}_{\pi}^0 \\ &\geq \|\boldsymbol{\lambda}\|^2 + \|\boldsymbol{\lambda}^0\|^2 - 2\boldsymbol{\lambda}^{\top} \boldsymbol{\lambda}^0 \\ &= \|\boldsymbol{\lambda} - \boldsymbol{\lambda}^0\|^2 \end{aligned}$$

and consequently

$$\|\boldsymbol{\lambda} - \boldsymbol{\lambda}^0\|^2 \leq N W_2(\hat{\mu}_{\boldsymbol{\lambda}}, \hat{\mu}_{\boldsymbol{\lambda}^0})^2. \quad (33)$$

Finally from (31), (32), (33), we obtain

$$\mathbb{E}_{\boldsymbol{\lambda}, \tilde{\boldsymbol{\lambda}}} [\|\boldsymbol{\lambda} - \tilde{\boldsymbol{\lambda}}\|^2] = \mathbb{E}_{\boldsymbol{\lambda}} [N W_2(\hat{\mu}_{\boldsymbol{\lambda}}, \hat{\mu}_{\boldsymbol{\lambda}^0})^2]. \quad (34)$$

Lemma H.6 in Appendix H.3 allows to conclude the proof. \square

A.4 Proof of theorem 1

By proposition 2, the free energies $F_N(\gamma)$ (defined in (18)) and $\tilde{F}_N(\gamma)$ (defined in (23)), satisfy

$$|F_N^{(1)}(\gamma) - F_N^{(2)}(\gamma)| \leq \frac{\gamma}{4N} \left(\sqrt{\mathbb{E}_{\boldsymbol{\lambda}} [\|\boldsymbol{\lambda}\|^2]} + \sqrt{\mathbb{E}_{\tilde{\boldsymbol{\lambda}}} [\|\tilde{\boldsymbol{\lambda}}\|^2]} \right) \sqrt{\mathbb{E}_{\boldsymbol{\lambda}, \tilde{\boldsymbol{\lambda}}} [\|\boldsymbol{\lambda} - \tilde{\boldsymbol{\lambda}}\|^2]}. \quad (35)$$

The term $\frac{1}{N} \|\boldsymbol{\lambda}\|^2 = \frac{1}{N} \sum \lambda_i^2$ is the second moment of the empirical spectral distribution of \mathbf{S} , which is almost surely bounded by assumption 1.B. So, $\frac{1}{N} \mathbb{E}_{\boldsymbol{\lambda}} [\|\boldsymbol{\lambda}\|^2]$ is bounded uniformly in N . Moreover, $\frac{1}{N} \mathbb{E} [\|\tilde{\boldsymbol{\lambda}}\|^2] = \frac{1}{N} \sum \lambda_i^0{}^2$ is also bounded uniformly in N . By lemma A.2, $\lim_{N \rightarrow \infty} \frac{1}{N} \mathbb{E}_{\boldsymbol{\lambda}, \tilde{\boldsymbol{\lambda}}} [\|\boldsymbol{\lambda} - \tilde{\boldsymbol{\lambda}}\|^2] = 0$. Therefore

$$\lim_{N \rightarrow \infty} |F_N(\gamma) - \tilde{F}_N(\gamma)| = 0. \quad (36)$$

Proposition 1 together with (36) conclude the proof. \square

B Proof of Theorem 2 and rotation invariance of the MMSE estimator

In this section we show how to use the RIE class in order to prove Theorem 2 under the extra assumption 1.B. Recall that an estimator $\hat{\Xi}(\mathbf{Y})$ is called *rotation invariant* if for any orthogonal matrix $\mathbf{O}\hat{\Xi}(\mathbf{Y})\mathbf{O}^\top = \hat{\Xi}(\mathbf{O}\mathbf{Y}\mathbf{O}^\top)$. Such an estimator has the same eigenvectors as the matrix \mathbf{Y} and denoting the eigenvectors of \mathbf{Y} by $\mathbf{y}_1, \dots, \mathbf{y}_N$, it can be expressed as $\hat{\Xi}(\mathbf{Y}) = \sum_{i=1}^N \hat{\xi}_i \mathbf{y}_i \mathbf{y}_i^\top$ where $\hat{\xi}_1, \dots, \hat{\xi}_N$ are the eigenvalues of the estimator. The best RIE estimator corresponds to eigenvalues chosen to minimize the mean-square-error in the RIE class and a heuristic calculation using the replica method leads to

$$\begin{cases} \hat{\Xi}^*(\mathbf{Y}) = \sum_{i=1}^N \xi_i^* \mathbf{y}_i \mathbf{y}_i^\top \\ \xi_i^* = \sum_{j=1}^N \lambda_j^S (\mathbf{s}_j^\top \mathbf{y}_i)^2 = \frac{1}{\sqrt{\gamma}} (\lambda_i^Y - 2\pi \mathbf{H}[\rho_Y](\lambda_i^Y)) \end{cases} \quad (37)$$

where $(\lambda_i^Y)_{1 \leq i \leq N}$ are the eigenvalues of \mathbf{Y} , and $\mathbf{H}[\rho_Y]$ is the *Hilbert transform* of the limiting spectral distribution of \mathbf{Y} defined as:

$$\mathbf{H}[\rho_Y](z) := \text{PV} \frac{1}{\pi} \int \frac{\rho_Y(x)}{z-x} dx. \quad (38)$$

We will need the following properties of the Hilbert transform. A proof can be found in lemma 3.1 of [60].

Lemma B.1. *If $f : \mathbb{R} \rightarrow \mathbb{R}$ is compactly supported and sufficiently regular, then one has the identities*

$$\int_{\mathbb{R}} f(x) (\mathbf{H}[f](x))^2 dx = \frac{1}{3} \int_{\mathbb{R}} f^3(x) dx, \quad (39)$$

$$\int_{\mathbb{R}} \mathbf{H}[f](x) x f(x) dx = \frac{1}{2\pi} \left(\int_{\mathbb{R}} f(x) dx \right)^2. \quad (40)$$

Proof of theorem 2. As explained in the main text the best RIE estimator is optimal in the sense $\text{MMSE}_N(\gamma) = \text{MMSE}_{\text{RIE},N}(\gamma)$ so our proof proceeds by a computation of the limit of the r.h.s (the optimality follows from rotation invariance of the MMSE estimator $\mathbb{E}(\mathbf{S}|\mathbf{Y})$ and this rotation invariance is checked later for completeness). From assumption 2, it suffices to compute the limit of $\frac{1}{N} \mathbb{E} \|\mathbf{S} - \hat{\Xi}^*(\mathbf{Y})\|^2$. Denoting the eigenvectors of \mathbf{S} by $\mathbf{s}_1, \dots, \mathbf{s}_N$. Expanding the MSE, we find

$$\|\mathbf{S} - \hat{\Xi}^*(\mathbf{Y})\|_F^2 = \sum_{i=1}^N \left[\lambda_i^{S^2} + \xi_i^{*2} - 2\xi_i^* \sum_{j=1}^N \lambda_j^S (\mathbf{s}_j^\top \mathbf{y}_i)^2 \right] = \sum_{i=1}^N (\lambda_i^{S^2} - \xi_i^{*2}) \quad (41)$$

where we used (37) to get the last equality. Using again (37) we have

$$\begin{aligned} \|\mathbf{S} - \hat{\Xi}^*(\mathbf{Y})\|_F^2 &= \sum_{i=1}^N (\lambda_i^{S^2} - \xi_i^{*2}) \\ &= \sum_{i=1}^N \lambda_i^{S^2} - \frac{1}{\gamma} (\lambda_i^Y - 2\pi \mathbf{H}[\rho_Y](\lambda_i^Y))^2 \\ &= \sum_{i=1}^N \lambda_i^{S^2} - \frac{1}{\gamma} \sum_{i=1}^N \lambda_i^{Y^2} - \frac{4\pi^2}{\gamma} \sum_{i=1}^N (\mathbf{H}[\rho_Y](\lambda_i^Y))^2 + \frac{4\pi}{\gamma} \sum_{i=1}^N \mathbf{H}[\rho_Y](\lambda_i^Y) \lambda_i^Y \end{aligned} \quad (42)$$

From linearity of expectation and, as the Hilbert transform $\mathbf{H}[\rho_Y]$ is continuous on the support of ρ_Y [45], we find

$$\begin{aligned} \lim_{N \rightarrow \infty} \frac{1}{N} \mathbb{E} \|\mathbf{S} - \hat{\Xi}^*(\mathbf{Y})\|_F^2 &= \int x^2 \rho_S(x) dx - \frac{1}{\gamma} \int x^2 \rho_Y(x) dx - \frac{4\pi^2}{\gamma} \int \rho_Y(x) (\mathbf{H}[\rho_Y](x))^2 dx \\ &\quad + \frac{4\pi}{\gamma} \int \mathbf{H}[\rho_Y](x) x \rho_Y(x) dx \end{aligned} \quad (43)$$

By the independence of \mathbf{S} and \mathbf{Z} , we have:

$$\begin{aligned} \int x^2 \rho_Y(x) dx &= \lim_{N \rightarrow \infty} \frac{1}{N} \mathbb{E} \text{Tr} \mathbf{Y}^2 \\ &= \lim_{N \rightarrow \infty} \frac{1}{N} \gamma \mathbb{E} \text{Tr} \mathbf{S}^2 + \lim_{N \rightarrow \infty} \frac{1}{N} \text{Tr} \mathbf{Z}^2 + \lim_{N \rightarrow \infty} \frac{2}{N} \mathbb{E} \text{Tr} \mathbf{S} \mathbf{Z} \end{aligned}$$

$$= \gamma \int x^2 \rho_S(x) dx + 1 \quad (44)$$

Finally, using the identities in lemma B.1, we get

$$\lim_{N \rightarrow \infty} \frac{1}{N} \mathbb{E} \|\mathbf{S} - \hat{\mathbf{S}}\|_F^2 = -\frac{1}{\gamma} - \frac{4\pi^2}{3\gamma} \int \rho_Y^3(x) dx + \frac{2}{\gamma} = \frac{1}{\gamma} \left(1 - \frac{4\pi^2}{3} \int \rho_Y^3(x) dx \right). \quad (45)$$

□

For completeness we provide a check that the MMSE estimator belongs to the RIE class. The posterior mean given \mathbf{Y} is

$$\mathbb{E}[\mathbf{S}|\mathbf{Y}] = \frac{\int d\mathbf{X} P_{S,N}(\mathbf{X}) \mathbf{X} e^{-\frac{N}{4} \|\mathbf{Y} - \sqrt{\gamma} \mathbf{X}\|_F^2}}{\int d\mathbf{X} P_{S,N}(\mathbf{X}) e^{-\frac{N}{4} \|\mathbf{Y} - \sqrt{\gamma} \mathbf{X}\|_F^2}}. \quad (46)$$

By rotation invariance of $P_{S,N}(\mathbf{X})$ under any orthogonal transformation $\mathbf{X} \rightarrow \mathbf{O}\mathbf{X}\mathbf{O}^\top$ with Jacobian $|\det \mathbf{O}| = 1$ we have

$$\begin{aligned} \mathbb{E}[\mathbf{S}|\mathbf{O}\mathbf{Y}\mathbf{O}^\top] &= \frac{\int d\mathbf{X} P_{S,N}(\mathbf{X}) \mathbf{X} e^{-\frac{N}{4} \|\mathbf{O}\mathbf{Y}\mathbf{O}^\top - \sqrt{\gamma} \mathbf{X}\|_F^2}}{\int d\mathbf{X} P_{S,N}(\mathbf{X}) e^{-\frac{N}{4} \|\mathbf{O}\mathbf{Y}\mathbf{O}^\top - \sqrt{\gamma} \mathbf{X}\|_F^2}} \\ &= \frac{\int d\mathbf{X} P_{S,N}(\mathbf{X}) \mathbf{O}\mathbf{X}\mathbf{O}^\top e^{-\frac{N}{4} \|\mathbf{O}\mathbf{Y}\mathbf{O}^\top - \sqrt{\gamma} \mathbf{O}\mathbf{X}\mathbf{O}^\top\|_F^2}}{\int d\mathbf{X} P_{S,N}(\mathbf{X}) e^{-\frac{N}{4} \|\mathbf{O}\mathbf{Y}\mathbf{O}^\top - \sqrt{\gamma} \mathbf{O}\mathbf{X}\mathbf{O}^\top\|_F^2}} \\ &= \mathbf{O} \left\{ \frac{\int d\mathbf{X} P_{S,N}(\mathbf{X}) \mathbf{X} e^{-\frac{N}{4} \|\mathbf{Y} - \sqrt{\gamma} \mathbf{X}\|_F^2}}{\int d\mathbf{X} P_{S,N}(\mathbf{X}) e^{-\frac{N}{4} \|\mathbf{Y} - \sqrt{\gamma} \mathbf{X}\|_F^2}} \right\} \mathbf{O}^\top \\ &= \mathbf{O} \mathbb{E}[\mathbf{S}|\mathbf{Y}] \mathbf{O}^\top. \end{aligned} \quad (47)$$

Therefore the posterior mean estimator is an RIE.

C Proof of theorem 3: explicit expression of the mutual information

We derive an explicit expression for the asymptotic mutual information using the I-MMSE relation [25] and basic results in free probability. This derivation is completely independent of Theorem 1 in which the asymptotic mutual information is expressed using the asymptotic spherical integral, $\mathcal{J}[\rho_{\sqrt{\gamma}S}, \rho_{\sqrt{\gamma}S} \boxplus \rho_{\text{sc}}]$.

Proof of Theorem 3. An important property of the Gaussian channel is the I-MMSE relation relating the MMSE to the derivative of the mutual information w.r.t the SNR. The concavity of the mutual information w.r.t. SNR, implies that this relation also holds in the limit $N \rightarrow \infty$. Integrating this relation we have

$$I(\mathbf{S}; \mathbf{Y}) = \frac{1}{4} \int_0^\gamma \text{MMSE}(t) dt + \text{constant} \quad (48)$$

where $I(\mathbf{S}; \mathbf{Y}) := \lim_{N \rightarrow \infty} \frac{1}{N^2} I_N(\mathbf{S}; \mathbf{Y})$ and $\text{MMSE}(t) = \lim_{N \rightarrow +\infty} \text{MMSE}_N(t)$.

Since for $\gamma = 0$, $I(\mathbf{S}; \mathbf{Y}) = 0$ the integration constant vanishes. Therefore, we just need to compute the integral over the asymptotic MMSE given by Theorem 2. From results in free probability as explained in the main text

$$\text{MMSE}(\gamma) = \frac{1}{\gamma} \left(1 - \Phi(\sqrt{\gamma}S + Z) \right) \quad (49)$$

where S is a non-commutative random variable associated to the density ρ_S , and a semi-circular non-commutative

variable Z free from S . Thus

$$\begin{aligned}
I(\mathbf{S}; \mathbf{Y}) &= \frac{1}{4} \int_0^\gamma \left(\frac{1}{t} - \frac{1}{t} \Phi(\sqrt{t}S + Z) \right) dt \\
&= \frac{1}{4} \int_0^\gamma \left(\frac{1}{t} - \frac{1}{t^2} \Phi\left(S + \sqrt{\frac{1}{t}}Z\right) \right) dt \\
&= \frac{1}{4} \int_{\frac{1}{\gamma}}^\infty \left(\frac{1}{x} - \Phi\left(S + \sqrt{x}Z\right) \right) dx \quad \left(\frac{1}{t} \rightarrow x\right) \\
&= \frac{1}{4} \int_{\frac{1}{\gamma}}^\infty \left(\frac{1}{x} - \gamma \Phi(\sqrt{\gamma}S + \sqrt{\gamma x}Z) \right) dx \quad \left(\Phi(aX) = \frac{1}{a^2} \Phi(X) \text{ for } a > 0\right) \\
&= \frac{1}{4} \int_1^\infty \left(\frac{1}{y} - \Phi(\sqrt{\gamma}S + \sqrt{y}Z) \right) dy \quad (\gamma x \rightarrow y) \\
&= \frac{1}{4} \int_0^\infty \left(\frac{1}{t+1} - \Phi(\sqrt{\gamma}S + \sqrt{t+1}Z) \right) dt \quad (y \rightarrow t+1) \\
&= \frac{1}{4} \int_0^\infty \left(\frac{1}{t+1} - \Phi(\sqrt{\gamma}S + Z_0 + \sqrt{t}Z) \right) dt \quad (Z \text{ and } Z_0 \text{ free semi-circulars}) \\
&= \frac{1}{2} \chi(\sqrt{\gamma}S + Z_0) - \frac{1}{4} \ln 2\pi - \frac{1}{4} \quad (\text{from Eq. [14] in the main part of the paper})
\end{aligned} \tag{50}$$

Therefore, we obtain

$$\lim_{N \rightarrow \infty} \frac{1}{N^2} I_N(\mathbf{S}; \mathbf{Y}) = \frac{1}{2} \iint \ln |s - t| \rho_Y(s) \rho_Y(t) ds dt + \frac{1}{8} \tag{51}$$

where $\rho_Y = \rho_{\sqrt{\gamma}S} \boxplus \rho_{sc}$. □

D Discussion of models with rotation invariant noise

Suppose that the noise matrix \mathbf{Z} in our basic model is the realization of a rotation invariant ensemble. While we are not quite able to treat this case, we can generalize Theorem 3 to the setting $\mathbf{Y}_\epsilon = \sqrt{\gamma}\mathbf{S} + \mathbf{Z}_\epsilon$ where $\mathbf{Z}_\epsilon = \mathbf{Z} + \sqrt{\epsilon}\boldsymbol{\zeta}$ with $\boldsymbol{\zeta}$ from the Gaussian Wigner ensemble, and $\epsilon > 0$ (so the noise is non-Gaussian rotation invariant). We call this model the *Additive Rotation Invariant Noise* (ARIN) model.

Proposition 3 (Explicit Mutual Information for the ARIN model). *Assume that the conditions in assumption 1 hold for both \mathbf{S} and \mathbf{Z} . Then, we have for the ARIN model:*

$$\frac{I_N(\mathbf{S}; \mathbf{Y}_\epsilon)}{N^2} \xrightarrow{N \rightarrow \infty} \frac{1}{2} \iint \ln |s - t| \rho_{Y_\epsilon}(s) \rho_{Y_\epsilon}(t) ds dt - \frac{1}{2} \iint \ln |s - t| \rho_{Z_\epsilon}(s) \rho_{Z_\epsilon}(t) ds dt. \tag{52}$$

The proof leverages only on the simple formula for the mutual information for Gaussian noise in theorem 3, and does not really hinge on assumption 2 (in main text). Finally we would like to take the limit $\epsilon \rightarrow 0$. This however is a subtle problem which would require more specific hypothesis on the rotation invariant ensemble of \mathbf{Z} . For example it is quite apparent that one would need the existence of a density for the limiting empirical measures ρ_Z and ρ_{Y_0} . Moreover, this also requires an argument to permute the limits $N \rightarrow +\infty$ and $\epsilon \rightarrow 0$.

Proof. Set $\mathbf{X} = \sqrt{\gamma}\mathbf{S} + \mathbf{Z}$. We have the information theoretic equalities (\mathcal{H}_N are Shannon entropies)

$$\begin{aligned}
I_N(\mathbf{Y}_\epsilon; \mathbf{S}) &= \mathcal{H}_N(\mathbf{Y}_\epsilon) - \mathcal{H}_N(\mathbf{Y}_\epsilon | \mathbf{S}) \\
&= \mathcal{H}_N(\mathbf{Y}_\epsilon) - \mathcal{H}_N(\mathbf{Z}_\epsilon) \\
&= [\mathcal{H}_N(\mathbf{Y}_\epsilon) - \mathcal{H}_N(\boldsymbol{\zeta})] - [\mathcal{H}_N(\mathbf{Z}_\epsilon) - \mathcal{H}_N(\boldsymbol{\zeta})] \\
&= [\mathcal{H}_N(\mathbf{Y}_\epsilon) - \mathcal{H}_N(\mathbf{Y}_\epsilon | \mathbf{X})] - [\mathcal{H}_N(\mathbf{Z}_\epsilon) - \mathcal{H}_N(\mathbf{Z}_\epsilon | \mathbf{Z})] \\
&= I_N(\mathbf{Y}_\epsilon; \mathbf{X}) - I_N(\mathbf{Z}_\epsilon; \mathbf{Z}).
\end{aligned} \tag{53}$$

The two mutual informations in the last line correspond to the inference models for two AWGN models with strength ϵ , namely $\mathbf{Y}_\epsilon = \mathbf{X} + \sqrt{\epsilon}\boldsymbol{\zeta}$ and $\mathbf{Z}_\epsilon = \mathbf{Z} + \sqrt{\epsilon}\boldsymbol{\zeta}$, and inputs from rotation invariant ensembles. By the formula in Theorem 2 which holds for these channels we obtain

$$\lim_{N \rightarrow +\infty} \frac{1}{N^2} I_N(\mathbf{Y}_\epsilon; \mathbf{S}) = \frac{1}{2} \iint \ln |s - t| \rho_{Y_\epsilon}(s) \rho_{Y_\epsilon}(t) ds dt - \frac{1}{2} \iint \ln |s - t| \rho_{Z_\epsilon}(s) \rho_{Z_\epsilon}(t) ds dt. \tag{54}$$

□

E Replica symmetric formula for sub-linear rank matrix factorization

In this section, we provide the heuristic approach based on the replica symmetric method from statistical physics to derive the mutual information and minimum mean-square error of sub-linear rank matrix factorization (Statement 4). In order to be self-contained, we first recall the definition of the model.

The ground-truth matrix signal $\mathbf{X} = (X_{ik}) \in \mathbb{R}^{N \times M}$ with $M = \lfloor N^\alpha \rfloor$ is generated from a prior distribution assumed to be fully factorized

$$P_{X,N}(\mathbf{X}) = \prod_{i \leq N} \prod_{k \leq M} p_X(X_{ik}) \quad (55)$$

for a law p_X with finite variance, symmetric $p_X(x) = p_X(-x)$ and hence centered $\int dp_X(x)x = 0$. Let $\mathbf{Z} = \mathbf{Z}^\top \in \mathbb{R}^{N \times N}$ a noise Wigner matrix with p.d.f.

$$P_{Z,N}(\mathbf{Z}) \propto \exp\left(-\frac{1}{4}\text{Tr}\mathbf{Z}^2\right).$$

Note the scaling here which corresponds to eigenvalues of order $O(\sqrt{N})$ for \mathbf{Z} . The symmetric data matrix $\mathbf{Y} = (Y_{ij}) \in \mathbb{R}^{N \times N}$ has entries generated through the following observation channel

$$\mathbf{Y} = \sqrt{\frac{\gamma}{N}} \mathbf{X} \mathbf{X}^\top + \mathbf{Z}. \quad (56)$$

Matrix $\sqrt{\frac{\gamma}{N}} \mathbf{X} \mathbf{X}^\top$ has $O(\sqrt{N})$ eigenvalues like the noise (and generically $O(1)$ entries), hence the scaling $\sqrt{\frac{\gamma}{N}}$ of the signal-to-noise ratio. After basic simplifications the Bayesian posterior reads

$$dP_{X|Y,N}(\mathbf{x} | \mathbf{Y}) = \frac{1}{\mathcal{Z}(\mathbf{Y})} dP_{X,N}(\mathbf{x}) \exp \frac{1}{2} \text{Tr} \left(\sqrt{\frac{\gamma}{N}} \mathbf{Y} \mathbf{x} \mathbf{x}^\top - \frac{\gamma}{2N} (\mathbf{x} \mathbf{x}^\top)^2 \right).$$

The mutual information $I(\mathbf{Y}; \mathbf{X})$, which we aim at computing, is

$$I(\mathbf{Y}; \mathbf{X}) = -\mathbb{E} \ln \int dP_{X,N}(\mathbf{x}) \exp \frac{1}{2} \text{Tr} \left(\sqrt{\frac{\gamma}{N}} \mathbf{Y} \mathbf{x} \mathbf{x}^\top - \frac{\gamma}{2N} (\mathbf{x} \mathbf{x}^\top)^2 \right) + \frac{\gamma}{4N} \mathbb{E} \text{Tr}(\mathbf{X} \mathbf{X}^\top)^2$$

where the first term is minus the expected free entropy defined as

$$\mathbb{E} f_N := \frac{1}{MN} \mathbb{E} \ln \mathcal{Z}(\mathbf{Y}).$$

It is useful to note that model (56) is equivalent to

$$\begin{cases} Y_{ij} \sim \mathcal{N}(\sqrt{\frac{\gamma}{N}} \langle \mathbf{X}_i, \mathbf{X}_j \rangle, 1) & \text{for } i < j \in [N]^2, \\ Y_{ii} \sim \mathcal{N}(\sqrt{\frac{\gamma}{N}} \|\mathbf{X}_i\|^2, 2) & \text{for } i \in [N]. \end{cases}$$

The average free entropy then concretely reads

$$\begin{aligned} \mathbb{E} f_N &= \frac{1}{NM} \mathbb{E} \ln \int dP_{X,N}(\mathbf{x}) \exp \frac{1}{2} \sum_{i \leq N} \left(\sqrt{\frac{\gamma}{N}} Y_{ii} \|\mathbf{x}_i\|^2 - \frac{\gamma}{2N} \|\mathbf{x}_i\|^4 \right) \\ &\quad \times \exp \sum_{i < j}^{1,N} \left(\sqrt{\frac{\gamma}{N}} Y_{ij} \langle \mathbf{x}_i, \mathbf{x}_j \rangle - \frac{\gamma}{2N} \langle \mathbf{x}_i, \mathbf{x}_j \rangle^2 \right). \end{aligned} \quad (57)$$

E.1 Replica method: first steps

The approach starts from the replica trick:

$$\lim_{N \rightarrow +\infty} \mathbb{E} f_N = \lim_{N \rightarrow +\infty} \lim_{u \rightarrow 0_+} \frac{1}{NMu} \ln \mathbb{E} \mathcal{Z}(\mathbf{Y})^u = \lim_{u \rightarrow 0_+} \lim_{N \rightarrow +\infty} \frac{1}{NMu} \ln \mathbb{E} \mathcal{Z}(\mathbf{Y})^u. \quad (58)$$

As it is standard in the replica method, we assume that the u and N limits commute, and that the formulas derived for integer u can be "analytically continued" to real $u \rightarrow 0_+$. We therefore evaluate the expectation $\mathbb{E} \mathcal{Z}(\mathbf{Y})^u$ of the

replicated partition function for integer u . We directly integrate the quenched Gaussian observations in (57) using the following useful formula:

$$Y \sim \mathcal{N}\left(\sqrt{\frac{\gamma}{N}}f_0, t\right) \Rightarrow \mathbb{E}_{Y|f_0} \prod_{a \leq u} \exp \frac{1}{t} \left(\sqrt{\frac{\gamma}{N}} Y f_a - \frac{\gamma}{2N} f_a^2 \right) = \prod_{a < b}^{0,u} \exp \frac{\gamma}{tN} f_a f_b. \quad (59)$$

In the Bayes-optimal setting the ground-truth \mathbf{X} plays the role of one additional replica, so we rename it $\mathbf{x}^0 := \mathbf{X}$. We set $\mathbf{x}_i^a = (x_{ik}^a)_{k \leq M} \in \mathbb{R}^M$ and introduce the notation

$$\int dP_{X,N}(\{\mathbf{x}\}_0^u) \cdots := \int_{\mathbb{R}^{MN(u+1)}} \prod_{a=0}^u \prod_{i \leq N} \prod_{k \leq M} dp_{X,N}(x_{ik}^a) \cdots$$

For replica indices $0 \leq a < b \leq u$, define the $M \times M$ overlap matrices

$$\mathbf{Q}^{ab} := \left(\frac{1}{N} \sum_{i \leq N} x_{ik}^a x_{i\ell}^b \right)_{k, \ell \leq M} = \frac{1}{N} (\mathbf{x}^a)^\top \mathbf{x}^b = (\mathbf{Q}^{ba})^\top. \quad (60)$$

Then the above formula (59) yields

$$\begin{aligned} \mathbb{E} \mathcal{Z}(\mathbf{Y})^u &= \int dP_{X,N}(\{\mathbf{x}\}_0^u) \prod_{a < b}^{0,u} \exp \left(\frac{\gamma}{2N} \sum_{i \leq N} \|\mathbf{x}_i^a\|^2 \|\mathbf{x}_i^b\|^2 + \frac{\gamma}{N} \sum_{i < j}^{1,N} \langle \mathbf{x}_i^a, \mathbf{x}_j^a \rangle \langle \mathbf{x}_i^b, \mathbf{x}_j^b \rangle \right) \\ &= \int dP_{X,N}(\{\mathbf{x}\}_0^u) \prod_{a < b}^{0,u} \exp \frac{\gamma}{2} N \sum_{k, \ell \leq M} \left(\frac{1}{N} \sum_{i \leq N} x_{ik}^a x_{i\ell}^b \right)^2 \\ &= \int dP_{X,N}(\{\mathbf{x}\}_0^u) \prod_{a < b}^{0,u} \exp \frac{\gamma}{2} N \text{Tr} \mathbf{Q}^{ab} (\mathbf{Q}^{ab})^\top. \end{aligned} \quad (61)$$

We introduce Dirac delta functions and their Fourier representation in order to linearize the above quadratic term in the overlaps (and thus quartic in the replicas (\mathbf{x}^a))

$$\begin{aligned} \mathbb{E} \mathcal{Z}(\mathbf{Y})^u &= \int dP_{X,N}(\{\mathbf{x}\}_0^u) \prod_{a < b}^{0,u} d\mathbf{Q}^{ab} \delta((\mathbf{x}^a)^\top \mathbf{x}^b - N\mathbf{Q}^{ab}) \exp \frac{\gamma}{2} N \text{Tr} \mathbf{Q}^{ab} (\mathbf{Q}^{ab})^\top \\ &= \int dP_{X,N}(\{\mathbf{x}\}_0^u) \prod_{a < b}^{0,u} d\mathbf{Q}^{ab} d\mathbf{R}^{ab} \exp \text{Tr} \left((\mathbf{R}^{ab})^\top (\mathbf{x}^a)^\top \mathbf{x}^b - N(\mathbf{R}^{ab})^\top \mathbf{Q}^{ab} + \frac{\gamma}{2} N \mathbf{Q}^{ab} (\mathbf{Q}^{ab})^\top \right). \end{aligned}$$

In this expression we used the notations $d\mathbf{Q}^{ab} = \prod_{k, \ell \leq M} dQ_{k\ell}^{ab}$ and similarly for $d\mathbf{R}^{ab}$. We have

$$\text{Tr}(\mathbf{R}^{ab})^\top (\mathbf{x}^a)^\top \mathbf{x}^b = \sum_{i \leq N} \sum_{k, \ell \leq M} R_{k\ell}^{ab} x_{ik}^a x_{i\ell}^b.$$

This implies that the integral can be re-written as

$$\begin{aligned} \mathbb{E} \mathcal{Z}(\mathbf{Y})^u &= \int \prod_{a < b}^{0,u} d\mathbf{Q}^{ab} d\mathbf{R}^{ab} \exp N \text{Tr} \left(-(\mathbf{R}^{ab})^\top \mathbf{Q}^{ab} + \frac{\gamma}{2} \mathbf{Q}^{ab} (\mathbf{Q}^{ab})^\top \right) \\ &\quad \times \prod_{i \leq N} \int \prod_{a=0}^u \prod_{k \leq M} dp_X(x_{ik}^a) \exp \sum_{a < b}^{0,u} \sum_{k, \ell \leq M} R_{k\ell}^{ab} x_{ik}^a x_{i\ell}^b \\ &= \int \prod_{a < b}^{0,u} d\mathbf{Q}^{ab} d\mathbf{R}^{ab} \exp N \text{Tr} \left(-(\mathbf{R}^{ab})^\top \mathbf{Q}^{ab} + \frac{\gamma}{2} \mathbf{Q}^{ab} (\mathbf{Q}^{ab})^\top \right) \\ &\quad \times \exp N \ln \int \prod_{a=0}^u dP_X(\mathbf{y}^a) \exp \sum_{a < b}^{0,u} (\mathbf{y}^a)^\top \mathbf{R}^{ab} \mathbf{y}^b \end{aligned} \quad (62)$$

where $\mathbf{y}^a = (y_k^a)_{k \leq M} \in \mathbb{R}^M$ and $dP_X(\mathbf{y}^a) = \prod_{k \leq M} dp_X(y_k^a)$. The factorization of the above integral over $i \leq N$ is the first key mechanism.

We will use the singular value decompositions (SVDs)

$$Q^{ab} = A^{ab} \sigma^{ab} (B^{ab})^\top, \quad R^{ab} = C^{ab} \tau^{ab} (D^{ab})^\top,$$

where $(A^{ab}, B^{ab}, C^{ab}, D^{ab})$ are orthogonal matrices of singular vectors, and (σ^{ab}, τ^{ab}) are positive semi-definite diagonal matrices of singular values. All matrices are of size $M \times M$. For diagonal matrices we simply index their non-zero entries with a single index. We also introduce the Vandermonde determinant

$$\Delta(\sigma) := \prod_{k < \ell} (\sigma_k - \sigma_\ell)$$

and the Haar measure μ_M over the orthogonal group of orthogonal $M \times M$ matrices. Vandermonde determinants appear as Jacobians when introducing the SVDs. Thus

$$\begin{aligned} \mathbb{E}Z(\mathbf{Y})^u &= \int \prod_{a < b}^{0,u} d\sigma^{ab} d\tau^{ab} |\Delta((\sigma^{ab})^2) \Delta((\tau^{ab})^2)| \exp N \frac{\gamma}{2} \text{Tr}(\sigma^{ab})^2 \\ &\quad \times \int \prod_{a < b}^{0,u} d\mu_M(C^{ab}) d\mu_M(D^{ab}) \exp N \ln \int \prod_{a=0}^u dP_X(\mathbf{y}^a) \exp \sum_{a < b}^{0,u} (\mathbf{y}^a)^\top C^{ab} \tau^{ab} (D^{ab})^\top \mathbf{y}^b \\ &\quad \times \int \prod_{a < b}^{0,u} d\mu_M(A^{ab}) d\mu_M(B^{ab}) \exp N \text{Tr}(-D^{ab} \tau^{ab} (C^{ab})^\top A^{ab} \sigma^{ab} (B^{ab})^\top). \end{aligned} \quad (63)$$

The singular values $(\sigma_k^{ab})_{k \leq M}$ and $(\tau_k^{ab})_{k \leq M}$ are considered ordered in decreasing order

$$\sigma_1^{ab} \geq \sigma_2^{ab} \geq \dots \geq \sigma_M^{ab}, \quad \tau_1^{ab} \geq \tau_2^{ab} \geq \dots \geq \tau_M^{ab},$$

and the integration over these variables takes that ordering into account (their permutations are taken into account by the integration over the singular vectors). The second key mechanism is the fact that we can absorb the singular vectors of R^{ab} into those of Q^{ab} in the last line of (63) when integrating $(A^{ab}, B^{ab})_{a < b}$: we change $(B^{ab})^\top D^{ab} \rightarrow (B^{ab})^\top$ and $(C^{ab})^\top A^{ab} \rightarrow A^{ab}$; these transformations have unit Jacobian. This decouples the integration over the orthogonal matrices in the second and last lines.

E.2 Integration over the orthogonal group by saddle point

In this section we are going to evaluate certain integrals by saddle point and Laplace methods. In spin glass models, when doing so, it may happen that due to the replica limit $u \rightarrow 0_+$, instead of maximizing the exponent, one must minimize it; see, e.g., [54, 61]. This, however, does not happen in the present setting due to the Bayes-optimality which implies that the model lies on its Nishimori line [62]. Therefore, we will follow the ‘‘normal’’ recipes of saddle point and Laplace methods even in the limit $u \rightarrow 0_+$.

We argue that, in the regime $M = \lfloor N^\alpha \rfloor$, $\alpha \in (0, 1)$, the last two terms in (63) can be integrated out by the saddle point method. Indeed, in both terms the exponent is $\Theta(NM) = \Theta(N^{1+\alpha})$ while the number of degrees of freedom over which we integrate is much smaller $\Theta(M^2) = \Theta(N^{2\alpha})$ (as long as $\alpha < 1$). Moreover, in this regime Gaussian fluctuations around the saddle points are sub-leading.

First saddle point

We start with the last term appearing in (63) corresponding to the rectangular spherical integral [63]

$$\begin{aligned} &\int d\mu_M(A^{ab}) d\mu_M(B^{ab}) \exp N \text{Tr}(-\tau^{ab} A^{ab} \sigma^{ab} (B^{ab})^\top) \\ &= C_M \exp(o(NM)) \sum_* \exp(-N \text{Tr} \tau^{ab} A_*^{ab} \sigma^{ab} (B_*^{ab})^\top) \end{aligned} \quad (64)$$

where the sum \sum_* is over all saddle points (A_*^{ab}, B_*^{ab}) and C_M is a volume factor coming from the normalization of the Haar measure. From now on C_M or C_N denotes a generic irrelevant constant that can change from place to place and that may include $\exp(o(NM))$ corrections. We focus on a given pair of replica indices (ab) so we drop this notation when there is no ambiguity. To find the saddle point equation we perturb the matrices (A, B) as $(A(I_M + \delta S), B(I_M + \delta T))$ for two generic anti-symmetric matrices $S^\top = -S$ and $T^\top = -T$ and a small δ . Then at a saddle point the first order variation in δ of $\text{Tr} \tau A \sigma B^\top$ under this perturbation must cancel, namely,

$$\left| \left(\frac{\partial}{\partial \delta} \text{Tr} \tau A(I_M + \delta S) \sigma(I_M - \delta T) B^\top \right)_{\delta=0} \right| = |\text{Tr} B^\top \tau A (S \sigma - \sigma T)| = 0. \quad (65)$$

This trace being zero means that, given $(\boldsymbol{\tau}, \boldsymbol{\sigma})$, the matrix $\mathbf{B}^\top \boldsymbol{\tau} \mathbf{A}$ lies in the orthogonal complement of $(\mathbf{S}\boldsymbol{\sigma} - \boldsymbol{\sigma}\mathbf{T})^\top$ under the Hilbert-Schmidt inner product $\text{Tr} \mathbf{X} \mathbf{Y}^\top$. As will see, the only way to find a solution is to look for symmetric saddle points belonging to the subspace of matrices verifying $\mathbf{B} = \mathbf{A}$; this is strongly suggested by the $\mathbf{A} \leftrightarrow \mathbf{B}$ symmetry of $\text{Tr} \boldsymbol{\tau} \mathbf{A} \boldsymbol{\sigma} \mathbf{B}^\top$. The argument goes as follows. Because $\boldsymbol{\sigma}$ is diagonal and \mathbf{S}, \mathbf{T} have zero diagonal (by antisymmetry), both $\mathbf{S}\boldsymbol{\sigma}$ and $\boldsymbol{\sigma}\mathbf{T}$ have zero entries on their diagonal as well. The orthogonal complement of the set of matrices with vanishing diagonal is the set of diagonal matrices. Therefore $\text{Tr} \mathbf{B}^\top \boldsymbol{\tau} \mathbf{A} (\mathbf{S}\boldsymbol{\sigma} - \boldsymbol{\sigma}\mathbf{T}) = 0$ if and only if $\mathbf{B}^\top \boldsymbol{\tau} \mathbf{A}$ is diagonal. This is possible only if $\mathbf{A} = \mathbf{B}$ is a (possibly signed) permutation matrix (because $\boldsymbol{\tau}$ is already diagonal and the set of signed permutation matrices is the normalizer of the diagonal matrices in the group of orthogonal matrices). So for any perturbation (\mathbf{S}, \mathbf{T}) and choice of $(\boldsymbol{\sigma}, \boldsymbol{\tau})$, if $\mathbf{A} = \mathbf{B}$ belongs to the set

$$\Pi_M := \{\boldsymbol{\pi} : \boldsymbol{\pi} \text{ is a } M \times M \text{ permutation matrix with signed non-zero entries}\},$$

then the first order variation around $\mathbf{A} = \mathbf{B}$ cancels. This means that the set of saddle points is Π_M . Denoting

$$\boldsymbol{\pi}(\boldsymbol{\sigma}) := \boldsymbol{\pi} \boldsymbol{\sigma} \boldsymbol{\pi}^\top, \quad \sigma_{\pi_k} := \boldsymbol{\pi}(\boldsymbol{\sigma})_k,$$

where $\boldsymbol{\pi}(\boldsymbol{\sigma})$ is the permuted diagonal matrix $\boldsymbol{\sigma}$, (64) becomes

$$C_M \sum_{\Pi_M} \exp \left(-N \sum_{k \leq M} \tau_k^{ab} \sigma_{\pi_k}^{ab} \right). \quad (66)$$

The above sum on Π_M , whose cardinal is $2^M M! = \Theta(\exp(M \ln M))$, is over exponentially large terms of order $\exp(\Theta(MN))$. Therefore it can be estimated by Laplace approximation. In other words only the dominating terms matter, so we need to understand which choices of permutations minimize $\sum_k \tau_k^{ab} \sigma_{\pi_k}^{ab}$. By the *rearrangement inequality* [59] this corresponds to the permutation which orders $(\tau_k^{ab})_k$ and $(\sigma_k^{ab})_k$ in opposite order. Therefore (66) becomes

$$\int d\mu_M(\mathbf{A}^{ab}) d\mu_M(\mathbf{B}^{ab}) \exp N \text{Tr} \left(-\boldsymbol{\tau}^{ab} \mathbf{A}^{ab} \boldsymbol{\sigma}^{ab} (\mathbf{B}^{ab})^\top \right) = C_M \exp \left(-N \sum_{k \leq M} \tau_k^{ab} \sigma_{M+1-k}^{ab} \right) \quad (67)$$

where $\tau_k^{ab} \geq \tau_{k+1}^{ab}$ and $\sigma_k^{ab} \geq \sigma_{k+1}^{ab}$ for all $k \leq M$.

Second saddle point

We now consider the second term appearing in (63). Let \mathbb{E}_μ be the joint expectation over the Haar distributed matrices $(\mathbf{C}^{ab}, \mathbf{D}^{ab})_{a < b}$. We need to compute

$$\mathbb{E}_\mu \exp N \phi_M((\mathbf{C}^{ab}, \mathbf{D}^{ab}, \boldsymbol{\tau}^{ab})_{a < b}), \quad (68)$$

where ϕ_M , which plays the role of effective action for $(\mathbf{C}^{ab}, \mathbf{D}^{ab})_{a < b}$, is

$$\phi_M((\mathbf{C}^{ab}, \mathbf{D}^{ab}, \boldsymbol{\tau}^{ab})_{a < b}) := \ln \int \prod_{a=0}^u dP_X(\mathbf{y}^a) \exp \sum_{a < b}^{0,u} (\mathbf{y}^a)^\top \mathbf{C}^{ab} \boldsymbol{\tau}^{ab} (\mathbf{D}^{ab})^\top \mathbf{y}^b. \quad (69)$$

Note that it is of order M . A saddle point approximation to the integral over the orthogonal matrices yields

$$\mathbb{E}_\mu \exp N \phi_M((\mathbf{C}^{ab}, \mathbf{D}^{ab}, \boldsymbol{\tau}^{ab})_{a < b}) = C_M \sum_{*} \exp N \phi_M((\mathbf{C}_*^{ab}, \mathbf{D}_*^{ab}, \boldsymbol{\tau}^{ab})_{a < b}), \quad (70)$$

where $(\mathbf{C}_*^{ab}, \mathbf{D}_*^{ab})_{a < b, *}$ are the saddle points. Symmetry suggests again that $\mathbf{C}_*^{ab} = \mathbf{D}_*^{ab}$. We are going to argue that the saddle points are the elements of Π_M as in the previous saddle point estimate. We consider a generic perturbation $(\mathbf{C}^{ab}(\mathbf{I}_M + \delta \mathbf{S}^{ab}), \mathbf{D}^{ab}(\mathbf{I}_M + \delta \mathbf{T}^{ab}))$ for anti-symmetric matrices $(\mathbf{S}^{ab})^\top = -\mathbf{S}^{ab}$ and $(\mathbf{T}^{ab})^\top = -\mathbf{T}^{ab}$. Then the first order variation in δ of the action reads

$$\left| \left(\frac{\partial}{\partial \delta} \phi_M((\mathbf{C}^{ab}(\mathbf{I}_M + \delta \mathbf{S}^{ab}), \mathbf{D}^{ab}(\mathbf{I}_M + \delta \mathbf{T}^{ab}), \boldsymbol{\tau}^{ab})) \right)_{\delta=0} \right| = \left| \sum_{a < b} \text{Tr}(\mathbf{D}^{ab})^\top \langle \mathbf{y}^b (\mathbf{y}^a)^\top \rangle \mathbf{C}^{ab} (\boldsymbol{\tau}^{ab} \mathbf{T}^{ab} - \mathbf{S}^{ab} \boldsymbol{\tau}^{ab}) \right|. \quad (71)$$

The expectation $\langle \cdot \rangle$ acting on $(\mathbf{y}^a)_{a=0}^u$ is induced by the Hamiltonian defined by the exponent in (69) with generic matrices $(\mathbf{C}^{ab}, \mathbf{D}^{ab})_{a < b}$, under the reference measure P_X and at fixed $(\boldsymbol{\tau}^{ab})_{a < b}$:

$$\langle f((\mathbf{y}^a)) \rangle := \frac{\int \prod_{a=0}^u dP_X(\mathbf{y}^a) f((\mathbf{y}^a)) \exp \sum_{a < b}^{0,u} (\mathbf{y}^a)^\top \mathbf{C}^{ab} \boldsymbol{\tau}^{ab} (\mathbf{D}^{ab})^\top \mathbf{y}^b}{\int \prod_{a=0}^u dP_X(\mathbf{y}^a) \exp \sum_{a < b}^{0,u} (\mathbf{y}^a)^\top \mathbf{C}^{ab} \boldsymbol{\tau}^{ab} (\mathbf{D}^{ab})^\top \mathbf{y}^b}. \quad (72)$$

We assume that in order to make the sum (71) vanish, each terms in the sum must cancel. For a given pair $a < b$, the trace in (71) can thus cancel only if $(\mathbf{D}^{ab})^\top \langle \mathbf{y}^b(\mathbf{y}^a)^\top \rangle \mathbf{C}^{ab}$ lies in the orthogonal complement of $(\boldsymbol{\tau}^{ab} \mathbf{T}^{ab} - \mathbf{S}^{ab} \boldsymbol{\tau}^{ab})^\top$. Because as before $\boldsymbol{\tau}^{ab} \mathbf{T}^{ab} - \mathbf{S}^{ab} \boldsymbol{\tau}^{ab}$ has zero diagonal, it thus requires $(\mathbf{D}^{ab})^\top \langle \mathbf{y}^b(\mathbf{y}^a)^\top \rangle \mathbf{C}^{ab}$ to be diagonal. We now show that a sufficient condition for this is that $\mathbf{C}^{ab} = \mathbf{D}^{ab} = \boldsymbol{\pi}^{ab} \in \Pi_M$. In this case we can see from (69) that y_k^a is independent of y_ℓ^b ,

$$\langle y_k^a y_\ell^b \rangle = \langle y_k^a \rangle \langle y_\ell^b \rangle \quad \forall a < b \text{ and } k \neq \ell. \quad (73)$$

This is because the following interaction matrices are diagonal:

$$\pi^{ab}(\boldsymbol{\tau}^{ab}) := \boldsymbol{\pi}^{ab} \boldsymbol{\tau}^{ab} (\boldsymbol{\pi}^{ab})^\top.$$

Thanks to the aforementioned decoupling taking place when considering $\mathbf{C}^{ab} = \mathbf{D}^{ab} = \boldsymbol{\pi}^{ab} \in \Pi_M$,

$$\langle y_k^a \rangle \propto \int \prod_{b=0}^u dp_X(y^b) y^a \exp\left(y^a \sum_{b(\neq a)}^{0,u} y^b \pi^{ab}(\boldsymbol{\tau}^{ab})_k\right). \quad (74)$$

This is the local mean magnetization of a spin system $(y^a)_{a=0}^u$. Because the prior is symmetric and centered, this local magnetization is null by the global sign symmetry $(y^a) \rightarrow (-y^a)$ of its associated Gibbs measure:

$$\langle y_k^a \rangle = 0 \quad \forall k, a.$$

Combined with (73) this implies that the matrix $\langle \mathbf{y}^b(\mathbf{y}^a)^\top \rangle = (\langle y_k^b y_\ell^a \rangle)_{k, \ell \leq M}$ is diagonal and thus the matrix $(\boldsymbol{\pi}^{ab})^\top \langle \mathbf{y}^b(\mathbf{y}^a)^\top \rangle \boldsymbol{\pi}^{ab}$ is also diagonal (as $\boldsymbol{\pi}^{ab} \in \Pi_M$). We thus have $\text{Tr}(\boldsymbol{\pi}^{ab})^\top \langle \mathbf{y}^b(\mathbf{y}^a)^\top \rangle \boldsymbol{\pi}^{ab} (\boldsymbol{\tau}^{ab} \mathbf{T}^{ab} - \mathbf{S}^{ab} \boldsymbol{\tau}^{ab}) = 0$ for any antisymmetric perturbations $(\mathbf{S}^{ab}, \mathbf{T}^{ab})$ and diagonal $(\boldsymbol{\tau}^{ab})$. So (71) does cancel in that case. This ends the argument that matrices in Π_M are again saddle points.

Showing that *only* the matrices in Π_M are saddle points requires showing that $\mathbf{M}^{ab} := (\mathbf{D}^{ab})^\top \langle \mathbf{y}^b(\mathbf{y}^a)^\top \rangle \mathbf{C}^{ab}$ cannot be diagonal if $\mathbf{C}^{ab} \neq \mathbf{D}^{ab}$ (but they are allowed to be permutations) or if $\mathbf{C}^{ab} = \mathbf{D}^{ab}$ is not a permutation. In both scenarios, $\langle \mathbf{y}^b(\mathbf{y}^a)^\top \rangle$ and \mathbf{M}^{ab} have no reasons to be diagonal. Having \mathbf{M}^{ab} diagonal would require finding interaction matrices $(\mathbf{C}^{ab} \boldsymbol{\tau}^{ab} (\mathbf{D}^{ab})^\top)_{a < b}$ entering the spin model associated to the log-partition function (69) such that $(\mathbf{C}^{ab}, \mathbf{D}^{ab})$ also represent the singular vectors of $\langle \mathbf{y}^b(\mathbf{y}^a)^\top \rangle$. We believe that this is not possible in general and thus make the assumption that Π_M contains all saddle points. Therefore (70) becomes

$$C_M \sum_{(\boldsymbol{\pi}^{ab})_{a < b} \in \Pi_M^{u(u+1)/2}} \exp\left(N \sum_{k \leq M} \ln \int \prod_{a=0}^u dp_X(y^a) \exp \sum_{a < b}^{0,u} y^a y^b \pi^{ab}(\boldsymbol{\tau}^{ab})_k\right). \quad (75)$$

E.3 Spectral replica symmetry and simplifications

Now we assume the following ‘‘spectral replica symmetric ansatz’’ for the order parameters:

$$\text{Spectral replica symmetry: } \boldsymbol{\tau}^{ab} = \boldsymbol{\tau} \text{ and } \boldsymbol{\sigma}^{ab} = \boldsymbol{\sigma} \quad \forall a < b. \quad (76)$$

The sum over the permutation matrices in (75) simply becomes

$$C_M \sum_{(\boldsymbol{\pi}^{ab})_{a < b} \in \Pi_M^{u(u+1)/2}} \exp\left(N \sum_{k \leq M} \ln \int \prod_{a=0}^u dp_X(y^a) \exp \sum_{a < b}^{0,u} y^a y^b \pi^{ab}(\boldsymbol{\tau})_k\right). \quad (77)$$

The sum (77) is over $(M!)^{u(u+1)/2}$ exponentially large terms of order $\exp(\Theta(MN))$ so a before it can be estimated by Laplace approximation. We thus need to understand which choices of permutations $(\boldsymbol{\pi}^{ab})_{a < b}$ maximize the ‘‘free entropy’’

$$g_M := \sum_{k \leq M} \ln \int \prod_{a=0}^u dp_X(y^a) \exp \sum_{a < b}^{0,u} y^a y^b \pi^{ab}(\boldsymbol{\tau})_k. \quad (78)$$

We assume here that there are only two potential candidates for the maximizers corresponding to opposite extreme cases: the fully ordered and fully disordered scenarios.

Ordered scenario

This corresponds to consider matrices $(\pi^{ab})_{a<b}$ all equal, i.e., an additional layer of replica symmetric ansatz:

$$\pi^{ab} = \pi \quad \forall a < b. \quad (79)$$

In this case the free entropy g_M reads

$$g_M = \sum_{k \leq M} \ln \int \prod_{a=0}^u dp_X(y^a) \exp\left(\tau_{\pi_k} \sum_{a<b}^{0,u} y^a y^b\right) = \sum_{k \leq M} \ln \int \prod_{a=0}^u dp_X(y^a) \exp\left(\tau_k \sum_{a<b}^{0,u} y^a y^b\right) \quad (80)$$

as this is the same for any permutation $\pi \in \Pi_M$. We call this the ‘‘ordered’’ scenario as this free entropy becomes, at fixed k , the one of a standard *ferromagnetic* model (i.e., with only positive interactions) without disorder, that is with same interaction strength $\tau_k > 0$ (which is a quenched random variable in this spin model) for all pairs of spins $(y^a, y^b)_{a<b}$. We can simplify it as follows. Let Z be an i.i.d. standard normal random variable. We thus compute

$$\begin{aligned} & \sum_{k \leq M} \ln \int \prod_{a=0}^u dp_X(y^a) \exp\left(\frac{1}{2}\left(\sqrt{\tau_k} \sum_a^{0,u} y^a\right)^2 - \frac{\tau_k}{2} \sum_a^{0,u} (y^a)^2\right) \\ &= \sum_{k \leq M} \ln \mathbb{E} \left(\int dp_X(y) \exp\left(\sqrt{\tau_k} Z y - \frac{\tau_k}{2} y^2\right) \right)^{u+1} \\ &= u \sum_{k \leq M} \mathbb{E} \int dp_X(y_0) \exp\left(\sqrt{\tau_k} Z y_0 - \frac{\tau_k}{2} y_0^2\right) \\ & \quad \times \ln \int dp_X(y) \exp\left(\sqrt{\tau_k} Z y - \frac{\tau_k}{2} y^2\right) + O(u^2) \\ &= u \sum_{k \leq M} \mathbb{E} \ln \int dp_X(y) \exp\left(\sqrt{\tau_k} Z y + \tau_k y Y_0 - \frac{\tau_k}{2} y^2\right) + O(u^2) \end{aligned} \quad (81)$$

using the change of variable $Z \rightarrow Z - \sqrt{\tau_{\pi_k}} y_0$ for the last step, and where $Y_0 \sim p_X$. So with this choice (75) would become

$$C_M \exp\left(uN \sum_{k \leq M} \mathbb{E} \ln \int dp_X(y) \exp\left(\sqrt{\tau_k} Z y + \tau_k y Y_0 - \frac{\tau_k}{2} y^2\right) + O(u^2)\right). \quad (82)$$

Disordered scenario

In the opposite scenario, the permutations $(\pi^{ab})_{a<b}$ are ‘‘typical’’ (i.e., taken randomly and independently for different pairs $a < b$). In this case, in the regime $M \gg 1$ with finitely many replicas, we have

$$\frac{g_M}{M} \approx \mathbb{E} \psi((\tau^{ab})_{a<b}) := \mathbb{E}_{(\tau^{ab})} \ln \int \prod_{a=0}^u dp_X(y^a) \exp \sum_{a<b}^{0,u} y^a y^b \tau^{ab} \quad (83)$$

where $(\tau^{ab})_{a<b}$ are i.i.d. random ferromagnetic interactions $\tau^{ab} \sim \rho_\tau$ whose law is the weak limit

$$\rho_\tau := \lim_{M \rightarrow \infty} \frac{1}{M} \sum_{k \leq M} \delta_{\tau_k}.$$

This is because picking a fixed diagonal entry k of random permutations $\pi^{ab}(\tau)_k$ of a diagonal matrix τ is the same as randomly picking diagonal entries of τ . Then $\mathbb{E} \psi$ is the average free entropy of a *disordered* mean-field ferromagnetic spin system.

Comparing the two scenarios

We now argue that the ordered scenario yields a greater free entropy than the disordered scenario, and therefore must be selected in the Laplace approximation to the sum (75), which implies that (75) equals (82) at leading order. To do so we are going to compare two random free entropies (we work in the large M limit directly). Let $\tau, (\tau^{ab})_{a<b}$ be random variables all i.i.d. with distribution ρ_τ defined above, and just for this section set $\tau := (\tau^{ab})_{a<b} \in \mathbb{R}_{>0}^{u(u+1)/2}$. Let

$$\psi(\tau) := \ln \int \prod_{a=0}^u dp_X(y^a) \exp \sum_{a<b}^{0,u} y^a y^b \tau^{ab}, \quad (84)$$

$$\xi(\tau) := \ln \int \prod_{a=0}^u dp_X(y^a) \exp\left(\tau \sum_{a<b}^{0,u} y^a y^b\right). \quad (85)$$

We also define the Gibbs measure for the disordered scenario:

$$\langle f((y^a)) \rangle_{\tau} := \frac{\int \prod_{a=0}^u dp_X(y^a) f((y^a)) \exp \sum_{a<b}^{0,u} y^a y^b \tau^{ab}}{\int \prod_{a=0}^u dp_X(y^a) \exp \sum_{a<b}^{0,u} y^a y^b \tau^{ab}}. \quad (86)$$

We denote it $\langle f((y^a)) \rangle_{\tau}$ for the ordered scenario where all $\tau^{ab} = \tau$.

Showing that the ordered scenario yields a greater free entropy than the disordered scenario is then equivalent (when M is large) to show that

$$\mathbb{E}\xi(\tau) \geq \mathbb{E}\psi(\tau). \quad (87)$$

Note that $\psi((\tau)) = \xi(\tau)$ (where (τ) is the constant vector), so in particular

$$\psi((\mathbb{E}\tau)) = \xi(\mathbb{E}\tau). \quad (88)$$

So the statement would follow if one could show the following equivalent inequality on the Jensen gaps:

$$\mathbb{E}\xi(\tau) - \xi(\mathbb{E}\tau) \geq \mathbb{E}\psi(\tau) - \psi((\mathbb{E}\tau)). \quad (89)$$

An heuristic suggesting the validity of (89) goes as follows. These two Jensen gaps can be approximated by evaluating the Laplacian

$$\Delta\xi(\tau) = \left\langle \left(\sum_{a<b}^{0,u} y^a y^b \right)^2 \right\rangle_{\tau} - \left\langle \sum_{a<b}^{0,u} y^a y^b \right\rangle_{\tau}^2 = \sum_{a<b}^{0,u} \sum_{c<d}^{0,u} (\langle y^a y^b y^c y^d \rangle_{\tau} - \langle y^a y^b \rangle_{\tau} \langle y^c y^d \rangle_{\tau}) \geq 0, \quad (90)$$

and comparing it to

$$\Delta\psi(\tau) = \sum_{a<b}^{0,u} (\langle (y^a y^b)^2 \rangle_{\tau} - \langle y^a y^b \rangle_{\tau}^2) \geq 0. \quad (91)$$

Because the models corresponding to the two free entropies ψ, ξ are ferromagnetic and invariant under spin-flip, the Griffiths inequality implies that each term in the double sum in (90) is non-negative, and thus suggests that $\Delta\xi(\tau) \geq \Delta\psi(\tau)$ may be true. This argument points towards ξ being “more convex” than ψ and thus that inequality (87) holds.

E.4 Replica symmetric free entropy

Under these assumptions we can combine everything to obtain an explicit formula for the replicated partition function. Recall that we assume that the saddle point over the singular values verifies (76). Thus

$$\begin{aligned} \mathbb{E}Z^u &= C_N \int d\sigma d\tau \exp NM \epsilon_N u \left(\frac{u+1}{2} \frac{1}{M^2} \sum_{k<\ell \leq M} \ln |\sigma_k^2 - \sigma_{\ell}^2| |\tau_k^2 - \tau_{\ell}^2| \right) \\ &\quad \times \exp NM u \left(-\frac{u+1}{2} \frac{1}{M} \sum_{k \leq M} \tau_k \sigma_{M+1-k} + \frac{u+1}{2} \frac{\gamma}{2M} \sum_{k \leq M} \sigma_k^2 \right) \\ &\quad \times \exp NM u \left(\frac{1}{M} \sum_{k \leq M} \mathbb{E} \ln \int dp_X(y) \exp \left(\sqrt{\tau_k} Z y + \tau_k y Y_0 - \frac{\tau_k}{2} y^2 \right) + O(u^2) \right) \end{aligned} \quad (92)$$

where C_N collects all irrelevant multiplicative constants and terms $\exp(o(NM))$. Note that the ordering of (τ_k) and (σ_k) enforced by (67) finally does not matter. Saddle point estimation and the replica trick (58) finally yields a variational formula for the average free entropy

$$\mathbb{E}f_N = \underset{\sigma, \tau \in \mathbb{R}_{>0}^M}{\text{extr}} \frac{1}{M} \sum_{k \leq M} \left\{ -\frac{1}{2} \tau_k \sigma_k + \frac{\gamma}{4} \sigma_k^2 + \mathbb{E} \ln \int dp_X(y) \exp \left(\sqrt{\tau_k} Z y + \tau_k y Y_0 - \frac{\tau_k}{2} y^2 \right) \right\} + o_N(1). \quad (93)$$

Note that in the present regime $M/N \rightarrow 0$ the terms coming from the Vandermonde does not play a role asymptotically. At fixed k , the bracket $\{\dots\}$ above is the usual formula for the rank-one case. And because different k indices do not interact, the solution is clearly the same for all k , so this formula collapses on the rank-one formula

$$\mathbb{E}f_N \xrightarrow{N \rightarrow \infty} \underset{\sigma, \tau \in \mathbb{R}_{>0}}{\text{extr}} \left\{ -\frac{1}{2} \tau \sigma + \frac{\gamma}{4} \sigma^2 + \mathbb{E} \ln \int dp_X(y) \exp \left(\sqrt{\tau} Z y + \tau y Y_0 - \frac{\tau}{2} y^2 \right) \right\}. \quad (94)$$

Solving for the saddle point equation for σ and using the connection between average free entropy and mutual information we obtain the rank-one prediction:

$$\frac{I_N(\mathbf{S}; \mathbf{Y})}{MN} \xrightarrow{N \rightarrow \infty} \inf_{\sigma \geq 0} \left\{ \frac{\gamma}{4} (\sigma - \rho)^2 + I(X; \sqrt{\gamma} \sigma X + Z) \right\} \quad (95)$$

where $X \sim p_X$, $Z \sim \mathcal{N}(0, 1)$ and ρ is the variance of p_X . Whenever it is unique, denoting σ_* the minimizer in the above variational formula, the MMSE reads (see [12, 19]):

$$\text{MMSE}_N(\gamma) \xrightarrow{N \rightarrow \infty} \rho^2 - \sigma_*^2. \quad (96)$$

Finally, we remark that the present derivation used that the rank M grows with N . But it can be verified numerically or analytically by studying the saddle point equations for the finite rank $M = O(1)$ that the replica prediction collapses onto the rank-one formulas when the prior is fully factorized as in the present setting.

F Sub-linear rank RIE and MSE

The signal matrix $\mathbf{S} \in \mathbb{R}^{N \times N}$ is taken from a rotationally invariant prior and observed through an additive channel,

$$\mathbf{Y} = \sqrt{\gamma} \mathbf{S} + \mathbf{Z}$$

where the noise $\mathbf{Z} \in \mathbb{R}^{N \times N}$ is also distributed according to a rotationally invariant ensemble. Here we allow non-Gaussian noise. It is assumed that \mathbf{S} has $M = \lfloor N^\alpha \rfloor$ non-zero i.i.d eigenvalues sampled from a distribution $\rho_S(x)$ with finite second moment and bounded support. By construction the empirical distribution of non-zero eigenvalues $\frac{1}{M} \sum_{i=1}^M \delta(x - \lambda_i^S)$ tends weakly to $\rho_S(x)$. Moreover we assume that \mathbf{Z} has a limiting spectral distribution ρ_Z . Since we are in the sub-linear regime, the limiting spectral measure of \mathbf{Y} (normalized by $1/N$) is the same as the one of \mathbf{Z} . But note that \mathbf{Y} may have sub-linear number of eigenvalues outside the support.

We propose a sub-linear rank RIE and an associated algorithm to estimate \mathbf{S} from \mathbf{Y} , which we conjecture to be optimal. Arguing as in the linear case it is not difficult to see that the *optimal* RIE (i.e., the one minimizing the MSE in the general RIE class) must have a MSE which equals the MMSE. We conjecture that the *proposed* RIE, and associated algorithm, are indeed the optimal. Evidence for this conjecture comes from numerics discussed below (at least for some range of α), but also from the particular case of Gaussian noise. Indeed for Gaussian noise we have the I-MMSE relation so by integrating the MMSE we find the mutual information. Thus our proposed sub-linear rank RIE predicts an expression for the mutual information. On the other hand the mutual information has recently been rigorously computed from the asymptotics of sub-linear rank spherical integrals [33]. By comparing the expressions obtained by these two independent approaches we validate the conjecture analytically, at least for Gaussian noise.

F.1 Sub-linear rank RIE

Let the eigen-decomposition of \mathbf{S} and \mathbf{Y} be $\mathbf{S} = \sum_{i=1}^M \lambda_i^S \mathbf{s}_i \mathbf{s}_i^\top$, $\mathbf{Y} = \sum_{i=1}^N \lambda_i^Y \mathbf{y}_i \mathbf{y}_i^\top$. For a RIE $\Xi(\mathbf{Y}) = \sum_{i=1}^N \xi_i \mathbf{y}_i \mathbf{y}_i^\top$, the MSE can be written as:

$$\begin{aligned} \frac{1}{M} \|\mathbf{S} - \Xi(\mathbf{Y})\|_F^2 &= \frac{1}{M} \left\| \sum_{i=1}^M \lambda_i^S \mathbf{s}_i \mathbf{s}_i^\top - \sum_{i=1}^N \xi_i \mathbf{y}_i \mathbf{y}_i^\top \right\|_F^2 \\ &= \frac{1}{M} \sum_{i=1}^M \lambda_i^{S^2} + \frac{1}{M} \sum_{i=1}^N \xi_i^2 - \frac{2}{M} \sum_{i=1}^N \xi_i \sum_{j=1}^M \lambda_j^S (\mathbf{s}_j^\top \mathbf{y}_i)^2. \end{aligned} \quad (97)$$

Minimizing (97) over ξ_i 's, the optimum is achieved at

$$\xi_i^* = \sum_{j=1}^M \lambda_j^S (\mathbf{s}_j^\top \mathbf{y}_i)^2 = \mathbf{y}_i^\top \mathbf{S} \mathbf{y}_i. \quad (98)$$

This estimator is called *oracle estimator* since it requires the knowledge of the signal.

To compute the optimal eigenvalues we need to know the overlap between the eigenvectors of the signal and the observation. For finite-rank additive perturbation, \mathbf{X} of a rotationally invariant matrix \mathbf{Z} , the eigenvalues and the overlap between the eigenvectors of the perturbation and the perturbed matrix $\mathbf{X} + \mathbf{Z}$ has been computed rigorously in [39]. In [46] this is extended to sub-linear rank perturbations. Essentially the same formulas (as for finite-rank perturbations) give the eigenvalues of the perturbed matrix and overlap in the large size limit.

These results could presumably be used to get a rigorous computation of the asymptotic MSE predicted by the oracle estimator but this is left for future work. Here we use these results in an heuristic way to propose a specific RIE and associated algorithm. We use the notation $a \rightarrow b$ to mean that $|a - b|$ tends to zero with high probability as $N \rightarrow +\infty$. Theorem 2.7 in [46] suggests

$$(\mathbf{s}_i^\top \mathbf{y}_i)^2 \rightarrow \begin{cases} \frac{-1}{\gamma \lambda_i^{S^2} G'_{\rho_Z} \left(G_{\rho_Z}^{-1} \left(\frac{1}{\sqrt{\gamma} \lambda_i^S} \right) \right)} & \text{if } \frac{1}{\sqrt{\gamma} \lambda_i^S} \in (G_{\rho_Z}(a^-), G_{\rho_Z}(b^+)), \\ 0 & \text{else.} \end{cases} \quad (99)$$

where $G_{\rho_Z}(z)$ is the *Cauchy transform* of ρ_Z , constrained on $\mathbb{R} \setminus \text{supp } \rho_Z$, and a, b are the infimum and supremum of the support of ρ_Z , and $G_{\rho_Z}(a^-) \equiv \lim_{z \rightarrow a^-} G_{\rho_Z}(z)$ and similarly for b^+ . The overlap in (99) is expressed in terms of eigenvalues of \mathbf{S} , but since the corresponding eigenvalue of \mathbf{Y} is affected by λ_i^S , we can express the overlap in terms of eigenvalues of \mathbf{Y} . Theorem 2.1 in [46] suggests

$$\lambda_i^Y \rightarrow \begin{cases} G_{\rho_Z}^{-1} \left(\frac{1}{\sqrt{\gamma} \lambda_i^S} \right) & \text{if } \frac{1}{\sqrt{\gamma} \lambda_i^S} \in (G_{\rho_Z}(a^-), G_{\rho_Z}(b^+)), \\ b & \text{if } \frac{1}{\sqrt{\gamma} \lambda_i^S} > G_{\rho_Z}(b^+), \\ a & \text{if } \frac{1}{\sqrt{\gamma} \lambda_i^S} > G_{\rho_Z}(a^-). \end{cases} \quad (100)$$

From (100), we can see that if an eigenvalue of \mathbf{Y} is outside the support of ρ_Z , then the corresponding eigenvalue of the signal can computed as $\lambda_i^S \approx \frac{1}{\sqrt{\gamma} G_{\rho_Z}(\lambda_i^Y)}$. From (99), (100) we deduce that for an eigenvalue $\lambda_i^Y \in (a, b)$ there is no spike aligned with \mathbf{y}_i , because otherwise λ_i^Y would be outside of the support of ρ_Z . So, the corresponding ξ_i^* 's are zero for the eigenvalues in (a, b) . On the other hand, since there are M spikes, at most M ξ_i^* 's are non-zero which makes the whole expression in (97) for the optimum ξ_i^* 's $O(1)$.

Finally the proposed RIE estimator is naturally constructed as follows

$$\begin{cases} \hat{\Xi}^*(\mathbf{Y}) = \sum_{i=1}^N \xi_i^* \mathbf{y}_i \mathbf{y}_i^\top, \\ \xi_i^* = -\frac{1}{\sqrt{\gamma}} \mathbb{I}(\lambda_i^Y \notin [a, b]) \frac{G_{\rho_Z}(\lambda_i^Y)}{G'_{\rho_Z}(\lambda_i^Y)}. \end{cases} \quad (101)$$

This provides an algorithm with the following steps to reconstruct the signal

- (i) Compute spectral data $(\lambda_i^Y, \mathbf{y}_i)$ from the matrix \mathbf{Y} .
- (ii) Apply the function f_Z to the eigenvalues

$$f_Z(x) = \begin{cases} -\frac{1}{\sqrt{\gamma}} \frac{G_{\rho_Z}(x)}{G'_{\rho_Z}(x)} & \text{if } x \notin [a, b] \\ 0 & \text{else.} \end{cases}$$

- (iii) Construct the estimate as $\hat{\mathbf{S}} = \sum_{i=1}^N f_Z(\lambda_i^Y) \mathbf{y}_i \mathbf{y}_i^\top$.

The second algorithmic step requires knowledge of the limiting distribution of the noise which can in principle be computed from its distribution.

F.2 Gaussian Noise

For $\rho_Z = \frac{1}{2\pi} \sqrt{4 - x^2}$, we have that $G_{\rho_{sc}}(z) = \frac{z - \text{sign}(z) \sqrt{z^2 - 4}}{2}$. Thus, given matrix \mathbf{Y} the estimator reads:

$$\begin{cases} \hat{\Xi}^*(\mathbf{Y}) = \sum_{i=1}^N \xi_i^* \mathbf{y}_i \mathbf{y}_i^\top, \\ \xi_i^* = \frac{1}{\sqrt{\gamma}} \mathbb{I}(|\lambda_i^Y| > 2) \text{sign}(\lambda_i^Y) \sqrt{\lambda_i^{Y^2} - 4}. \end{cases}$$

F.2.1 MSE

To compute the MSE, we use (99) which is in terms of the eigenvalues of \mathbf{S} . We have

$$(\mathbf{s}_i^\top \mathbf{y}_i)^2 \rightarrow \begin{cases} 1 - \frac{1}{\gamma \lambda_i^{S^2}} & \text{if } \gamma \lambda_i^{S^2} \geq 1, \\ 0 & \text{else,} \end{cases} \quad (102)$$

so the optimal eigenvalues of the estimator are

$$\xi_i^* \rightarrow \begin{cases} \lambda_i^S - \frac{1}{\gamma \lambda_i^S} & \text{if } \gamma \lambda_i^{S^2} \geq 1, \\ 0 & \text{else.} \end{cases} \quad (103)$$

The MSE can be written as,

$$\frac{1}{M} \|\mathbf{S} - \Xi^*(\mathbf{Y})\|_F^2 = \frac{1}{M} \sum_{i=1}^M \lambda_i^{S^2} - \frac{1}{M} \sum_{i=1}^N \xi_i^{*2} \quad (104)$$

where, we used that, in the limit $N \rightarrow \infty$, at most M number of ξ_i^* 's are non-zero. Taking the limit $N \rightarrow \infty$ (or $M \rightarrow \infty$), we find

$$\lim_{N \rightarrow \infty} \frac{1}{M} \|\mathbf{S} - \Xi^*(\mathbf{Y})\|_F^2 = \int x^2 \rho_S(x) dx - \int_{|x| \geq \frac{1}{\sqrt{\gamma}}} \left(x - \frac{1}{\gamma x}\right)^2 \rho_S(x) dx. \quad (105)$$

F.2.2 Mutual information in Gaussian noise

As already explained the MSE computed above should be equal to the MMSE, thus by integrating over γ we should recover the mutual information. Moreover, the mutual information can be computed using the limit of the spherical integrals of sub-linear rank [33]. In this section we explicitly check for a few priors that the two expressions indeed coincide.

We first present the main formula of [33]. The asymptotic mutual information between \mathbf{S} and the observation $\mathbf{Y} = \sqrt{\gamma} \mathbf{S} + \mathbf{Z}$ is

$$\lim_{N \rightarrow \infty} \frac{1}{MN} I_N(\mathbf{S}; \mathbf{Y}) = \frac{\gamma}{2} \int x^2 \rho_S(x) dx - \lim_{N \rightarrow \infty} \frac{1}{MN} \ln \int D\mathbf{U} e^{\frac{N}{2} \text{Tr} \sqrt{\gamma} \mathbf{S} \mathbf{U} \mathbf{Y} \mathbf{U}^\top}. \quad (106)$$

The integral $\int D\mathbf{U} e^{\frac{N}{2} \text{Tr} \sqrt{\gamma} \mathbf{S} \mathbf{U} \mathbf{Y} \mathbf{U}^\top}$ is the spherical integral of sub-linear rank, and its asymptotic limit has been studied in [33]. For matrix \mathbf{A} with M positive eigenvalues, by Theorem 2.5 in [33], we have that

$$\lim_{N \rightarrow \infty} \frac{1}{MN} \ln \int D\mathbf{U} e^{\frac{N}{2} \text{Tr} \mathbf{A} \mathbf{U} \mathbf{B} \mathbf{U}^\top} = \frac{1}{2} \lim_{N \rightarrow \infty} \frac{1}{M} \sum_{i=1}^M K(\theta_i, \lambda_i, \mu_B) \quad (107)$$

where θ_i 's are non-zero eigenvalues of \mathbf{A} , λ_i 's are the top eigenvalues of \mathbf{B} , and μ_B is the limiting spectral distribution of \mathbf{B} . Note that the result of [33] also covers the case of negative eigenvalues, however for simplicity we only consider matrices with positive eigenvalues. The function K is defined as

$$K(\theta, \lambda, \mu) = \theta \lambda' + (v - \lambda') G_\mu(v) - \ln |\theta| - \int \ln |v - x| d\mu(x) - 1$$

where $\lambda' = \max(\lambda, r(\mu))$ ($r(\mu)$ is the rightmost point of the support of μ),

$$v := v(\lambda, \theta) = \begin{cases} \lambda' & \text{when } 0 \leq G_\mu(\lambda') \leq \theta \text{ or } \theta \leq G_\mu(\lambda') \leq 0 \\ G_\mu^{-1}(\theta) & \text{else} \end{cases}$$

and G_μ is the Stieltjes transform of μ .

F.2.3 Example 1: Sub-linear Wishart signal

Consider the signal matrix \mathbf{S} to be $\frac{1}{N} \mathbf{X} \mathbf{X}^\top$, with $\mathbf{X} \in \mathbb{R}^{N \times M}$ has i.i.d. standard Gaussian entries, and $M = \lfloor N^\alpha \rfloor$. In the limit $N \rightarrow \infty$, one can show that the limiting distribution of non-zero eigenvalues of \mathbf{S} is $\delta(x - 1)$. For this example, the MSE given by (105) reads

$$\text{MSE}(\gamma) = \begin{cases} 1 & \text{if } \gamma \leq 1, \\ \frac{1}{\gamma} \left(2 - \frac{1}{\gamma}\right) & \text{if } \gamma \geq 1. \end{cases} \quad (108)$$

Integrating over γ , we find the mutual information to be:

$$\lim_{N \rightarrow \infty} \frac{1}{MN} I_N(\mathbf{S}; \mathbf{Y}) = \begin{cases} \frac{\gamma}{4} & \text{if } \gamma \leq 1, \\ \frac{1}{4} \frac{1}{\gamma} + \frac{1}{2} \ln \gamma & \text{if } \gamma \geq 1. \end{cases} \quad (109)$$

which is the mutual information in the rank-one case when the prior for the spike is a Gaussian vector.

Now, we compute the mutual information using spherical integrals. All the non-zero eigenvalues of sub-linear rank matrix $\sqrt{\gamma}\mathbf{S}$, θ_i 's, converge to a single number, $\sqrt{\gamma}$. By [39], the limiting top eigenvalues of \mathbf{Y} , λ_i 's, can also be computed. So, all the summands in r.h.s. of (107) are equal in the limit, and we have:

$$\lim_{N \rightarrow \infty} \frac{1}{MN} \ln \int D\mathbf{U} e^{\frac{N}{2} \text{Tr} \sqrt{\gamma} \mathbf{S} \mathbf{U} \mathbf{Y} \mathbf{U}^\top} = \begin{cases} \frac{1}{2} K(\sqrt{\gamma}, 2, \rho_{\text{sc}}) & \text{if } \gamma < 1, \\ \frac{1}{2} K(\sqrt{\gamma}, \sqrt{\gamma} + \frac{1}{\sqrt{\gamma}}, \rho_{\text{sc}}) & \text{if } \gamma \geq 1. \end{cases} \quad (110)$$

Case $\gamma < 1$: we have $\lambda' = 2$ and $v = G_{\rho_{\text{sc}}}^{-1}(\sqrt{\gamma}) = \sqrt{\gamma} + \frac{1}{\sqrt{\gamma}}$. Thus

$$\begin{aligned} K(\sqrt{\gamma}, 2, \rho_{\text{sc}}) &= 2\sqrt{\gamma} + \left(\sqrt{\gamma} + \frac{1}{\sqrt{\gamma}} - 2\right) G_{\rho_{\text{sc}}} \left(\sqrt{\gamma} + \frac{1}{\sqrt{\gamma}}\right) - \ln \sqrt{\gamma} \\ &\quad - \int_{-2}^2 \frac{\sqrt{4-x^2}}{2\pi} \ln \left| \sqrt{\gamma} + \frac{1}{\sqrt{\gamma}} - x \right| dx - 1 \\ &= 2\sqrt{\gamma} + \left(\sqrt{\gamma} + \frac{1}{\sqrt{\gamma}} - 2\right) \sqrt{\gamma} - \frac{1}{2} \ln \gamma - \left(\frac{\gamma}{2} - \frac{1}{2} \ln \gamma\right) - 1 \\ &= \frac{\gamma}{2} \end{aligned} \quad (111)$$

where we used the integral formula

$$\frac{1}{2\pi} \int_{-2}^2 \ln(A - Bx) \sqrt{4-x^2} dx = \frac{A}{A + \sqrt{A^2 - 4B^2}} + \ln(A + \sqrt{A^2 - 4B^2}) - \frac{1}{2} - \ln 2.$$

Case $\gamma \geq 1$: we have $\lambda' = \sqrt{\gamma} + \frac{1}{\sqrt{\gamma}}$ and $v = \lambda' = \sqrt{\gamma} + \frac{1}{\sqrt{\gamma}}$. Thus

$$\begin{aligned} K(\sqrt{\gamma}, \sqrt{\gamma} + \frac{1}{\sqrt{\gamma}}, \rho_{\text{sc}}) &= \sqrt{\gamma} \left(\sqrt{\gamma} + \frac{1}{\sqrt{\gamma}}\right) - \ln \sqrt{\gamma} - \int_{-2}^2 \frac{\sqrt{4-x^2}}{2\pi} \ln \left| \sqrt{\gamma} + \frac{1}{\sqrt{\gamma}} - x \right| dx - 1 \\ &= \gamma + 1 - \frac{1}{2} \ln \gamma - \left(\frac{1}{2} \frac{1}{\gamma} + \frac{1}{2} \ln \gamma\right) - 1 \\ &= \gamma - \frac{1}{2} \frac{1}{\gamma} - \ln \gamma. \end{aligned} \quad (112)$$

From (110), (111), and (112), we obtain

$$\lim_{N \rightarrow \infty} \frac{1}{MN} \ln \int D\mathbf{U} e^{\frac{N}{2} \text{Tr} \sqrt{\gamma} \mathbf{S} \mathbf{U} \mathbf{Y} \mathbf{U}^\top} = \begin{cases} \frac{\gamma}{4} & \text{if } \gamma < 1, \\ \frac{\gamma}{2} - \frac{1}{4} \frac{1}{\gamma} - \frac{1}{2} \ln \gamma & \text{if } \gamma \geq 1. \end{cases} \quad (113)$$

Replacing this result in (106) we get

$$\lim_{N \rightarrow \infty} \frac{1}{MN} I_N(\mathbf{S}; \mathbf{Y}) = \begin{cases} \frac{\gamma}{4} & \text{if } \gamma < 1, \\ \frac{1}{4} \frac{1}{\gamma} + \frac{1}{2} \ln \gamma & \text{if } \gamma \geq 1. \end{cases}$$

which is the same as the mutual information computed from the MSE, (109).

In Fig. 4, we compare the performance of the sub-linear RIE and the oracle estimator (98) with $M = \lfloor \sqrt{N} \rfloor$ for various values of N . We observe that the performance of the RIE is very close to the one of oracle estimator (which requires the knowledge of the signal). Moreover, the MSE is close to the theoretical predictions.

F.2.4 Example 2: Uniform distribution

Let ρ_S be the uniform distribution on $[1, 2]$. From (105), the MSE can be computed to be

$$\text{MSE}(\gamma) = \begin{cases} \frac{7}{3} & \text{for } 0 \leq \gamma \leq \frac{1}{4}, \\ -\frac{1}{3} + \frac{4}{\gamma} - \frac{8}{3\gamma^{3/2}} + \frac{1}{2\gamma^2} & \text{for } \frac{1}{4} \leq \gamma \leq 1, \\ \frac{2}{\gamma} - \frac{1}{2\gamma^2} & \text{for } 1 \leq \gamma. \end{cases} \quad (114)$$

Integrating over γ , we find the mutual information to be:

$$\lim_{N \rightarrow \infty} \frac{1}{MN} I_N(\mathbf{S}; \mathbf{Y}) = \begin{cases} \frac{7}{12} \gamma & \text{for } 0 \leq \gamma \leq \frac{1}{4}, \\ -\frac{\gamma}{12} + \ln \gamma + 2(\ln 2 - 1) + \frac{4}{3\sqrt{\gamma}} - \frac{1}{8\gamma} & \text{for } \frac{1}{4} \leq \gamma \leq 1, \\ \frac{1}{2} \ln \gamma + 2 \ln 2 - 1 + \frac{1}{8\gamma} & \text{for } 1 \leq \gamma. \end{cases} \quad (115)$$

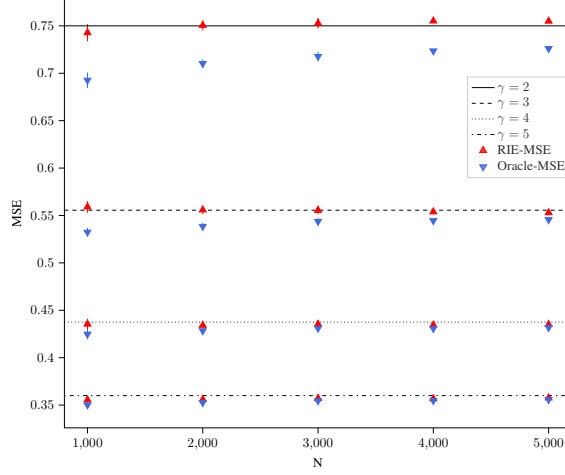


Figure 4: Comparison of the sub-linear RIE and the oracle estimator (98) for Gaussian noise with sub-linear Wishart signal with $M = \lfloor \sqrt{N} \rfloor$. Horizontal lines are MMSE computed from (108). Points are averaged over 10 experiments (error bars might be invisible).

Now, we proceed with the computation of the mutual information using the asymptotic of spherical integrals. In the limit $N \rightarrow \infty$, r.h.s. of (107) becomes an integral (expectation w.r.t. ρ_S). For $\rho_S = \mathcal{U}([1, 2])$ we have

$$\lim_{N \rightarrow \infty} \frac{1}{MN} \ln \int DU e^{\frac{N}{2} \text{Tr} \sqrt{\gamma} S U Y U^T} = \frac{1}{2} \int_1^2 K(\sqrt{\gamma}x, h(\sqrt{\gamma}x), \rho_{sc}) dx \quad (116)$$

with

$$h(\sqrt{\gamma}x) = \begin{cases} 2 & \text{if } \sqrt{\gamma}x \leq 1, \\ \sqrt{\gamma}x + \frac{1}{\sqrt{\gamma}x} & \text{if } \sqrt{\gamma}x \geq 1. \end{cases}$$

$$K(\sqrt{\gamma}x, h(\sqrt{\gamma}x), \rho_{sc}) = \begin{cases} \frac{1}{2}\gamma x^2 & \text{for } 0 < \gamma \leq \frac{1}{4}, \\ \frac{1}{2}\gamma x^2 & \text{for } \frac{1}{4} \leq \gamma \leq 1 \text{ and } x \leq \frac{1}{\sqrt{\gamma}}, \\ \gamma x^2 - \frac{1}{2} \frac{1}{\gamma x^2} - \ln \gamma - 2 \ln x & \text{for } \frac{1}{4} \leq \gamma \leq 1 \text{ and } x \geq \frac{1}{\sqrt{\gamma}}, \\ \gamma x^2 - \frac{1}{2} \frac{1}{\gamma x^2} - \ln \gamma - 2 \ln x & \text{for } 1 \leq \gamma. \end{cases}$$

Thus we find:

$$\lim_{N \rightarrow \infty} \frac{1}{MN} \ln \int DU e^{\frac{N}{2} \text{Tr} \sqrt{\gamma} S U Y U^T} = \begin{cases} \frac{7}{12}\gamma & \text{for } 0 \leq \gamma \leq \frac{1}{4}, \\ \frac{5}{4}\gamma - \ln \gamma + 2(1 - \ln 2) - \frac{4}{3\sqrt{\gamma}} + \frac{1}{8\gamma} & \text{for } \frac{1}{4} \leq \gamma \leq 1, \\ \frac{7}{6}\gamma - \frac{1}{2}\gamma + 1 - 2 \ln 2 - \frac{1}{8\gamma} & \text{for } 1 \leq \gamma. \end{cases} \quad (117)$$

Replacing in (106), we find the same mutual information as in (115).

In Fig. 5, we compare the performance of the sub-linear RIE and the oracle estimator (98) with $M = \lfloor \sqrt{N} \rfloor$ for various values of N as well as with theoretical predictions for a uniformly distributed signal.

F.3 Uniform Noise

We now consider non-Gaussian noise, a noise matrix with eigenvalues which are uniformly distributed $\rho_Z = \mathcal{U}([1, 2])$. We have $G_{\mathcal{U}([1,2])}(z) = \ln \frac{z-1}{z-2}$. Thus the eigenvalues of the proposed estimator are:

$$\xi_i^* = \frac{1}{\sqrt{\gamma}} \mathbb{I}(\lambda_i^Y \notin [1, 2]) \ln \frac{\lambda_i^Y - 1}{\lambda_i^Y - 2} (\lambda_i^Y - 1) (\lambda_i^Y - 2).$$

F.3.1 MSE

Writing the overlap in terms of the eigenvalues of the signal, for $1 \leq i \leq M$ we have

$$(\mathbf{s}_i^T \mathbf{y}_i)^2 \rightarrow \frac{1}{4} \frac{1}{\gamma \lambda_i^S} \left(\text{csch} \frac{1}{2\sqrt{\gamma} \lambda_i^S} \right)^2. \quad (118)$$

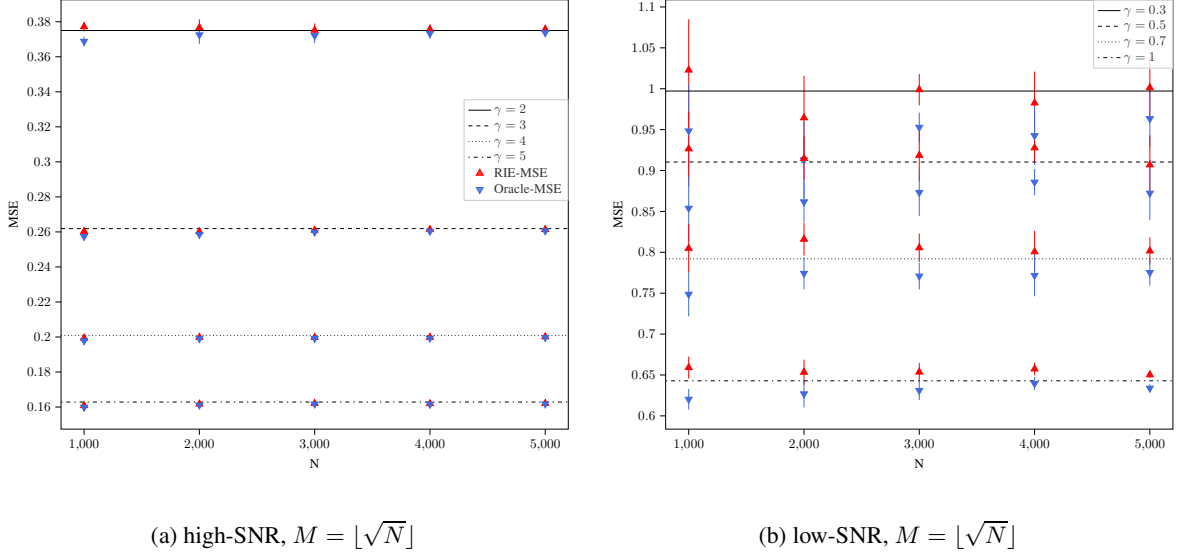


Figure 5: Comparison of the sub-linear RIE and the oracle estimator (98) for Gaussian noise with sub-linear signal with $\rho_S = \mathcal{U}([1, 2])$. Horizontal lines are MSE computed from (114). Points are averaged over 10 experiments (error bars might be invisible).

Note that, $G_{\mathcal{U}([1,2])}(1^-) = -\infty$ and $G_{\mathcal{U}([1,2])}(2^+) = +\infty$, so for any $\gamma > 0$ we have an outlier eigenvalue for each spike in the signal. From (118), the eigenvalues of the estimator are

$$\xi_i^* \rightarrow \frac{1}{4} \frac{1}{\gamma \lambda_i^S} \left(\operatorname{csch} \frac{1}{2\sqrt{\gamma} \lambda_i^S} \right)^2. \quad (119)$$

Using (104) we find in the asymptotic limit

$$\lim_{N \rightarrow \infty} \frac{1}{M} \|\mathcal{S} - \Xi^*(\mathbf{Y})\|_F^2 = \int \left[x^2 - \frac{1}{16} \frac{1}{\gamma^2 x^2} \left(\operatorname{csch} \frac{1}{2\sqrt{\gamma} x} \right)^4 \right] \rho_S(x) dx. \quad (120)$$

F.3.2 Example: Sub-linear Wishart Signal

As mentioned in section F.2.3, the limiting measure of the signal in this case is $\rho_S = \delta_{+1}$, so the MSE is $1 - \frac{1}{16} \frac{1}{\gamma^2} \left(\operatorname{csch} \frac{1}{2\sqrt{\gamma}} \right)^4$. In Fig. 6, we compare the performance of the sub-linear RIE and the oracle estimator (98) for $M = \lfloor \sqrt{N} \rfloor$ for various values of N . We observe that the performance of the RIE is very close to the one of oracle estimator (which requires the knowledge of the signal). Moreover, the MSE is close to the theoretical predictions.

G Examples and numerical calculations for linear ranks

G.1 Signal with Rademacher spectrum

In this example, we consider the case where $\rho_S = \frac{1}{2} \delta_{-1} + \frac{1}{2} \delta_{+1}$. Using the technique introduced in [45], we compute $\rho_Y = \rho_{\sqrt{\gamma} S} \boxplus \rho_{\text{sc}}$ in Appendix I. Fig. 12 shows the support of ρ_Y which consists of two disjoint intervals when $\gamma \geq 1$, and one single open set when $\gamma < 1$. Therefore, we expect that a phase transition, if it exists, should happen at a value $\gamma_c = 1$. By Theorem 2 the MMSE is a continuous function of γ , and the phase transition (if it exists) is of the second or higher order. The MMSE and the performance of the RIE for this example are plotted in figure 7.

From the expression of ρ_Y in Appendix I and from Theorem 2 we provide integral representations of the derivatives of the MMSE w.r.t. γ . These integrals are computed numerically and the result illustrated in figures 8 (a-b-c) for the MMSE and its first and second derivatives. For the third and the fourth derivatives the integral representation become unwieldy, so we only computed it numerically from the second derivative, as shown in figures 8 (f),(g). Based on these plots, we see that the third derivative (of the MMSE) at $\gamma_c = 1$ does not seem to exist, and therefore the free energy (18) (or mutual information) might have a fourth order phase transition at this point. Further numerical analysis in appendix I is compatible with a behavior of the function $\text{MMSE}(\gamma)$ close to the point $\gamma_c = 1$ of the form

$$\text{MMSE}(\gamma) \approx \text{MMSE}(1) + \text{MMSE}'(1)(\gamma-1) + \frac{1}{2} \text{MMSE}''(1)(\gamma-1)^2 + \alpha(\gamma-1)^3 (\ln |\gamma-1| + \beta) + o((\gamma-1)^3) \quad (121)$$

with $\alpha \approx -0.06125$, $\beta \approx 1.411$.

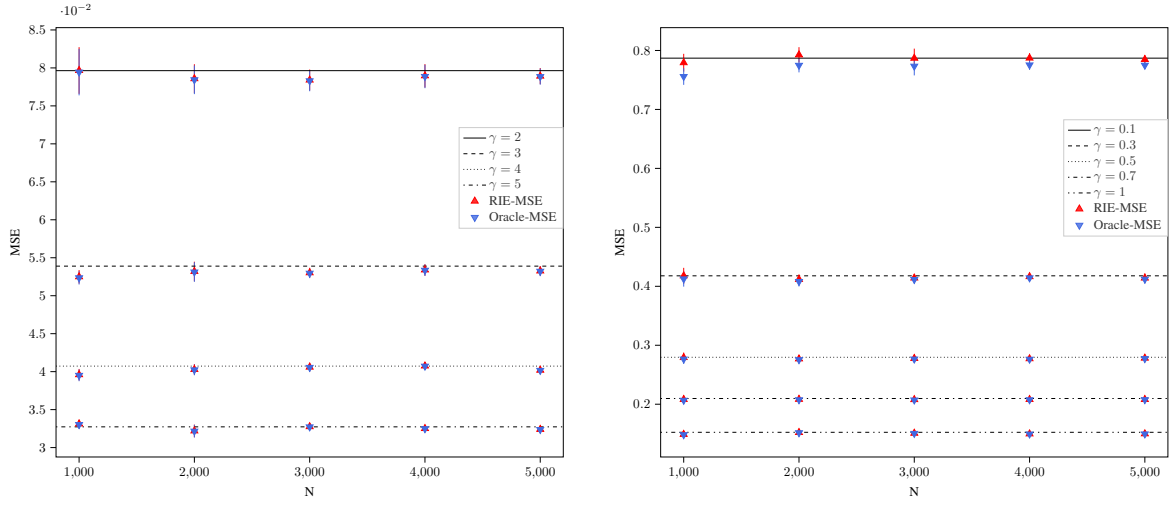


Figure 6: Comparison of the sub-linear RIE and the oracle estimator (98) for noise with uniform spectral distribution and sub-linear Wishart signal, for $M = \lfloor \sqrt{N} \rfloor$. Horizontal lines are MSE computed from $1 - \frac{1}{16} \frac{1}{\gamma^2} \left(\operatorname{csch} \frac{1}{2\sqrt{\gamma}} \right)^4$. Points are averaged over 10 experiments (error bars might be invisible). Note that unlike the Gaussian noise, for any SNR the estimation is possible and MSE is less than 1.

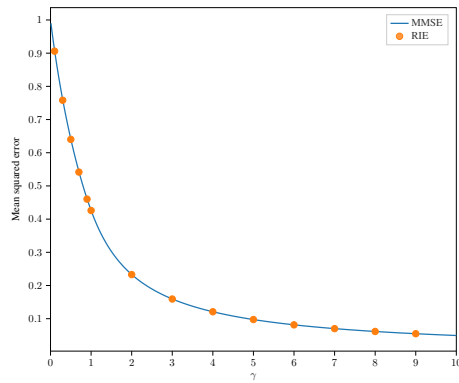


Figure 7: MMSE and the MSE of RIE (4) for the signal with spectrum $\rho_S = \frac{1}{2}\delta_{-1} + \frac{1}{2}\delta_{+1}$. The MMSE is continuous w.r.t. γ . The RIE is computed for $N = 1000$, and the results are averaged over 20 runs (error bars are invisible).

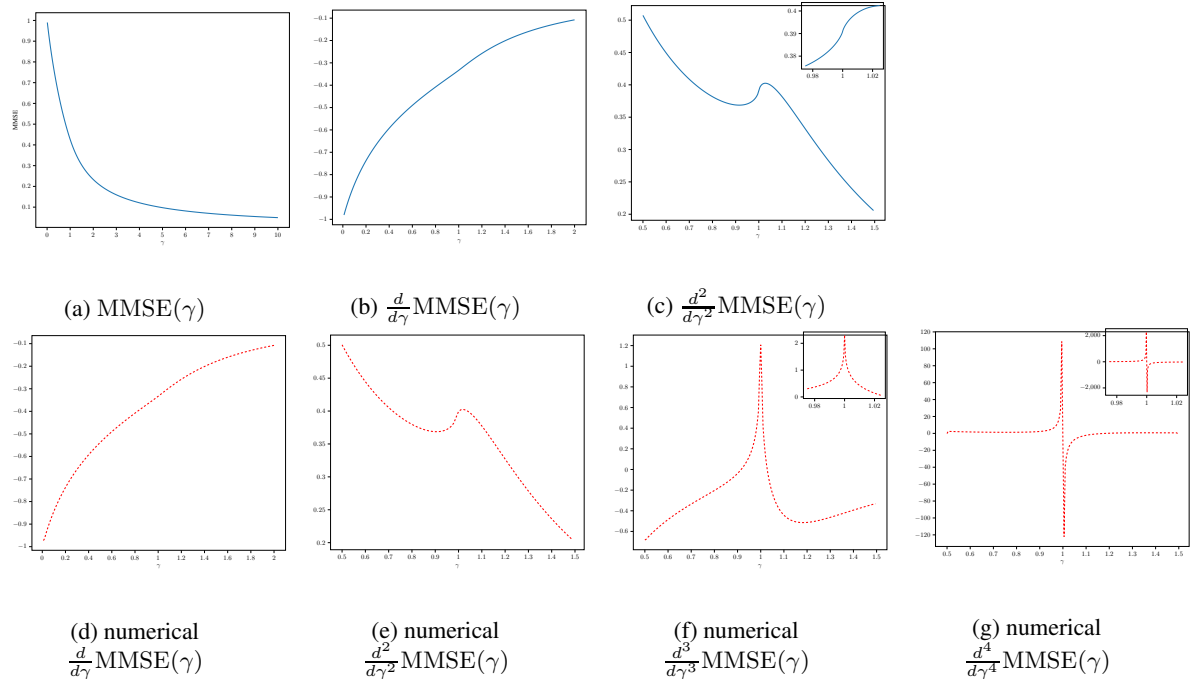


Figure 8: Analysis of the MMSE in example G.1. In plots (a),(b),(c) MMSE and its first and second derivatives are computed using the the expression (45). Plots (d), (e), (f) are the numerical differentiation of plots (a),(b), (c) respectively. The fourth derivative of the MMSE is computed from the curve in plot (c) by numerical second order differentiation. The first three plots shows that the MMSE, its first and second derivatives are continuous. But, plots (f), (g) suggests that the $\frac{d^2}{d\gamma^2} \text{MMSE}(\gamma)$ has a vertical tangent at $\gamma_c = 1$, and MMSE has a phase transition of third order at this point.

G.2 Signal with Bernoulli spectrum

Let $\rho_S = p\delta_0 + (1-p)\delta_{+1}$. The corresponding signal matrix is not full-rank but it has a rank linear in N . For this prior, the spectrum of $\rho_Y = \rho_{\sqrt{\gamma}S} \boxplus \rho_{\text{sc}}$ is computed in Appendix J using a similar technique as in the previous example. Depending on the SNR parameter γ the support of ρ_Y can be a single interval or is composed of two disjoint intervals as shown on figure 18. The MMSE and the MSE of RIE are illustrated in figure 9 for the two values $p = 0.9$ and $p = 0.3$.

In figure 10, the suitably normalized MMSE is plotted for the highly sparse case where p tends to 1. The MMSE is normalized by dividing by $p(1-p)$. We observe that as $p \rightarrow 1$ the MMSE approaches the MMSE of the rank-one symmetric matrix estimation problem, which has a phase transition at $\gamma_c = 1$.

G.3 Wishart Matrix

In this example, we consider the signal matrix \mathbf{S} to be $\frac{1}{N}\mathbf{X}\mathbf{X}^\top$, where $\mathbf{X} \in \mathbb{R}^{N \times M}$ has i.i.d. standard Gaussian entries. We look at the limit of aspect ratio $\frac{N}{M} \rightarrow q$. Then, the limiting spectral distribution of \mathbf{S} is a rescaling of the usual *Marchenko-Pastur* distribution by the factor α :

$$\rho_S(x) = \left(1 - \frac{1}{q}\right)^+ \delta(x) + \frac{\sqrt{\left(x - \left(\frac{1}{\sqrt{q}} - 1\right)^2\right) \left(\left(\frac{1}{\sqrt{q}} + 1\right)^2 - x\right)}}{2\pi x}. \quad (122)$$

The limiting spectral distribution of \mathbf{Y} is computed in Appendix K. For $q > 1$ the support of ρ_Y is the union of two disjoint intervals if $\gamma > q\left(\sqrt[3]{q} - 1\right)^{-3}$, and is a single interval otherwise. As in the previous example, we expect that in the high sparse regime, the MMSE behaves like the low-rank case. In figure 11 the MMSE is illustrated large q 's.

G.4 Finite-rank deformation of a Wigner matrix as signal

First, consider the case where \mathbf{S} is a standard Wigner matrix, then by independence of \mathbf{S} and \mathbf{Z} , \mathbf{Y} is also a Wigner matrix with variance $\gamma + 1$, and ρ_Y is a semi-circle law of variance $\gamma + 1$. From (51), we find that $\frac{1}{N^2} I_N(\mathbf{S}; \mathbf{Y})$ converges to $\frac{1}{4} \ln(\gamma + 1)$. This limit could also be obtained using the Gaussianity of entries of the matrices.

Now, let \mathbf{S} be a finite rank deformation of a Wigner matrix, $\mathbf{S} = \mathbf{A} + \mathbf{\zeta}$, where \mathbf{A} is a *finite-rank* symmetric matrix, and $\mathbf{\zeta} \in \mathbb{R}^{N \times N}$ is a symmetric Gaussian matrix with variance $\frac{1}{N}$ for non-diagonal, and $\frac{2}{N}$ for diagonal entries. We

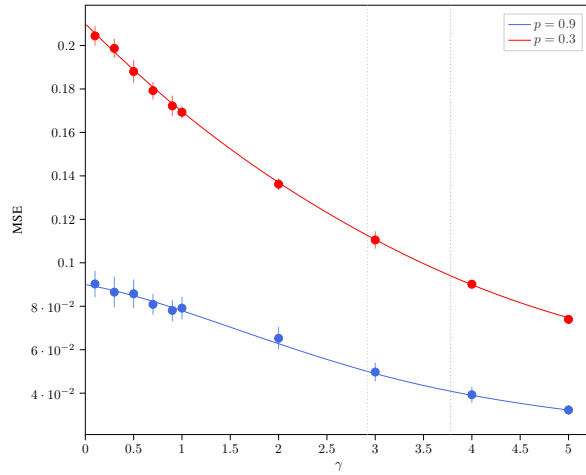


Figure 9: MMSE computed for the signal with Bernoulli spectrum $\rho_S = p\delta_0 + (1-p)\delta_{+1}$ for $p = 0.3$ and 0.9 . The MMSE is continuous w.r.t. γ . The vertical dashed lines corresponds to the values of γ , i.e., 2.92 for $p = 0.9$ and 3.78 for $p = 0.3$, where the disjoint intervals of the support of ρ_Y merge. We do not observe any phase transition for any low order derivative at these values. The MSE of RIE is computed for $N = 1000$, and the results are averaged over 20 runs.

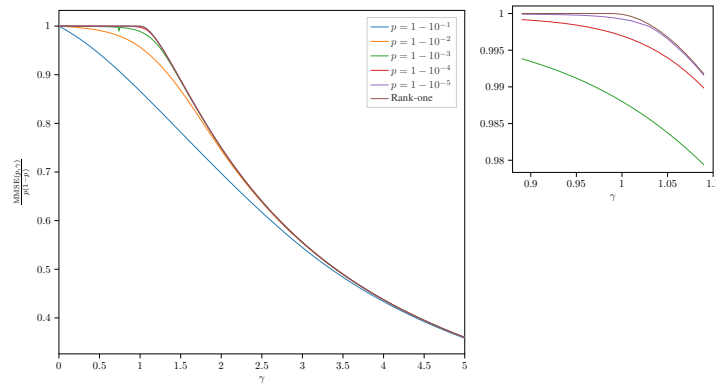


Figure 10: Normalized MMSE for the signal with spectrum $\rho_S = p\delta_0 + (1-p)\delta_{+1}$ for $p \rightarrow 1$. The MMSE of the rank-one problem is also plotted for comparison.

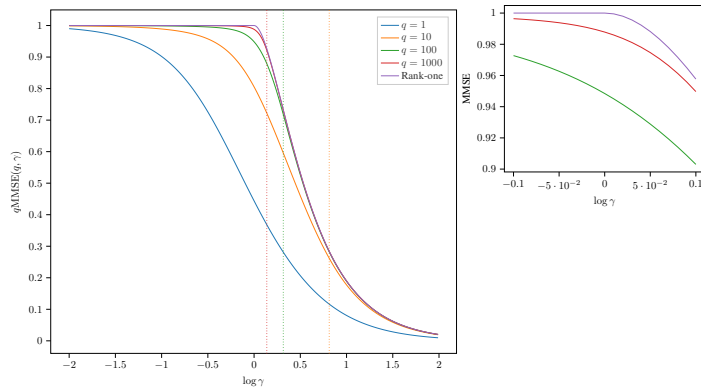


Figure 11: Normalized MMSE for the signal with the Marchenko-Pastur spectral distribution for large q 's. The MMSE of the rank-one problem is also plotted for comparison. The vertical dashed lines corresponds to the critical value where the support of ρ_Y splits into two intervals. We do not find any phase transition on low order derivatives

have the observation $\mathbf{Y} = \sqrt{\gamma}\mathbf{S} + \mathbf{Z}$. Since \mathbf{A} has finite rank, the limiting spectral measure of \mathbf{S} is the semicircle law, and average mutual information $\frac{1}{N^2}I_N(\mathbf{S}; \mathbf{Y})$ converges to $\frac{1}{4}\ln(\gamma + 1)$, (51). Since \mathbf{Z} and ζ are independent, the observation matrix \mathbf{Y} has the same distribution as the matrix $\tilde{\mathbf{Y}} = \sqrt{\gamma}\mathbf{A} + \sqrt{\gamma+1}\tilde{\mathbf{Z}}$, where $\tilde{\mathbf{Z}}$ is a symmetric Gaussian matrix, so $\mathcal{H}(\mathbf{Y}) = \mathcal{H}(\tilde{\mathbf{Y}})$. Define the matrix $\mathbf{Y}' = \sqrt{\frac{\gamma}{\gamma+1}}\mathbf{A} + \mathbf{Z}'$. By symmetry of the matrices, we have:

$$\mathcal{H}_N(\mathbf{Y}') = \mathcal{H}_N(\mathbf{Y}) - \frac{N(N+1)}{2} \ln \sqrt{\gamma+1}. \quad (123)$$

Here \mathbf{Y}' has the form of the observation matrix in the low-rank matrix estimation, which has been extensively studied in [12, 13], and in particular, it has been shown that under suitable assumptions, the average mutual information $\frac{1}{N}I_N(\mathbf{A}; \mathbf{Y}')$ converges to a finite value. By definition of mutual information, and (123), we have:

$$\begin{aligned} \frac{1}{N}I_N(\mathbf{A}; \mathbf{Y}') &= \frac{1}{N}\mathcal{H}_N(\mathbf{Y}') - \frac{1}{N}\mathcal{H}_N(\mathbf{Z}') \\ &= \frac{1}{N}\mathcal{H}_N(\mathbf{Y}) - \frac{1}{N}\mathcal{H}_N(\mathbf{Z}') - \frac{N+1}{4} \ln(\gamma+1) \\ &= \frac{1}{N}I_N(\mathbf{S}; \mathbf{Y}) - \frac{N+1}{4} \ln(\gamma+1). \end{aligned} \quad (124)$$

Dividing by N and taking the limit, we find the asymptotic mutual information

$$\begin{aligned} \lim_{N \rightarrow \infty} \frac{1}{N^2}I_N(\mathbf{S}; \mathbf{Y}) &= \lim_{N \rightarrow \infty} \frac{1}{N^2}I_N(\mathbf{A}; \mathbf{Y}') + \frac{N+1}{4N} \ln(\gamma+1) \\ &= \frac{1}{4} \ln(\gamma+1). \end{aligned} \quad (125)$$

where we used the fact that $\frac{1}{N}I_N(\mathbf{A}; \mathbf{Y}')$ has a finite limit. Moreover, from (124) the finite-size correction term for the asymptotic average mutual information can be derived as

$$\lim_{N \rightarrow \infty} N \left(\frac{1}{N^2}I_N(\mathbf{S}; \mathbf{Y}) - \frac{1}{4} \ln(\gamma+1) \right) = \lim_{N \rightarrow \infty} \frac{1}{N}I_N(\mathbf{A}; \mathbf{Y}') + \frac{1}{4} \ln(\gamma+1). \quad (126)$$

Therefore when \mathbf{S} is a finite rank deformation of the Wigner matrix, the finite-size correction term is directly related to the mutual information in the low-rank matrix estimation problem, which may exhibit a phase transition.

Now, let \mathbf{A} be a *rank-one* matrix. $\mathbf{S} = \frac{\sqrt{\eta}}{N}\mathbf{x}\mathbf{x}^\top + \zeta$ where $\mathbf{x} \in \mathbb{R}^N$ has i.i.d. components distributed according to the standard normal distribution. The matrix $\mathbf{Y}' = \frac{\sqrt{\frac{\eta\gamma}{\gamma+1}}}{N}\mathbf{x}\mathbf{x}^\top + \mathbf{Z}'$ is a rescaling of the rank-one model studied in [13], and since mutual information is invariant under rescaling, using Theorem 1 in [13], we have:

$$\lim_{N \rightarrow \infty} \frac{1}{N}I_N(\mathbf{x}; \mathbf{Y}') = \begin{cases} \frac{1}{4} \frac{\eta\gamma}{\gamma+1} & \text{if } \frac{\eta\gamma}{\gamma+1} \leq 1, \\ \frac{1}{4} \frac{\gamma+1}{\eta\gamma} + \frac{1}{2} \ln \frac{\eta\gamma}{\gamma+1} & \text{else.} \end{cases} \quad (127)$$

Fix $\eta \leq 1$. For all $\gamma > 0$, we have $\frac{\eta\gamma}{\gamma+1} \leq 1$ and there is no phase transition in the mutual information. On the other hand, for $\eta > 1$ mutual information has a phase transition at $\gamma = \frac{1}{\eta-1}$. From random matrix theory [39], we know that For $\eta \leq 1$, in the limit $N \rightarrow \infty$, all the eigenvalues of \mathbf{S} are inside the bulk, whereas for $\eta > 1$ one eigenvalue (which is the largest one) is outside the bulk. Therefore, for this particular signal, we can relate the phase transition of the correction term to the existence of an eigenvalue outside the bulk of ρ_S in the asymptotic limit.

H Further details for proof of Theorem 1

H.1 Proof of lemma A.1

To prove lemma A.1 we first need four preliminary lemmas.

Lemma H.1. For any N , and $N \times N$ symmetric matrices \mathbf{A}, \mathbf{B} with spectral radius $r^{(\mathbf{A})}, r^{(\mathbf{B})}$

$$-\frac{1}{2}r^{(\mathbf{A})}r^{(\mathbf{B})} \leq \mathcal{J}_N(\mathbf{A}, \mathbf{B}) \leq \frac{1}{2}r^{(\mathbf{A})}r^{(\mathbf{B})}.$$

Proof. Let $\mathbf{A} = \mathbf{U}_A \mathbf{\Lambda}_A \mathbf{U}_A^\top$, $\mathbf{B} = \mathbf{U}_B \mathbf{\Lambda}_B \mathbf{U}_B^\top$ be the eigendecomposition of \mathbf{A} , \mathbf{B} . We can write

$$\mathcal{I}_N(\mathbf{A}, \mathbf{B}) = \int D\mathbf{U} e^{\frac{N}{2} \text{Tr} \mathbf{U} \mathbf{\Lambda}_A \mathbf{U}^\top \mathbf{\Lambda}_B} = \int D\mathbf{U} e^{\frac{N}{2} \sum_{i,j} \lambda_i^{(\mathbf{A})} \lambda_j^{(\mathbf{B})} U_{ij}^2}.$$

For each for all $i, j \in \{1, \dots, N\}$, $-\lambda_i^{(\mathbf{A})} \lambda_j^{(\mathbf{B})} \leq r^{(\mathbf{A})} r^{(\mathbf{B})}$. Therefore, we get

$$\begin{aligned} \mathcal{I}_N(\mathbf{A}, \mathbf{B}) &= \int D\mathbf{U} e^{\frac{N}{2} \sum_{i,j} \lambda_i^{(\mathbf{A})} \lambda_j^{(\mathbf{B})} U_{ij}^2} \\ &\leq \int D\mathbf{U} e^{\frac{N}{2} r^{(\mathbf{A})} r^{(\mathbf{B})} \sum_{i,j} U_{ij}^2} \\ &= \int D\mathbf{U} e^{\frac{N}{2} r^{(\mathbf{A})} r^{(\mathbf{B})}} \\ &= e^{\frac{N}{2} r^{(\mathbf{A})} r^{(\mathbf{B})}}. \end{aligned}$$

Similarly we can obtain $\mathcal{I}_N(\mathbf{A}, \mathbf{B}) \geq e^{-\frac{N}{2} r^{(\mathbf{A})} r^{(\mathbf{B})}}$. Therefore

$$-\frac{1}{2} r^{(\mathbf{A})} r^{(\mathbf{B})} \leq \mathcal{J}_N(\mathbf{A}, \mathbf{B}) \leq \frac{1}{2} r^{(\mathbf{A})} r^{(\mathbf{B})}.$$

□

Lemma H.2. Let $r^{(\tilde{\mathbf{Y}})}$ denote the spectral radius of the matrix $\tilde{\mathbf{Y}} = \sqrt{\gamma} \mathbf{\Lambda}^0 + \tilde{\mathbf{Z}}$. For $k > 2 + \sqrt{\gamma}C$, we have

$$\mathbb{P}\{r^{(\tilde{\mathbf{Y}})} \geq k\} \leq 4e^{-\frac{N}{4}(k - \sqrt{\gamma}C - 2)^2}.$$

Proof. Denote the top and bottom eigenvalues of $\tilde{\mathbf{Y}}$ by $\lambda_{\max}^{(\tilde{\mathbf{Y}})}$, $\lambda_{\min}^{(\tilde{\mathbf{Y}})}$. By Weyls' inequality,

$$\begin{aligned} \lambda_{\max}^{(\tilde{\mathbf{Y}})} &\leq \sqrt{\gamma} \max_i \lambda_i^0 + \lambda_{\max}^{(\tilde{\mathbf{Z}})} \leq \sqrt{\gamma}C + \lambda_{\max}^{(\tilde{\mathbf{Z}})} \\ \lambda_{\min}^{(\tilde{\mathbf{Y}})} &\geq \sqrt{\gamma} \min_i \lambda_i^0 + \lambda_{\min}^{(\tilde{\mathbf{Z}})} \geq -\sqrt{\gamma}C + \lambda_{\min}^{(\tilde{\mathbf{Z}})} \end{aligned}$$

where $\lambda_{\max}^{(\tilde{\mathbf{Z}})}, \lambda_{\min}^{(\tilde{\mathbf{Z}})}$ are the top and bottom eigenvalues of $\tilde{\mathbf{Z}}$. Thus, we can write

$$\begin{aligned} \mathbb{P}\{\lambda_{\max}^{(\tilde{\mathbf{Y}})} \geq k\} &\leq \mathbb{P}\{\lambda_{\max}^{(\tilde{\mathbf{Z}})} + \sqrt{\gamma}C \geq k\} \\ &= \mathbb{P}\{\lambda_{\max}^{(\tilde{\mathbf{Z}})} \geq k - \sqrt{\gamma}C\}. \end{aligned}$$

By [64] (Theorem II.11), for $k - \sqrt{\gamma}C > 2$, we have

$$\mathbb{P}\{\lambda_{\max}^{(\tilde{\mathbf{Z}})} \geq k - \sqrt{\gamma}C\} \leq e^{-\frac{N}{4}(k - \sqrt{\gamma}C - 2)^2}$$

and therefore we get

$$\mathbb{P}\{\lambda_{\max}^{(\tilde{\mathbf{Y}})} \geq k\} \leq e^{-\frac{N}{4}(k + \sqrt{\gamma}C - 2)^2}. \quad (128)$$

For the bottom eigenvalue we have

$$\begin{aligned} \mathbb{P}\{\lambda_{\min}^{(\tilde{\mathbf{Y}})} \leq -k\} &\leq \mathbb{P}\{-\sqrt{\gamma}C + \lambda_{\min}^{(\tilde{\mathbf{Z}})} \leq -k\} \\ &= \mathbb{P}\{\lambda_{\min}^{(\tilde{\mathbf{Z}})} \leq \sqrt{\gamma}C - k\} \\ &\leq e^{-\frac{N}{4}(k - \sqrt{\gamma}C - 2)^2}. \end{aligned} \quad (129)$$

From (128), (129), we get

$$\begin{aligned} \mathbb{P}\{r^{(\tilde{\mathbf{Y}})} \geq k\} &\leq \mathbb{P}\{|\lambda_{\max}^{(\tilde{\mathbf{Y}})}| \geq k\} + \mathbb{P}\{|\lambda_{\min}^{(\tilde{\mathbf{Y}})}| \geq k\} \\ &\leq \mathbb{P}\{\lambda_{\max}^{(\tilde{\mathbf{Y}})} \geq k\} + \mathbb{P}\{\lambda_{\max}^{(\tilde{\mathbf{Y}})} \leq -k\} + \mathbb{P}\{\lambda_{\min}^{(\tilde{\mathbf{Y}})} \geq k\} + \mathbb{P}\{\lambda_{\min}^{(\tilde{\mathbf{Y}})} \leq -k\} \\ &\leq 2\mathbb{P}\{\lambda_{\max}^{(\tilde{\mathbf{Y}})} \geq k\} + 2\mathbb{P}\{\lambda_{\min}^{(\tilde{\mathbf{Y}})} \leq -k\} \\ &\leq 4e^{-\frac{N}{4}(k - \sqrt{\gamma}C - 2)^2} \end{aligned}$$

for $k > 2 + \sqrt{\gamma}C$.

□

Lemma H.3. For any polynomial function g , and k a sufficiently large constant, we have that

$$\lim_{n \rightarrow \infty} \mathbb{E}[g(r(\tilde{\mathbf{Y}})) \mathbb{I}\{r(\tilde{\mathbf{Y}}) \geq k\}] = 0.$$

Proof. By linearity of expectation, it is enough to consider the case $g(x) = x^i$. Let $X = r(\tilde{\mathbf{Y}})^i \mathbb{I}\{r(\tilde{\mathbf{Y}}) \geq k\}$ a non-negative random variable. We have

$$\begin{aligned} \mathbb{E}[X] &= \int_0^\infty \mathbb{P}(X \geq x) dx \\ &= i \int_0^\infty \mathbb{P}(X \geq x^i) x^{i-1} dx \\ &= i \int_0^\infty \mathbb{P}(r(\tilde{\mathbf{Y}})^i \mathbb{I}\{r(\tilde{\mathbf{Y}}) \geq k\} \geq x^i) x^{i-1} dx \\ &= i \int_0^\infty \mathbb{P}(r(\tilde{\mathbf{Y}}) \geq k, r(\tilde{\mathbf{Y}}) \geq x) x^{i-1} dx \\ &= i \int_0^k \mathbb{P}(r(\tilde{\mathbf{Y}}) \geq k) x^{i-1} dx + i \int_k^\infty \mathbb{P}(r(\tilde{\mathbf{Y}}) \geq x) x^{i-1} dx \\ &\leq 4e^{-\frac{N}{4}(k-\sqrt{\gamma}C-2)^2} k^i + 4i \int_k^\infty e^{-\frac{N}{4}(x-\sqrt{\gamma}C-2)^2} dx \\ &\leq 4e^{-\frac{N}{4}(k-\sqrt{\gamma}C-2)^2} k^i + 4i \int_0^\infty e^{-\frac{N}{4}(x-\sqrt{\gamma}C-2)^2} x^{i-1} dx. \end{aligned}$$

The first term converges to 0 as $N \rightarrow \infty$. The second term involves moments of a Gaussian with variance $\frac{1}{2N}$, one can see that the second term also converges to 0. Thus, $\lim_{N \rightarrow \infty} \mathbb{E}[X] = 0$. \square

Lemma H.4. For the sequence of random matrices $\tilde{\mathbf{Y}}$, the log spherical integral $\mathcal{J}_N(\sqrt{\gamma}\boldsymbol{\Lambda}^0, \tilde{\mathbf{Y}})$ converges almost surely to a well-defined limit, denoted by $\mathcal{J}[\rho_{\sqrt{\gamma}S}, \rho_{\sqrt{\gamma}S} \boxplus \rho_{\text{sc}}]$.

Proof. By assumption 1.A the support of $\hat{\mu}_{\sqrt{\gamma}\boldsymbol{\Lambda}^0}^{(N)}$ is included in a compact subset of $\mathbb{R}, [-\sqrt{\gamma}C, \sqrt{\gamma}C]$, for all $N \in \mathbb{N}$. Moreover, by the law of large numbers, $\hat{\mu}_{\sqrt{\gamma}\boldsymbol{\Lambda}^0}^{(N)}$ converges weakly towards $\rho_{\sqrt{\gamma}S}$.

Consider the sequence $\sqrt{\gamma}\boldsymbol{\Lambda}^0 + \tilde{\mathbf{Z}}$. For each matrix in the sequence, the second moment of the empirical spectral distribution is:

$$\frac{1}{N} \text{Tr}(\sqrt{\gamma}\boldsymbol{\Lambda}^0 + \tilde{\mathbf{Z}})^2 = \frac{1}{N} \gamma \text{Tr}\boldsymbol{\Lambda}^{0^2} + \frac{2}{N} \sqrt{\gamma} \text{Tr}\boldsymbol{\Lambda}^0 \tilde{\mathbf{Z}} + \frac{1}{N} \text{Tr}\tilde{\mathbf{Z}}^2.$$

The first term is bounded (for all N) by the construction of $\boldsymbol{\Lambda}^0$. The last term is also bounded since the second moment of the sequence of Wigner matrices converges to 1 almost surely. For the second term, we have

$$\begin{aligned} \frac{1}{N} \text{Tr}\boldsymbol{\Lambda}^0 \tilde{\mathbf{Z}} &\leq \frac{1}{N} \sqrt{\sum \gamma_i^{0^2}} \sqrt{\text{Tr}\tilde{\mathbf{Z}}^2} \\ &\leq C \sqrt{\frac{1}{N} \text{Tr}\tilde{\mathbf{Z}}^2} \end{aligned}$$

which is bounded for all N , since $\frac{1}{N} \text{Tr}\tilde{\mathbf{Z}}^2$ is a convergent sequence (a.s.). Therefore, the sequence of matrices $\sqrt{\gamma}\boldsymbol{\Lambda}^0 + \tilde{\mathbf{Z}}$ has bounded second moment for all N almost surely. Moreover, according to [41], by the independence of $\boldsymbol{\Lambda}^0$ and $\tilde{\mathbf{Z}}$, the empirical spectral distribution of this sequence converges weakly, almost surely to the free additive convolution of $\rho_{\sqrt{\gamma}S}$ with the semi-circle law ρ_{sc} .

Therefore, the conditions of theorem 1 in [43] hold a.s. for the sequence $\boldsymbol{\Lambda}^0, \sqrt{\gamma}\boldsymbol{\Lambda}^0 + \tilde{\mathbf{Z}}$. Hence, $\mathcal{J}_N(\sqrt{\gamma}\boldsymbol{\Lambda}^0, \tilde{\mathbf{Y}})$ has a well-defined limit which is a function of $\rho_{\sqrt{\gamma}S}$ and $\rho_{\sqrt{\gamma}S} \boxplus \rho_{\text{sc}}$, and is denoted by $\mathcal{J}[\rho_{\sqrt{\gamma}S}, \rho_{\sqrt{\gamma}S} \boxplus \rho_{\text{sc}}]$. \square

Now, we are ready to prove lemma A.1.

Proof. of lemma A.1. For simplicity of notation, we denote $\mathcal{J}_N(\sqrt{\gamma}\boldsymbol{\Lambda}^0, \tilde{\mathbf{Y}})$ by \mathcal{J}_N , and $\mathcal{J}[\rho_{\sqrt{\gamma}S}, \rho_{\sqrt{\gamma}S} \boxplus \rho_{\text{sc}}]$ by \mathcal{J} . By Jensen's inequality (note that the expectation is over the matrix $\tilde{\mathbf{Z}}$), we have

$$|\mathbb{E}[\mathcal{J}_N] - \mathcal{J}| \leq \mathbb{E}[|\mathcal{J}_N - \mathcal{J}|]. \quad (130)$$

Let $X_N \equiv \mathcal{J}_N - \mathcal{J}$. For $\epsilon > 0$ We can write

$$\begin{aligned} \mathbb{E}[|X_N|] &= \mathbb{E}[|X_N| \mathbb{I}\{|X_N| \leq \epsilon\}] + \mathbb{E}[|X_N| \mathbb{I}\{|X_N| > \epsilon\}] \\ &\leq \epsilon + \mathbb{E}[|X_N| \mathbb{I}\{|X_N| > \epsilon\}]. \end{aligned} \quad (131)$$

By lemma H.1, $|\mathcal{J}_N| \leq \frac{1}{2}\sqrt{\gamma}Cr^{(\tilde{\mathcal{Y}})}$, so the second term in (131) can be bounded as,

$$\mathbb{E}[|X_N| \mathbb{I}\{|X_N| > \epsilon\}] \leq \mathbb{E}[|W_N| \mathbb{I}\{|X_N| > \epsilon\}] \quad (132)$$

where

$$W_N = \max \left\{ \left| \mathcal{J} - \frac{1}{2}\sqrt{\gamma}Cr^{(\tilde{\mathcal{Y}})} \right|, \left| \mathcal{J} + \frac{1}{2}\sqrt{\gamma}Cr^{(\tilde{\mathcal{Y}})} \right| \right\} = \frac{1}{2}\sqrt{\gamma}Cr^{(\tilde{\mathcal{Y}})} + \text{sign}(\mathcal{J})\mathcal{J}.$$

For any positive constant t , we have

$$\begin{aligned} \mathbb{E}[|W_N| \mathbb{I}\{|X_N| > \epsilon\}] &= \mathbb{E}[|W_N| \mathbb{I}\{|X_N| > \epsilon\} \mathbb{I}\{|W_N| \leq t\}] + \mathbb{E}[|W_N| \mathbb{I}\{|X_N| > \epsilon\} \mathbb{I}\{|W_N| > t\}] \\ &\leq \mathbb{E}[|W_N| \mathbb{I}\{|X_N| > \epsilon\} \mathbb{I}\{|W_N| \leq t\}] + \mathbb{E}[|W_N| \mathbb{I}\{|W_N| > t\}] \end{aligned} \quad (133)$$

For the first term in (133) we can write

$$\begin{aligned} \mathbb{E}[|W_N| \mathbb{I}\{|X_N| > \epsilon\} \mathbb{I}\{|W_N| \leq t\}] &\leq t \mathbb{E}[\mathbb{I}\{|X_N| > \epsilon\}] \\ &\leq t \mathbb{P}(|X_N| > \epsilon) \end{aligned} \quad (134)$$

and the second term in (133) can be rewritten as

$$\mathbb{E}[|W_N| \mathbb{I}\{|W_N| > t\}] = \mathbb{E} \left[|W_N| \mathbb{I} \left\{ r^{(\tilde{\mathcal{Y}})} > \frac{2}{\sqrt{\gamma}C} (t - \text{sign}(\mathcal{J})\mathcal{J}) \right\} \right]. \quad (135)$$

From (132), (133), (134), we obtain

$$\mathbb{E}[|X_N| \mathbb{I}\{|X_N| > \epsilon\}] \leq t \mathbb{P}(|X_N| > \epsilon) + \mathbb{E} \left[|W_N| \mathbb{I} \left\{ r^{(\tilde{\mathcal{Y}})} > \frac{2}{\sqrt{\gamma}C} (t - \text{sign}(\mathcal{J})\mathcal{J}) \right\} \right]. \quad (136)$$

Notice that W_N is a polynomial function of $r^{(\tilde{\mathcal{Y}})}$, so by lemma H.3, vanishes as $N \rightarrow \infty$ for sufficiently large constant t . By lemma H.4, $\mathbb{P}(|X_N| > \epsilon) \xrightarrow{N \rightarrow \infty} 0$. For a fixed $t > 0$, the first term in (136) goes to 0 in the limit $N \rightarrow \infty$. Therefore, taking the limit of both sides in (131), for any $\epsilon > 0$, we find:

$$\lim_{N \rightarrow \infty} \mathbb{E}[|X_N|] \leq \epsilon. \quad (137)$$

From which, by (130), we deduce that $\lim_{N \rightarrow \infty} \mathbb{E}[\mathcal{J}_N] = \mathcal{J}$. \square

H.2 Proof of proposition 2

Consider two matrices with the same eigenvectors, $\mathbf{S} = \mathbf{U}\mathbf{\Lambda}\mathbf{U}^\top$ and $\tilde{\mathbf{S}} = \mathbf{U}\tilde{\mathbf{\Lambda}}\mathbf{U}^\top$, where \mathbf{U} is a Haar orthogonal matrix, and $\boldsymbol{\lambda}, \tilde{\boldsymbol{\lambda}}$ are distributed according to $P_N^{(1)}(\boldsymbol{\lambda}), P_N^{(2)}(\tilde{\boldsymbol{\lambda}})$, respectively. For two such matrices, we write $(\mathbf{S}, \tilde{\mathbf{S}}) \sim Q_N(\mathbf{U}, \boldsymbol{\lambda}, \tilde{\boldsymbol{\lambda}})$, where $Q_N(\mathbf{U}, \boldsymbol{\lambda}, \tilde{\boldsymbol{\lambda}})$ is the joint p.d.f. of $\mathbf{U}, \boldsymbol{\lambda}, \tilde{\boldsymbol{\lambda}}$,

$$dQ_N(\mathbf{U}, \boldsymbol{\lambda}, \tilde{\boldsymbol{\lambda}}) = d\mu_N(\mathbf{U}) P_N^{(1)}(\boldsymbol{\lambda}) d\boldsymbol{\lambda} P_N^{(2)}(\tilde{\boldsymbol{\lambda}}) d\tilde{\boldsymbol{\lambda}}.$$

For $t \in [0, 1]$ an interpolating parameter, consider the following observation model:

$$\begin{cases} \mathbf{Y}_1^{(t)} = \sqrt{\gamma t} \mathbf{S} + \mathbf{Z}_1 \\ \mathbf{Y}_2^{(t)} = \sqrt{\gamma(1-t)} \tilde{\mathbf{S}} + \mathbf{Z}_2 \end{cases} \quad (138)$$

where $\mathbf{Z}_1, \mathbf{Z}_2$ are Wigner matrices independent of each other, and $(\mathbf{S}, \tilde{\mathbf{S}}) \sim Q_N(\mathbf{U}, \boldsymbol{\lambda}, \tilde{\boldsymbol{\lambda}})$. The free energy for this model can be written as :

$$\begin{aligned} F_N(t) &= -\frac{1}{N^2} \mathbb{E}_{\mathbf{Y}_1^{(t)}, \mathbf{Y}_2^{(t)}} \left[\ln \int dQ_N(\mathbf{U}, \boldsymbol{\lambda}, \tilde{\boldsymbol{\lambda}}) e^{\frac{N}{2} \text{Tr}[\sqrt{\gamma t} \mathbf{X} \mathbf{Y}_1^{(t)} - \frac{\gamma t}{2} \mathbf{X}^2 + \sqrt{\gamma(1-t)} \tilde{\mathbf{X}} \mathbf{Y}_2^{(t)} - \frac{\gamma(1-t)}{2} \tilde{\mathbf{X}}^2]} \right] \\ &= -\frac{1}{N^2} \mathbb{E}_{\mathbf{Y}_1^{(t)}, \mathbf{Y}_2^{(t)}} \left[\ln \int dQ_N(\mathbf{U}, \boldsymbol{\lambda}, \tilde{\boldsymbol{\lambda}}) e^{\frac{N}{2} \text{Tr}[\gamma t \mathbf{X} \mathbf{S} + \sqrt{\gamma t} \mathbf{X} \mathbf{Z}_1 - \frac{\gamma t}{2} \mathbf{X}^2 + \gamma(1-t) \tilde{\mathbf{X}} \tilde{\mathbf{S}} + \sqrt{\gamma(1-t)} \tilde{\mathbf{X}} \mathbf{Z}_2 - \frac{\gamma(1-t)}{2} \tilde{\mathbf{X}}^2]} \right] \end{aligned}$$

where \mathbf{X} , $\tilde{\mathbf{X}}$ has the same eigenspace, $\mathbf{X} = \mathbf{U}\mathbf{\Lambda}\mathbf{U}^\top$, $\tilde{\mathbf{X}} = \mathbf{U}\tilde{\mathbf{\Lambda}}\mathbf{U}^\top$. Note that, for $t = 0$ the only term depending on $\boldsymbol{\lambda}$ (in both the inner and outer expectation) is the pdf $P_N^{(1)}(\boldsymbol{\lambda})$ and we can integrate over $\boldsymbol{\lambda}$ in both of the expectations, to get $F_N(0) = F_N^{(2)}(\gamma)$. Similarly, we have $F_N(1) = F_N^{(1)}(\gamma)$.

Taking the derivative w.r.t. t , we get:

$$\begin{aligned} \frac{d}{dt}F_N(t) &= -\frac{1}{N}\mathbb{E}\left[\frac{\gamma}{2}\text{Tr}\langle\mathbf{X}\mathbf{S}\rangle_t + \frac{1}{4}\sqrt{\frac{\gamma}{t}}\text{Tr}\mathbf{Z}_1\langle\mathbf{X}\rangle_t - \frac{\gamma}{4}\text{Tr}\langle\mathbf{X}^2\rangle_t\right. \\ &\quad \left. - \frac{\gamma}{2}\text{Tr}\langle\tilde{\mathbf{X}}\tilde{\mathbf{S}}\rangle_t - \frac{1}{4}\sqrt{\frac{\gamma}{1-t}}\text{Tr}\mathbf{Z}_2\langle\tilde{\mathbf{X}}\rangle_t + \frac{\gamma}{4}\text{Tr}\langle\tilde{\mathbf{X}}^2\rangle_t\right] \end{aligned}$$

where $\langle\cdot\rangle_t$ denotes the expectation with respect to the posterior distribution of the model (138). By integration by parts, we have

$$\mathbb{E}[\text{Tr}\mathbf{Z}_1\langle\mathbf{X}\rangle_t] = \sqrt{\gamma t}\mathbb{E}[\text{Tr}\langle\mathbf{X}^2\rangle_t - \text{Tr}\langle\mathbf{X}\rangle_t^2], \quad \mathbb{E}[\text{Tr}\mathbf{Z}_2\langle\tilde{\mathbf{X}}\rangle_t] = \sqrt{\gamma(1-t)}\mathbb{E}[\text{Tr}\langle\tilde{\mathbf{X}}^2\rangle_t - \text{Tr}\langle\tilde{\mathbf{X}}\rangle_t^2]$$

Therefore,

$$\begin{aligned} \frac{d}{dt}F_N(t) &= -\frac{1}{N}\frac{\gamma}{4}\mathbb{E}\left[2\text{Tr}\langle\mathbf{X}\mathbf{S}\rangle_t - \text{Tr}\langle\mathbf{X}\rangle_t^2 - 2\text{Tr}\langle\tilde{\mathbf{X}}\tilde{\mathbf{S}}\rangle_t + \text{Tr}\langle\tilde{\mathbf{X}}\rangle_t^2\right] \\ &= \frac{1}{N}\frac{\gamma}{4}\mathbb{E}[\text{Tr}\langle\mathbf{X}\mathbf{S}\rangle_t - \langle\tilde{\mathbf{X}}\tilde{\mathbf{S}}\rangle_t] \quad (\text{By a Nishimori identity}). \end{aligned}$$

We have

$$\begin{aligned} \frac{4N}{\gamma}\left|\frac{d}{dt}F_N(t)\right| &= \left|\mathbb{E}\left[\left\langle\text{Tr}[\mathbf{S}(\mathbf{X} - \tilde{\mathbf{X}}) - (\tilde{\mathbf{S}} - \mathbf{S})\tilde{\mathbf{X}}]\right\rangle_t\right]\right| \\ &\leq \mathbb{E}\left[\left\langle\left|\text{Tr}[\mathbf{S}(\mathbf{X} - \tilde{\mathbf{X}}) - (\tilde{\mathbf{S}} - \mathbf{S})\tilde{\mathbf{X}}]\right|\right\rangle_t\right] \quad (\text{By Jensen}) \\ &\leq \mathbb{E}\left[\left\langle\left|\text{Tr}\mathbf{S}(\mathbf{X} - \tilde{\mathbf{X}})\right|\right\rangle_t\right] + \mathbb{E}\left[\left\langle\left|\text{Tr}(\tilde{\mathbf{S}} - \mathbf{S})\tilde{\mathbf{X}}\right|\right\rangle_t\right] \\ &\leq \mathbb{E}\left[\|\mathbf{S}\|_F\langle\|\mathbf{X} - \tilde{\mathbf{X}}\|_F\rangle_t\right] + \mathbb{E}\left[\|\mathbf{S} - \tilde{\mathbf{S}}\|_F\langle\|\tilde{\mathbf{X}}\|_F\rangle_t\right] \\ &\leq \sqrt{\mathbb{E}\left[\|\mathbf{S}\|_F^2\right]}\mathbb{E}\left[\langle\|\mathbf{X} - \tilde{\mathbf{X}}\|_F^2\rangle_t\right] + \sqrt{\mathbb{E}\left[\|\mathbf{S} - \tilde{\mathbf{S}}\|_F^2\right]}\mathbb{E}\left[\langle\|\tilde{\mathbf{X}}\|_F^2\rangle_t\right] \quad (\text{By Cauchy-Schwarz}) \\ &\leq \sqrt{\mathbb{E}\left[\|\mathbf{S}\|_F^2\right]}\mathbb{E}\left[\langle\|\mathbf{X} - \tilde{\mathbf{X}}\|_F^2\rangle_t\right] + \sqrt{\mathbb{E}\left[\|\mathbf{S} - \tilde{\mathbf{S}}\|_F^2\right]}\mathbb{E}\left[\langle\|\tilde{\mathbf{X}}\|_F^2\rangle_t\right] \quad (\text{By Cauchy-Schwarz}) \\ &= \sqrt{\mathbb{E}\left[\|\mathbf{S}\|_F^2\right]}\mathbb{E}\left[\|\mathbf{S} - \tilde{\mathbf{S}}\|_F^2\right] + \sqrt{\mathbb{E}\left[\|\mathbf{S} - \tilde{\mathbf{S}}\|_F^2\right]}\mathbb{E}\left[\|\tilde{\mathbf{S}}\|_F^2\right] \quad (\text{By Nishimori}) \\ &= \left(\sqrt{\mathbb{E}\left[\|\mathbf{S}\|_F^2\right]} + \sqrt{\mathbb{E}\left[\|\tilde{\mathbf{S}}\|_F^2\right]}\right)\sqrt{\mathbb{E}\left[\|\mathbf{S} - \tilde{\mathbf{S}}\|_F^2\right]} \\ &= \left(\sqrt{\mathbb{E}_{\boldsymbol{\lambda}}\left[\|\boldsymbol{\lambda}\|^2\right]} + \sqrt{\mathbb{E}_{\tilde{\boldsymbol{\lambda}}}\left[\|\tilde{\boldsymbol{\lambda}}\|^2\right]}\right)\sqrt{\mathbb{E}_{\boldsymbol{\lambda},\tilde{\boldsymbol{\lambda}}}\left[\|\boldsymbol{\lambda} - \tilde{\boldsymbol{\lambda}}\|^2\right]}. \end{aligned}$$

We obtain the result by integrating over t from 0 to 1. □

H.3 Proof of technical lemmas

Lemma H.5. *Given two vectors $\mathbf{u}, \mathbf{v} \in \mathbb{R}^N$, denote their empirical distributions by μ, ν respectively. We have*

$$W_2(\mu, \nu) = \sqrt{\min_{\pi \in \mathcal{S}_N} \frac{1}{N} \|\mathbf{u} - \mathbf{v}_\pi\|^2}$$

where \mathbf{v}_π is a permutation of \mathbf{v} .

Proof. By definition we have

$$W_2(\mu, \nu)^2 = \inf_{\gamma \in \Gamma(\mu, \nu)} \mathbb{E}_{\gamma(x,y)}[(x-y)^2].$$

Any measure in $\Gamma(\mu, \nu)$ can be represented by a doubly stochastic $N \times N$ matrix. Thus, we have

$$W_2(\mu, \nu)^2 = \inf_{\mathbf{P} \in \mathcal{B}_N} \frac{1}{N} \sum_{i,j} P_{ij}(u_i - v_j)^2$$

where \mathcal{B}_N denotes the set of doubly stochastic matrices. This minimization problem is a linear optimization problem on the bounded convex set \mathcal{B}_N . By Choquet's theorem, the solutions to this problem exist and are the extremal points of \mathcal{B}_N , which are permutation matrices (by Birkhoff's theorem). Therefore, the minimization can be written on the set of permutation matrices to get:

$$W_2(\mu, \nu)^2 = \min_{\pi \in \mathcal{S}_N} \frac{1}{N} \sum_{i,j} (u_i - v_{\pi(i)})^2.$$

□

Lemma H.6. *Suppose $\lambda \in \mathbb{R}^N$ is distributed according to $P_{S,N}(\lambda)$, and λ^0 is generated with i.i.d. elements from ρ_S . Let $\hat{\mu}_\lambda, \hat{\mu}_{\lambda^0}$ be their empirical distribution. We have:*

$$\lim_{N \rightarrow \infty} \mathbb{E}_\lambda [W_2(\hat{\mu}_\lambda, \hat{\mu}_{\lambda^0})^2] = 0.$$

Proof. By the triangle inequality

$$W_2(\hat{\mu}_\lambda, \hat{\mu}_{\lambda^0}) \leq W_2(\hat{\mu}_\lambda, \rho_S) + W_2(\hat{\mu}_{\lambda^0}, \rho_S). \quad (139)$$

The first term approaches 0 as $N \rightarrow \infty$ almost surely, by remark 2. By lemma H.7, the second term also converges 0 as $N \rightarrow \infty$. Therefore, we have $W_2(\hat{\mu}_\lambda, \hat{\mu}_{\lambda^0}) \rightarrow 0$ almost surely. Consequently, we have that $W_2(\hat{\mu}_\lambda, \hat{\mu}_{\lambda^0})^2 \rightarrow 0$ almost surely. Denote $W_2(\hat{\mu}_\lambda, \hat{\mu}_{\lambda^0})^2$ by X_N which is a non-negative random variable. We have:

$$\begin{aligned} \mathbb{E}[X_N] &= \mathbb{E}[X_N \mathbb{I}\{X_N \leq \epsilon\}] + \mathbb{E}[X_N \mathbb{I}\{X_N > \epsilon\}] \\ &\leq \epsilon + \mathbb{E}[X_N \mathbb{I}\{X_N > \epsilon\}]. \end{aligned} \quad (140)$$

By definition, one can see that $W_2(\hat{\mu}_\lambda, \hat{\mu}_{\lambda^0})^2 \leq 2(m_{\hat{\mu}_\lambda}^{(2)} + m_{\hat{\mu}_{\lambda^0}}^{(2)})$, where $m_{\hat{\mu}_\lambda}^{(2)} = \frac{1}{N} \sum \lambda_i^2$ and $m_{\hat{\mu}_{\lambda^0}}^{(2)} = \frac{1}{N} \sum \lambda_i^{0^2}$. For the second term in (140) we have

$$\begin{aligned} \mathbb{E}[X_N \mathbb{I}\{X_N > \epsilon\}] &\leq 2\mathbb{E}[(m_{\hat{\mu}_\lambda}^{(2)} + m_{\hat{\mu}_{\lambda^0}}^{(2)}) \mathbb{I}\{X_N > \epsilon\}] \\ &= 2m_{\hat{\mu}_{\lambda^0}}^{(2)} \mathbb{E}[\mathbb{I}\{X_N > \epsilon\}] + 2\mathbb{E}[m_{\hat{\mu}_\lambda}^{(2)} \mathbb{I}\{X_N > \epsilon\}] \\ &= 2m_{\hat{\mu}_{\lambda^0}}^{(2)} \mathbb{P}[X_N > \epsilon] + 2\mathbb{E}[m_{\hat{\mu}_\lambda}^{(2)} \mathbb{I}\{X_N > \epsilon\}]. \end{aligned} \quad (141)$$

For the last term in (141) is decomposed as

$$\begin{aligned} \mathbb{E}[m_{\hat{\mu}_\lambda}^{(2)} \mathbb{I}\{X_N > \epsilon\}] &= \mathbb{E}[m_{\hat{\mu}_\lambda}^{(2)} \mathbb{I}\{X_N > \epsilon\} \mathbb{I}\{m_{\hat{\mu}_\lambda}^{(2)} \leq t\}] + \mathbb{E}[m_{\hat{\mu}_\lambda}^{(2)} \mathbb{I}\{X_N > \epsilon\} \mathbb{I}\{m_{\hat{\mu}_\lambda}^{(2)} > t\}] \\ &\leq t\mathbb{P}[X_N > \epsilon] + \mathbb{E}[m_{\hat{\mu}_\lambda}^{(2)} \mathbb{I}\{m_{\hat{\mu}_\lambda}^{(2)} > t\}] \end{aligned} \quad (142)$$

where t is a fixed sufficiently large constant such that $t > C$. From (140), (141), (142), we get:

$$\mathbb{E}[X_N] \leq \epsilon + 2m_{\hat{\mu}_{\lambda^0}}^{(2)} \mathbb{P}[X_N > \epsilon] + 2t\mathbb{P}[X_N > \epsilon] + 2\mathbb{E}[m_{\hat{\mu}_\lambda}^{(2)} \mathbb{I}\{m_{\hat{\mu}_\lambda}^{(2)} > t\}]. \quad (143)$$

Since $W_2(\hat{\mu}_\lambda, \hat{\mu}_{\lambda^0})^2 \rightarrow 0$ almost surely, $\mathbb{P}[X_N > \epsilon]$ approaches 0 as $N \rightarrow \infty$. By construction $m_{\hat{\mu}_{\lambda^0}}^{(2)}$ is bounded (by the constant C), so the second and the third terms approaches 0 as $N \rightarrow \infty$. The last term also converges 0, by lemma H.8. Therefore, for arbitrary $\epsilon > 0$ we find

$$\lim_{N \rightarrow \infty} \mathbb{E}[X_N] \leq \epsilon.$$

□

Lemma H.7. *Let X_1, \dots, X_N be i.i.d. random variables distributed according to distribution μ , which has finite support. Let μ_N denote their empirical distribution. Then*

$$\lim_{N \rightarrow \infty} W_2(\mu_N, \mu) = 0 \quad \text{almost surely.}$$

Proof. By the law of large numbers, $\mu_N \rightarrow \mu$ almost surely. Moreover, since μ has bounded support, the second moment of μ_N converges to the one of μ . By Theorem 7.12 in [58], we have the convergence in the Wasserstein-2 metric almost surely. □

Lemma H.8. *Under assumption 1.B, for t large enough, we have:*

$$\lim_{N \rightarrow \infty} \mathbb{E} [m_{\hat{\mu}_\lambda}^{(2)} \mathbb{I}\{m_{\hat{\mu}_\lambda}^{(2)} > t\}] = 0.$$

Proof. Boundedness and almost sure convergence of $m_{\hat{\mu}_\lambda}^{(2)}$ imply that $\lim_{N \rightarrow \infty} \mathbb{E}[m_{\hat{\mu}_\lambda}^{(2)}] = m_{\rho_S}^{(2)}$, which is bounded since ρ_S has compact support. Denote $X_N = m_{\hat{\mu}_\lambda}^{(2)} \mathbb{I}\{m_{\hat{\mu}_\lambda}^{(2)} \leq t\}$. Then, $X_N \rightarrow m_{\rho_S}^{(2)}$ a.s. and by bounded convergence we also have that $\lim_{N \rightarrow \infty} \mathbb{E}[X_N] = m_{\rho_S}^{(2)}$. Therefore,

$$\lim_{N \rightarrow \infty} \mathbb{E} [m_{\hat{\mu}_\lambda}^{(2)} \mathbb{I}\{m_{\hat{\mu}_\lambda}^{(2)} > t\}] = \lim_{N \rightarrow \infty} \mathbb{E} [m_{\hat{\mu}_\lambda}^{(2)} - X_N] = 0.$$

□

I Derivation of the limiting spectral distribution for the model G.1

Suppose we want to find the density $\mu(x)$, which is the free convolution of the density $\rho(x)$ with the semi-circle density $\rho_{sc}(x)$. This density is given in [45] by

$$\begin{aligned} \mu(\psi(u)) &= \frac{v(u)}{\pi} \\ \psi(u) &= u + \int_{\mathbb{R}} \frac{u-x}{(u-x)^2 + v(u)^2} \rho(x) dx, \quad v(u) = \inf \left\{ w \geq 0 \mid \int_{\mathbb{R}} \frac{\rho(x)}{(u-x)^2 + w^2} dx \leq 1 \right\}. \end{aligned} \quad (144)$$

This result will be used repeatedly.

To compute the density $\rho_Y = \rho_{\sqrt{\gamma}S} \boxplus \rho_{sc}$ where $\rho_{\sqrt{\gamma}S}(x) = \frac{1}{2}\delta(x + \sqrt{\gamma}) + \frac{1}{2}\delta(x - \sqrt{\gamma})$, we compute functions $v(u)$ and $\psi(u)$

$$\begin{aligned} \text{if } \gamma < 1: \quad v(u) &= \begin{cases} \frac{1}{\sqrt{2}} \sqrt{1 - 2(u^2 + \gamma) + \sqrt{1 + 16\gamma u^2}} & \text{if } |u| \leq \frac{1}{\sqrt{2}} \sqrt{1 + 2\gamma + \sqrt{1 + 8\gamma}} \\ 0 & \text{else.} \end{cases} \\ \psi(u) &= \begin{cases} \frac{1+8u^2 - \sqrt{1+16\gamma u^2}}{4u} & \text{if } |u| \leq \frac{1}{\sqrt{2}} \sqrt{1 + 2\gamma + \sqrt{1 + 8\gamma}} \\ \frac{u(u^2 - \gamma + 1)}{u^2 - \gamma} & \text{else.} \end{cases} \end{aligned} \quad (145)$$

$$\begin{aligned} \text{if } \gamma \geq 1: \\ v(u) &= \begin{cases} \frac{1}{\sqrt{2}} \sqrt{1 - 2(u^2 + \gamma) + \sqrt{1 + 16\gamma u^2}} & \text{if } \frac{1}{\sqrt{2}} \sqrt{1 + 2\gamma - \sqrt{1 + 8\gamma}} \leq |u| \leq \frac{1}{\sqrt{2}} \sqrt{1 + 2\gamma + \sqrt{1 + 8\gamma}} \\ 0 & \text{else.} \end{cases} \\ \psi(u) &= \begin{cases} \frac{1+8u^2 - \sqrt{1+16\gamma u^2}}{4u} & \text{if } \frac{1}{\sqrt{2}} \sqrt{1 + 2\gamma - \sqrt{1 + 8\gamma}} \leq |u| \leq \frac{1}{\sqrt{2}} \sqrt{1 + 2\gamma + \sqrt{1 + 8\gamma}} \\ \frac{u(u^2 - \gamma + 1)}{u^2 - \gamma} & \text{else.} \end{cases} \end{aligned} \quad (146)$$

Solving the equation $\rho_Y(\psi(u)) = \frac{v(u)}{\pi}$, we find:

$$\begin{aligned} \text{if } \gamma < 1: \quad \rho_Y(x) &= \begin{cases} \frac{1}{\sqrt{2\pi}} \sqrt{1 - 2(\gamma + \frac{1}{2304}A^2) + \sqrt{1 + \frac{\gamma}{144}A^2}} & \text{if } |x| \leq U(\gamma) \\ 0 & \text{else.} \end{cases} \\ \text{if } \gamma \geq 1: \quad \rho_Y(x) &= \begin{cases} \frac{1}{\sqrt{2\pi}} \sqrt{1 - 2(\gamma + \frac{1}{2304}A^2) + \sqrt{1 + \frac{\gamma}{144}A^2}} & \text{if } L(\gamma) \leq |x| \leq U(\gamma) \\ 0 & \text{else.} \end{cases} \end{aligned} \quad (147)$$

where

$$A = 16x + \frac{32 \times 2^{1/3}(-3 + 3\gamma + x^2)}{B} + 2^{2/3}B \quad (148)$$

$$\begin{aligned} B &= \sqrt[3]{576x + 1152\gamma x - 128x^3 + 64\sqrt{x^2(9 + 18\gamma - 2x^2)^2 - 4(-3 + 3\gamma + x^2)^3}} \\ L(\gamma) &= \frac{(-3 + \sqrt{1 + 8\gamma})\sqrt{1 + 2\gamma - \sqrt{1 + 8\gamma}}}{\sqrt{2}(-1 + \sqrt{1 + 8\gamma})}, \quad U(\gamma) = \frac{(3 + \sqrt{1 + 8\gamma})\sqrt{1 + 2\gamma + \sqrt{1 + 8\gamma}}}{\sqrt{2}(1 + \sqrt{1 + 8\gamma})} \end{aligned} \quad (149)$$

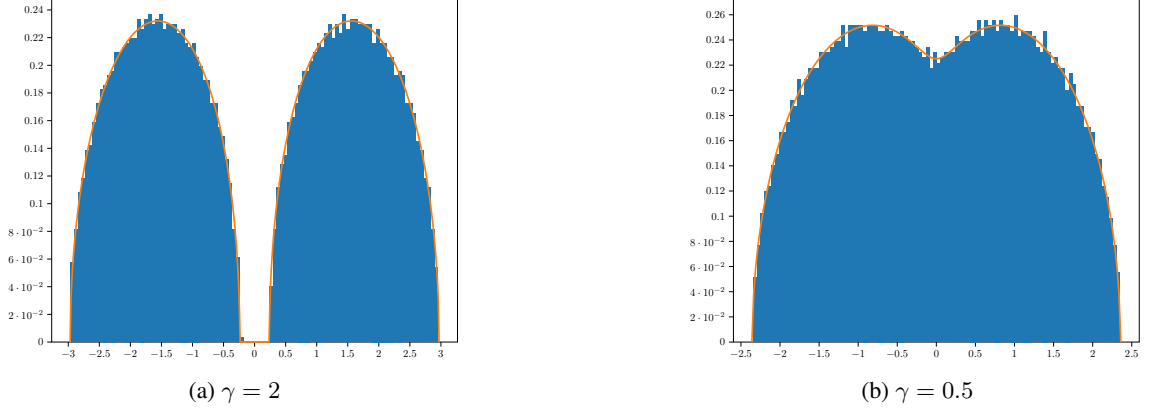


Figure 12: The continuous line is the asymptotic spectral density of the observation matrix \mathbf{Y} in example G.1. $\rho_Y(x) = \rho_{\sqrt{\gamma}S} \boxplus \rho_{sc}$ where $\rho_{\sqrt{\gamma}S}(x) = \frac{1}{2}\delta(x + \sqrt{\gamma}) + \frac{1}{2}\delta(x - \sqrt{\gamma})$ for $\gamma = 2$ and $\gamma = 0.5$. Compared to the histogram of a realization of size $N = 5000$.

From (147), one can see that the support of ρ_Y is constituted of two disjoint intervals for $\gamma \geq 1$, and of one single interval for $\gamma < 1$.

Once we have the expression (147), we get from Theorem 2 an explicit integral representation for $\text{MMSE}(\gamma)$, as well as for the derivatives. We show the details here for $\gamma \geq 1$. Since in this example $\rho_Y(x)$ is symmetric we have for $\gamma > 1$

$$\text{MMSE}(\gamma) = \frac{1}{\gamma} \left(1 - \frac{8\pi^2}{3} \int_{L(\gamma)}^{U(\gamma)} \rho_Y^3(x) dx \right). \quad (150)$$

By the Leibniz integral rule (all derivatives are w.r.t γ) we have using that ρ_Y vanishes at the end-points of the interval $[L(\gamma), U(\gamma)]$

$$\begin{aligned} \text{MMSE}'(\gamma) &= -\frac{1}{\gamma^2} + \frac{1}{\gamma^2} \frac{8\pi^2}{3} \int_{L(\gamma)}^{U(\gamma)} \rho_Y^3(x) dx \\ &\quad - \frac{1}{\gamma} \frac{8\pi^2}{3} \left(\rho_Y^3(U(\gamma))U'(\gamma) - \rho_Y^3(L(\gamma))L'(\gamma) + \int_{L(\gamma)}^{U(\gamma)} 3\rho_Y^2(x)\rho_Y'(x) dx \right) \\ &= -\frac{1}{\gamma^2} + \frac{1}{\gamma^2} \frac{8\pi^2}{3} \int_{L(\gamma)}^{U(\gamma)} \rho_Y^3(x) dx - \frac{8\pi^2}{\gamma} \int_{L(\gamma)}^{U(\gamma)} \rho_Y^2(x)\rho_Y'(x) dx. \end{aligned} \quad (151)$$

Moreover, $\rho_Y^2(x)\rho_Y'(x)$ can also be checked to vanishes at the end-points of the interval $[L(\gamma), U(\gamma)]$ so

$$\begin{aligned} \text{MMSE}''(\gamma) &= \frac{2}{\gamma^3} - \frac{1}{\gamma^3} \frac{16\pi^2}{3} \int_{L(\gamma)}^{U(\gamma)} \rho_Y^3(x) dx + \frac{16\pi^2}{\gamma^2} \int_{L(\gamma)}^{U(\gamma)} \rho_Y^2(x)\rho_Y'(x) dx \\ &\quad - \frac{8\pi^2}{\gamma} \int_{L(\gamma)}^{U(\gamma)} [2\rho_Y(x)(\rho_Y'(x))^2 + \rho_Y^2(x)\rho_Y''(x)] dx. \end{aligned} \quad (152)$$

A similar and somewhat simpler calculation also provides integral representations for $\gamma < 1$.

It is not clear how to compute these integrals analytically but precise results can be obtained from numerical integration. Integral representations of higher derivatives can also be obtained in principle but become unwieldy. In fact the numerical integration of the formula for the second derivative is precise enough to get a good numerical calculation of the third and fourth derivatives. All numerical results are summarized in figure 13.

Plots (f),(g) in figure 13 suggest the existence of a third-order phase transition at $\gamma_c = 1$. Note that this is the point where the support of ρ_Y transitions from a single to two intervals. Since the singularity seems to appear in the third derivative we define the function

$$f(\gamma) = \text{MMSE}(\gamma) - \text{MMSE}(1) + \text{MMSE}'(1)(\gamma - 1) + \frac{1}{2}\text{MMSE}''(1)(\gamma - 1)^2.$$

If one tries the ansatz $f(\gamma) = c|\gamma - 1|^\alpha$ with $2 < \alpha \leq 3$, or in other words $\log |f(\gamma)| \approx \log |c| + \alpha \log |\gamma - 1|$ we find $\alpha \approx 2.929$. This is shown in figure 14 where $f(\gamma)$ is plotted on a log-log scale on both sides of $\gamma_c = 1^\pm$. However, the appearance of this exponent is not consistent with the fact that the expression for ρ_Y (147) is fully algebraic and an exact integration could only give an integer exponent or a logarithmic singularity. To further investigate the

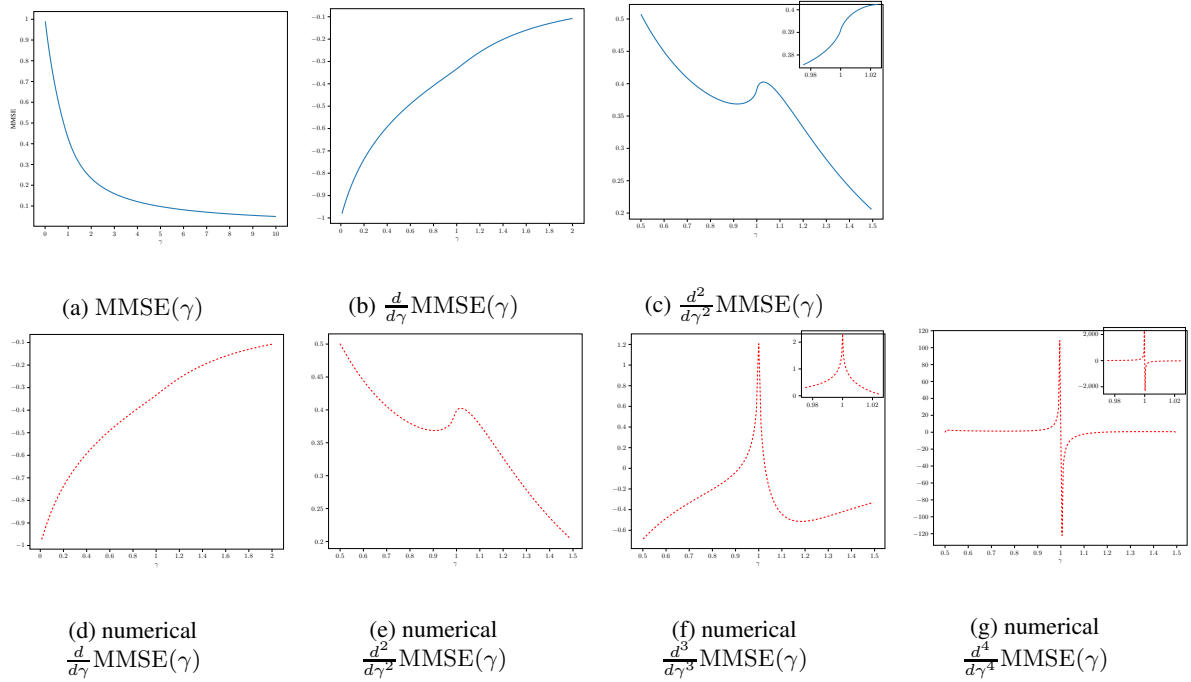
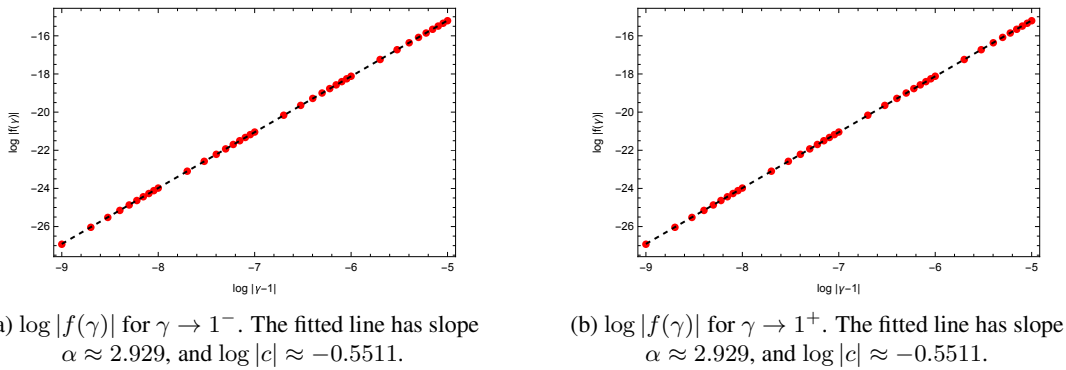


Figure 13: Analysis of the MMSE in example G.1. In (a), MMSE is plotted from (150) for $0 < \gamma \leq 10$ with step-size $h = 0.01$. The numerical first derivative of the curve in (a) is illustrated in (d), which is computed using five-point stencil [65] $f'(x) \approx \frac{-f(x+2h)+8f(x+h)-8f(x-h)+f(x-2h)}{12h}$. In (b), the first derivative is plotted from (151) with step-size $h = 0.01$, and its numerical first derivative is plotted in (e). The second derivative of MMSE, computed from (152), is depicted in (c) with step-size $h = 0.005$. The inset plot is with step-size $h = 0.00025$. The third derivative of MMSE in (f) is obtained from the numerical differentiation of the curve in (c). The fourth derivative is computed using the five-point stencil $f'''(x) \approx \frac{-f(x+2h)+16f(x+h)-30f(x)+16f(x-h)-f(x-2h)}{12h^2}$ from the curve in (c).



(a) $\log |f(\gamma)|$ for $\gamma \rightarrow 1^-$. The fitted line has slope $\alpha \approx 2.929$, and $\log |c| \approx -0.5511$.

(b) $\log |f(\gamma)|$ for $\gamma \rightarrow 1^+$. The fitted line has slope $\alpha \approx 2.929$, and $\log |c| \approx -0.5511$.

Figure 14: $\log |f(\gamma)|$ as a function of $\log |\gamma - 1|$

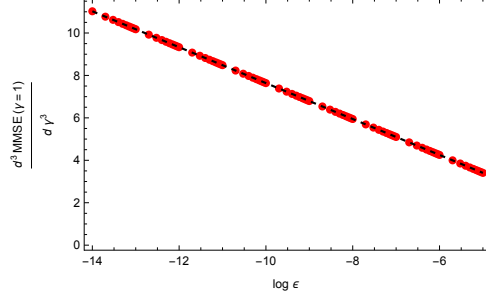
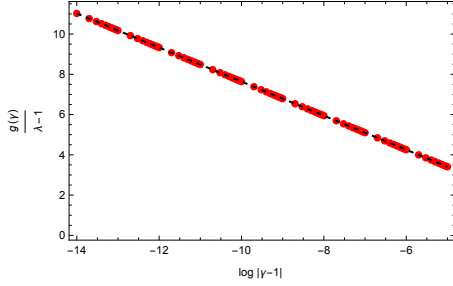
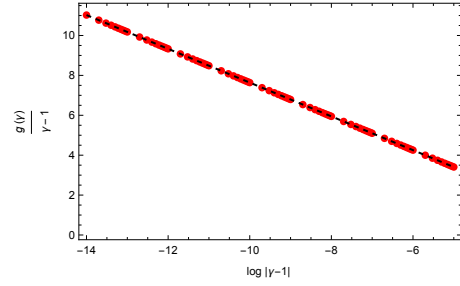


Figure 15: Numerical third derivative of MMSE at $\gamma = 1$ computed from $\frac{\text{MMSE}''(1+\epsilon) - \text{MMSE}''(1-\epsilon)}{2\epsilon}$ as a function of $\log \epsilon$. A linear function $-0.8463 \log \epsilon - 0.8249$ is fitted to the points.



(a) $\frac{g(\gamma)}{\gamma-1}$ for $\gamma \rightarrow 1^-$. The fitted line has slope $a \approx -0.8463$, and $ab \approx -0.8249$.



(b) $\frac{g(\gamma)}{\gamma-1}$ for $\gamma \rightarrow 1^+$. The fitted line has slope $a \approx -0.8463$, and $ab \approx -0.8249$.

Figure 16: $\frac{g(\gamma)}{\gamma-1}$ as a function of $\log |\gamma - 1|$

behavior of the MMSE, we study the third numerical derivative obtained from the curve of $\text{MMSE}''(\gamma)$ using the relation $\frac{d^3}{d\gamma^3} \text{MMSE}(1) \approx \frac{\text{MMSE}''(1+\epsilon) - \text{MMSE}''(1-\epsilon)}{2\epsilon}$. As plotted in figure 15, $\frac{d^3}{d\gamma^3} \text{MMSE}(1)$ diverges linearly as ϵ decays exponentially. This suggests that the behavior of the correction term for the second derivative is of the form $a(\gamma - 1)(\log |\gamma - 1| + b)$. Define the function

$$g(\gamma) = \text{MMSE}''(\gamma) - \text{MMSE}''(1) \quad (153)$$

for γ close to 1, we have:

$$\frac{g(\gamma)}{\gamma-1} \approx a \log |\gamma - 1| + ab \quad (154)$$

From the plots in figure 16, we deduce that $a \approx -0.8463$ and $b \approx 0.9746$. Therefore, the $\text{MMSE}''(\gamma)$ can be described by the following expansion close to the point $\gamma = 1$

$$\text{MMSE}''(\gamma) = \text{MMSE}''(1) + a(\gamma - 1)(\log |\gamma - 1| + b) + o((\gamma - 1)). \quad (155)$$

From this expansion, we conjecture that the MMSE has a third-order phase transition at $\gamma = 1$.

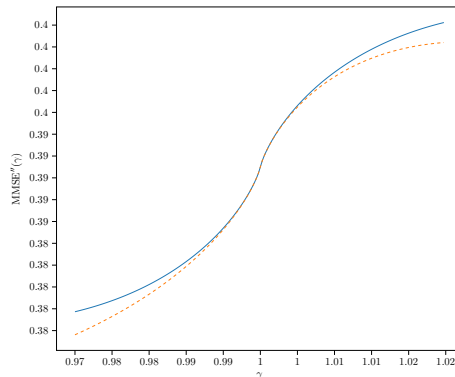


Figure 17: Comparison of the second derivative of the $\text{MMSE}(\gamma)$ and the expansion (155) (plotted with dashed line).

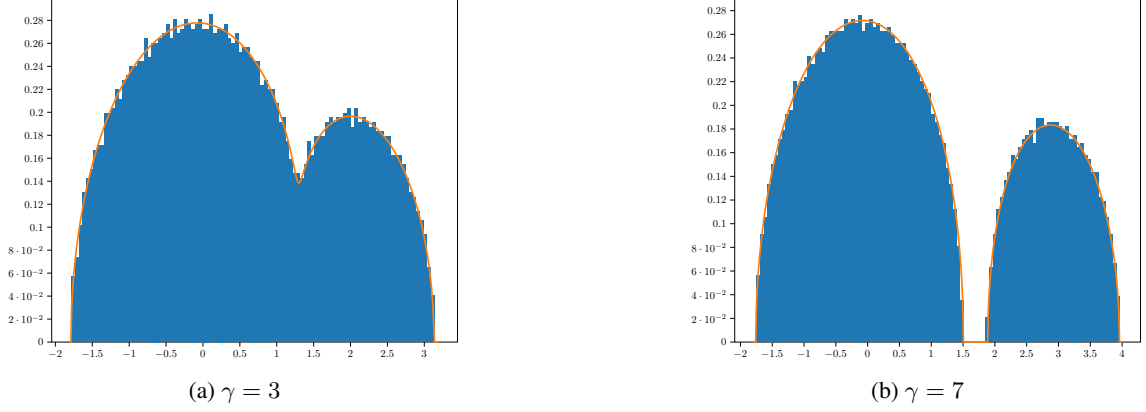


Figure 18: The continuous line is plotted from the analytical expression for the asymptotic spectral density of the observation matrix \mathbf{Y} in example G.2 for $p = 0.7$. $\rho_Y(x) = \rho_{\sqrt{\gamma}S} \boxplus \rho_{SC}$ where $\rho_{\sqrt{\gamma}S}(x) = 0.7\delta(x) + 0.3\delta(x - \sqrt{\gamma})$ for $\gamma = 3$ and $\gamma = 7$. The critical value for $p = 0.7$ is $\gamma^c \approx 3.78$. This is compared to the histogram of a realization of size $N = 5000$.

J Derivation of the limiting spectral distribution for the model G.2

We indicate the main steps to compute the density $\rho_Y = \rho_{\sqrt{\gamma}S} \boxplus \rho_{SC}$ where $\rho_{\sqrt{\gamma}S}(x) = p\delta(x) + (1-p)\delta(x - \sqrt{\gamma})$. Following the same procedure as in the previous example, functions $v(u)$ and $\psi(u)$ can be derived as :

$$v(u) = \begin{cases} \sqrt{\frac{1}{2} \left[-2u^2 + 2\sqrt{\gamma}u + \sqrt{\sqrt{\gamma}(\sqrt{\gamma} - 2u)(-2\sqrt{\gamma}u + \gamma + 4p - 2) + 1 - \gamma + 1} \right]} & \text{if } u \in \text{Supp}(v) \\ 0 & \text{else.} \end{cases}$$

$$\psi(u) = \begin{cases} \frac{-8u^2 + 6\sqrt{\gamma}u + \sqrt{\sqrt{\gamma}(\sqrt{\gamma} - 2u)(-2\sqrt{\gamma}u + \gamma + 4p - 2) + 1 - \gamma - 1}}{2(\sqrt{\gamma} - 2u)} & \text{if } u \in \text{Supp}(v) \\ u + \frac{p}{u} + \frac{1-p}{u - \sqrt{\gamma}} & \text{else.} \end{cases}$$

where

$$\text{Supp}(v) = \{u | g(u) < 0\}$$

and

$$g(u) = u^4 - 2\sqrt{\gamma}u^3 + (\gamma - 1)u^2 + 2p\sqrt{\gamma}u - p\gamma. \quad (156)$$

Solving the equation $\rho_Y(\psi(u)) = \frac{v(u)}{\pi}$, we find the analytical expression for $\rho_Y(x)$ which we omit here.

The set $\text{Supp}(v)$ determines the support of ρ_Y . For a given $0 < p < 1$ the degree four polynomial $g(u)$ has either two or four real roots, depending on γ . The former case corresponds to the situation where the support of ρ_Y is a single interval, and the latter corresponds to the case where the support of ρ_Y is a union of two intervals. Using Theorem 3.7 in [66], a critical value γ_c is found such that for $\gamma < \gamma_c$ the polynomial $g(u)$ has two real roots and for $\gamma > \gamma_c$ it has four real roots. We have

$$\gamma_c = 1 + 3\sqrt[3]{p^2(1-p)} + 3\sqrt[3]{p(1-p)^2}. \quad (157)$$

An example is illustrated in figure 18. But contrary to the previous example we have not identified any singularity in $\text{MMSE}(\gamma)$ due to the merging of the two intervals.

K Derivation of the limiting spectral distribution for the model G.3

In this example, we find the limiting spectral measure $\rho_Y = \rho_{\sqrt{\gamma}S} \boxplus \rho_{sc}$ directly using the free additive convolution formula. The limiting spectral measure of \mathbf{S} is the Marchenko-Pastur law rescaled by factor q , which we denote by ρ_{MP} . The R-transform is $\mathcal{R}_{\rho_{MP}} = \frac{1}{q} \frac{1}{1-z}$. Using the relation $\mathcal{R}_{a*\mu}(z) = a\mathcal{R}_\mu(az)$, we have that $R_{\rho_{\sqrt{\gamma}S}}(z) = \frac{\sqrt{\gamma}}{q} \frac{1}{1 - \sqrt{\gamma}z}$. The free additive convolution formula is $R_{\rho_{\sqrt{\gamma}S}}(z) + R_{\rho_{sc}}(z) = R_{\rho_Y}(z)$. Substituting z by the inverse of the Cauchy transform of ρ_Y , $G_{\rho_Y}^{-1}$, and using that $R_{\rho_{sc}}(z) = z$ we get:

$$G_{\rho_Y}(z) + \frac{\sqrt{\gamma}}{q} \frac{1}{1 - \sqrt{\gamma}G_{\rho_Y}(z)} + \frac{1}{G_{\rho_Y}(z)} = z. \quad (158)$$

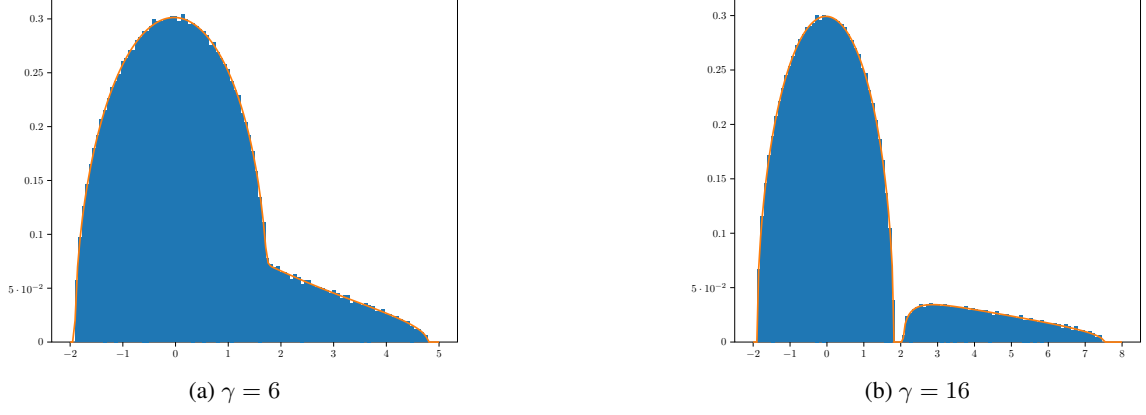


Figure 19: Asymptotic spectral density of the observation matrix Y in example G.3 for $q = 8$. $\gamma^c = 8$. It is Compared to the empirical density of a realization of size $N = 10000$.

Solving this equation for $G_{\rho_Y}(z)$, and using the Stieltjes inversion formula, $\mu(x) = \frac{1}{\pi} \lim_{\epsilon \rightarrow 0} \Im \mathcal{S}_\mu(x + i\epsilon)$, we find the density of ρ_Y to be

$$\rho_Y(x) = \begin{cases} \frac{\sqrt[3]{2A^2-2}(q\gamma(x^2-3)-q\sqrt{\gamma}x+q+3\gamma)}{\pi 2^{\frac{2}{3}} \sqrt{3q\gamma} \sqrt[3]{A}} & \text{if } x \in \text{Supp}(\rho_Y) \\ 0 & \text{else.} \end{cases} \quad (159)$$

where

$$A = q^{\frac{3}{2}}(\sqrt{\gamma}x - 2)(\gamma(2x^2 - 9) + \sqrt{\gamma}x - 1) + 9q^2\gamma(\sqrt{\gamma}x + 1) + \sqrt{f(x)} \quad (160)$$

where

$$f(x) = q\left(q(\sqrt{\gamma}x - 2)(2\gamma x^2 + \sqrt{\gamma}x - 9\gamma - 1) + 9(\gamma^{\frac{3}{2}}x + \gamma)\right)^2 - 4\left(q\gamma(x^2 - 3) - q\sqrt{\gamma}x + q + 3\gamma\right)^3 \quad (161)$$

and

$$\text{Supp}(\rho_Y) = \{x \mid f(x) \geq 0\}. \quad (162)$$

If $q \leq 1$, then the support of $\rho_{\sqrt{\gamma}S}$ is only a single interval, and the support of ρ_Y is also an interval. However, for $q > 1$, $\rho_{\sqrt{\gamma}S}$ has a delta at zero, and the support of ρ_Y can be a single interval or union of two intervals, depending on γ . For fixed $q > 1$, the intervals merge at the critical value $\gamma_c = \frac{q}{(\sqrt[3]{q}-1)^3}$: if $\gamma \leq \gamma_c$, $\text{Supp}(\rho_Y)$ is a single interval, while if $\gamma > \gamma_c$, $\text{Supp}(\rho_Y)$ is the union of two intervals. In Fig. 19, the density is plotted for $q = 8$, for which $\gamma_c = 8$.